Volume 6, Number 2, November 2022.
ISSN 2459-9484
seemedj.mefos.unios.hr

SEEMEDJ SOUTHEASTERN EUROPEAN MEDICAL JOURNAL

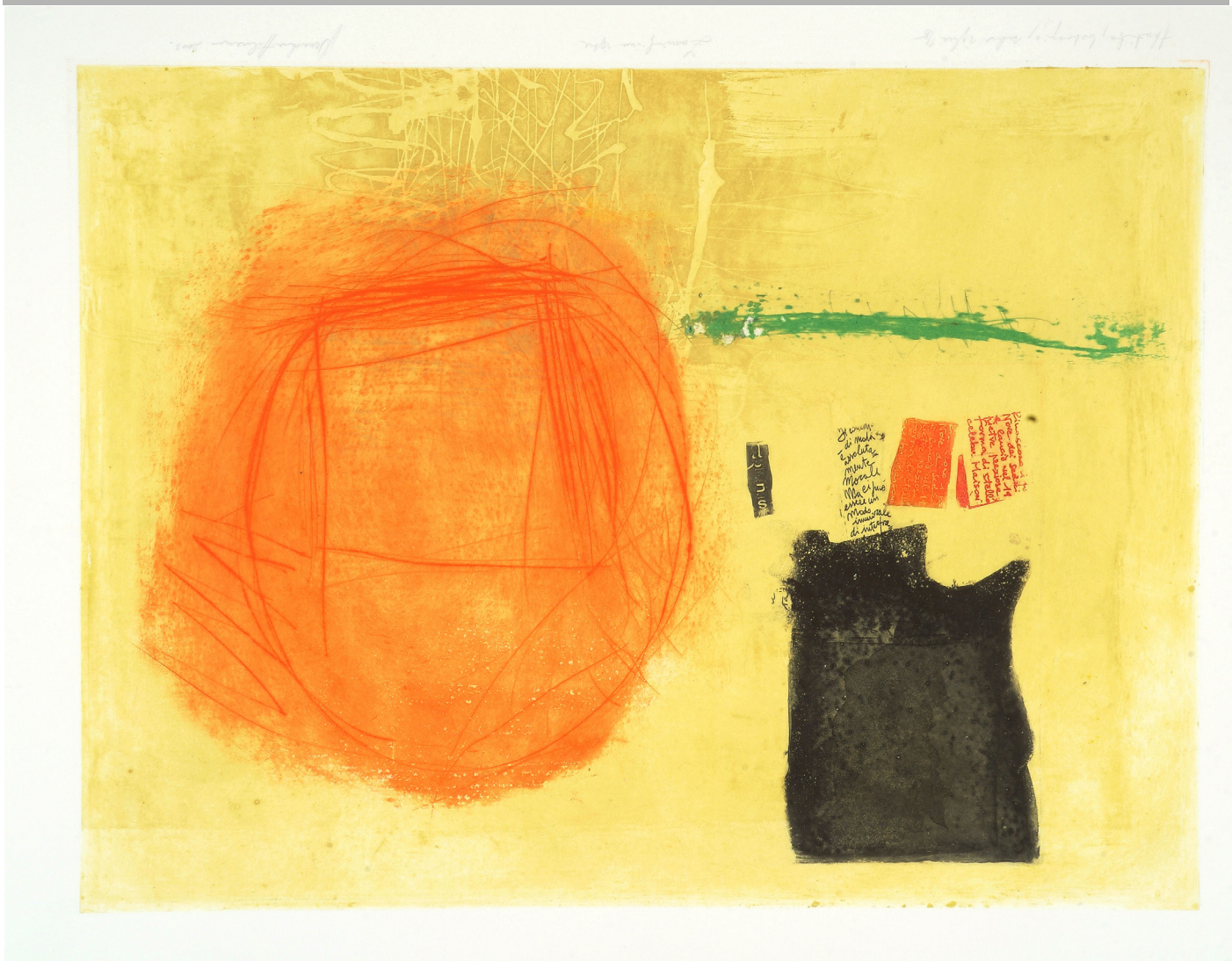

Nevenka Arbanas, An interesting game, 1996
Acquamonotype, copperplate, drypoint
MLU-4325

Josip Juraj Strossmayer University of Osijek
Faculty of Medicine

Arbanas, Nevenka, Croatian graphic artist (Batina, June 8, 1950). Graduated from the Academy in Zagreb (1975), and completed postgraduate studies with A. Kinert (1977); she trained in Paris and Prague (S. W. Hayter, L. Čepelak). He has been teaching at the School of Applied Art and Design in Zagreb since 1993. In the spirit of lyrical abstraction, in all graphic techniques and their combinations, he creates a distinctive and powerful graphic expression (Grafika 22, 1995). Published eight maps of graphics (Venice, verses by L. Paljetak, 1997; Novi listovi, 2008). She is the winner of the "Vladimir Nazor" Award for Lifetime Achievement (2018).

Citation:
Arbanas, Nevenka. Croatian encyclopedia, online edition. Miroslav Krleža Lexicographic Institute, 2021. Accessed on November 8, 2022.
http://www.enciklopedija.hr/Natuknica.aspx?ID=3566

Arbanas, Nevenka.

Croatian graphic artist (Batina, June 8, 1950). Graduated from the Academy in Zagreb (1975), and completed postgraduate studies with A. Kinert (1977); she trained in Paris and Prague (S. W. Hayter, L. Čepelak). He has been teaching at the School of Applied Art and Design in Zagreb since 1993. In the spirit of lyrical abstraction, in all graphic techniques and their combinations, he creates a distinctive and powerful graphic expression (Grafika 22, 1995). Published eight maps of graphics (Venice, verses by L. Paljetak, 1997; Novi listovi, 2008). She is the winner of the "Vladimir Nazor" Award for Lifetime Achievement (2018).

Citation:

Arbanas, Nevenka. Croatian encyclopedia, online edition. Miroslav Krleža Lexicographic Institute, 2021. Accessed on November 8, 2022. <http://www.enciklopedija.hr/Natuknica.aspx?ID=3566>.

Southeastern European Medical Journal (SEEMEDJ)
Published by
University Josip Juraj Strossmayer Osijek
Faculty of Medicine Osijek
for publisher: Ivica Mihaljević, MD, PhD, - Dean of Faculty of Medicine Osijek, Croatia

Published online:
http://seemedj.mefos.unios.hr
ISSN 2459-9484

Since 2021 the journal is published with the financial support of the
Ministry of Science, Education and Sports of the Republic of Croatia

Contents

SEEMEDJ SOUTHEASTERN EUROPEAN MEDICAL JOURNAL

Editorial SEEMEDJ 2022;6(2): 1-85

Dear colleagues,

Hereby, new 12th issue of SEEMEDJ is presented to you. This issue brings 7 articles with various topics. The molecular dynamics of the antigen-antibody reaction and the role of water molecules is presented in the article by Nemeth P. Iskandarov et al investigated bioactive components that affect blood coagulation system by fractionation of Vipera berus berus snake venom which may be utilized in biotechnology and medicine. Microcirculatory blood flow after acute exertional exercise was examined by Potočnik N. TFF3 is involved in the pathogenesis of sepsis, but the exact mechanism is not yet clear. This issue has been reviewed by Bazina and Baus Lončar. Comorbidities of psychiatric and somatic disease pose a major challenge to modern medicine and the multidisciplinary approach and cooperation in treatment are necessary to improve the patients' quality of life and life expectancy, as presented in a work by Marušić R et al. Vidović et al detected vitamin D deficiency in a population of medical students, which is significant problem noted elsewhere also. And finally, Krajina Kmoničekk et al reviewed the effects of iron chelators in COVID-19 disease.

We are happy to inform our potential authors that SEEMEDJ has been included to another citation bases: Crossref, Dimensions and Publons, thus widening our accessibility to readers. The art work at the cover page is authored by Nevenka Arbanas, Croatian graphic artist born in Batina, Baranja. This way, we continue to present our national but widely recognized artists with the origin from Easter Slavonia and Baranja.

I hope that readers will find relevant published articles for their work. On the behalf of the editorial board and my own, I warmly greet our readers and invite them to join us in the endeavor of publishing their own scientific work in SEEMEDJ.

Ines Drenjančević, MD, PhD
Editor-in-Chief
Southeastern European Medical Journal (SEEMEDJ)

FACULTY OF MEDICINE OSIJEK
Josip Juraj Strossmayer University of Osijek
J. Huttlera 4
Croatia – 31000 Osijek

seemedj@mefos.unios.hr
seemedj.mefos.unios.hr

Original article

Do Water Molecules Displaced by Hydrophobic Interactions Stabilize Antigen-Antibody Binding? Physico-chemical background of antigen-antibody reactions analyzed by fluorescent and Fourier-transform infrared spectroscopy on FITC – anti-FITC (IgG1) model

Peter Németh*

Department of Immunology and Biotechnology, Clinical Centre, University of Pécs Medical School, Pécs, Hungary

*Corresponding author: Peter Németh, nemeth.peter@pte.hu

Abstract

Background: Antigen-antibody reactions are a special field of molecular interactions. The physico-chemical nature of antigen-antibody binding and ligand-induced changes in the fine molecular structures of antigens during immunocomplex formation are less studied. However, these changes in the molecular appearance are extremely important for further molecular recognition. The major aim of this study is to clarify the physico-chemical modification of the antigen/hapten during immunobinding using model experiments.

Methods: An appropriate model system was designed for our investigations: fluorescein-isothiocyanate (FITC, isomer I) was used as the antigen (hapten), and its interactions with a specific antibody (monoclonal anti-FITC IgG1) were analyzed using spectrophotometry, different spectrofluorimetric methods and fluorescence polarization, and Fourier-transform infrared spectroscopic methods.

Results: Fluorescent polarization and infrared spectroscopic measurements detected a local decrease in the hydration degree in the submolecular area of the specific ligand between the small antigen (hapten) molecule and the hypervariable region of the specific IgG1, causing "rigidization" of molecular movements. Changes in hydration modified the molecular microenvironment, allowing them to influence further functions of both immunoglobulins and the antigen.

Conclusion: Hydrophobic interactions with exclusion of water molecules around the binding sites seem to be thermodynamically strong enough for stable molecular binding without a covalent chemical interaction between the antigen and the antibody. The results of this study, together with data obtained in previous research, help understand the molecular dynamics of the antigen-antibody reaction better.

(Németh P. Do Water Molecules Displaced by Hydrophobic Interactions Stabilize Antigen-Antibody Binding?. SEEMEDJ 2022; 6(2); 1-19)

Received: Oct 12, 2022; revised version accepted: Oct 27 2022; published: Nov 28, 2022

KEYWORDS: Antigen-antibody reaction, FITC, fluorescence, spectrum analysis

Introduction

Antigen-antibody interactions are special forms of molecular associations in vivo and in vitro. The influence of antigen molecules on specific immunoglobulins during the formation of immune complexes has been studied: modification of the physico-chemical character of immunoglobulins after the binding of an antigen can influence the biological functions of an antibody (e.g. complement fixation, Fc receptor functions, etc.) (1, 2, 3, 4). However, our knowledge about diverse modifications of the fine molecular structure of antigens, especially changes in the structure of low molecular weight antigens (or so-called haptens) by specific immunoglobulins, is limited (5, 6, 7). However, these physico-chemical changes in the fine structure of antigens cross-linked by immunoglobulins seem to be important in the further regulation of several other molecular interactions. Activation or inhibition of different receptors, enzymes, and transporter molecules interchange during immunocomplex formation. Both new physiological and pathological immune reactions occur by the modification of the primary physico-chemical appearance of the antigenic structure after binding with an immunoglobulin (8). The submolecular mechanism of immunobinding and consequential modifications of fine molecular structures are poorly understood (9, 10, 11). Simple electrostatic coherence between the antigen and immunoglobulins is not thermodynamically strong enough to form a stable molecular complex and cause remarkable modifications of physico-chemical appearances of participating molecules (12, 13).

An analysis of hapten-immunoglobulin interactions is more favourable for studying the physico-chemical nature of structural modifications of the antigen caused by immunobinding. We have developed an experimental model system that allows us to use spectrophotometry, spectrofluorimetry, different fluorescence polarization techniques, and Fourier-transform infrared spectroscopy (FT-IR) as delicate methods for a complex analysis of the physico-chemical nature of hapten-immunoglobulin interactions. A conventional fluorescent dye (FITC) was used as the antigen and a specific monoclonal antibody (anti-FITC IgG1) against this hapten molecule had been developed at our department earlier (14). Immunological recognition and the consequential physico-chemical changes in the antigen/hapten structure were studied by carrying out a comparative analysis of native and chemically cross-linked FITC molecules. The further aim of this study was to find theoretical explanations for the feature of strong molecular interactions between the antigen and antibody, which are thermodynamically equivalent to a covalent chemical bond, without a real chemical ligand formation (15).

Materials and Methods

Antigen:

Fluorescein-iso-thiocyanate (FITC, isomer I) was used as a hapten (Mw: 389.4, product of the Sigma Chemical Company, USA), and its interactions with a specific antibody were studied using spectrophotometry, different spectrofluorimetric methods, fluorescence polarization, and Fourier-transform infrared spectroscopic methods.

For the preparation of the standard antigen stock solution, 1 mg FITC was dissolved in 100 µl dimethyl-sulfoxide (DMSO, Sigma Chemical Company, USA), then diluted to 1 mg/ml concentration with PBS 0.15 M, pH 7.2 (phosphate buffered saline containing 5.4 mM Na2HPO4, 1.5 mM KH2PO4, 140 mM NaCl and 2.7 mM KCl). This stock solution was kept at 4 °C.

For the comparative analysis of free (native) FITC and the carrier cross-linked form, different protein molecules were labelled with FITC as bovine serum albumin (BSA, Sigma Chemical Company, USA), polyclonal anti-rat-IgG antibody (produced in sheep by our laboratory), and monoclonal mouse antibodies with IgG1 isotype (anti-FITC, anti-β hCG, anti-insulin produced by our department earlier). The FITC-labelling of proteins was carried out by following the method described (17). After protein labelling, the free, non-conjugated FITC

was removed from the reaction mixture by gel-filtration on a Sephadex G 25 FPLC column (Pharmacia, Sweden) equilibrated with PBS. Afterwards, the so-called conjugation rate – that is, the number of FITC molecules coupled onto one protein molecule – was determined semi-quantitatively by measuring the optical density of solutions of labelled proteins at 495 and 280 nm and by applying an empirical formula for the calculation:

$$X = \frac{2.87 * A_{495}}{A_{280} - 0.35 * A_{495}}$$

where x is the conjugation rate and A280 and A495 are the optical density of the solution measured at 280 and 495 nm, respectively (18).

The conjugation rate was 10.7 for FITC-BSA, 8.6 for FITC-anti-rat-(sheep) IgG, 12.4 for anti-FITC IgG1, 10.3 anti-βhCG, and 11.3 for anti-insulin IgG1 antibodies in our experiments.

Antibody:

The monoclonal anti-FITC antibody (mouse, IgG1) was developed at our department earlier (14). The mass of the antibody was produced by hybridoma fermentation using Harvestmouse (Serotec, UK) hollow-fibre fermenter and affinity-purified on a FITC-BSA-coupled Sepharose 4B column. The column was prepared as usual (16). In brief, 1.8 g of CNBr-activated Sepharose 4B (Pharmacia, Sweden) gel was suspended, swollen and washed five consecutive times in 50 ml 1 mM HCl. 100 mg BSA (Sigma Chemical Company, USA) was dissolved in 10 ml coupling buffer, that is 0.1 M $NaHCO_3$, pH 8.3, containing 0.5 M NaCl, and mixed with the gel. The mixture was being rotated end-over-end for two hours at room temperature. Following a thorough wash in the coupling buffer, the gel was left to react with 300 µg/ml FITC, generally following the FITC-labelling method described above (17). Afterwards, the reaction was stopped and all remaining active groups were blocked by washing in 50 ml 0.1 M pH 8 Tris-HCl buffer for two hours at room temperature. The gel was then washed in five cycles of alternating pH. Each cycle consisted of a wash with 0.1 M pH 8 acetate buffer containing 0.5 M NaCl. Following this washing procedure, the gel – adding up to 7 ml – was poured into a column and equilibrated with PBS containing 0.05% NaN_3.

The anti-FITC antibody was purified on the aforementioned column, thus ensuring that all antibody molecules would recognize the hapten selectively. 800 ml hybridoma supernatant was flown slowly through the column for 24 hours at 4 ˚C. The antibody was then eluted from the column with 0.1 M pH 2.5 glycine buffer. 1-ml fractions were collected and 100 µl 1 M pH 9 Tris-HCl was added instantly to each of them. Afterwards, the concentration was determined by measuring the optical density at 280 nm.

The purified monoclonal anti-FITC antibody was fragmented to Fab using papain as usual (19). The purified anti-FITC antibody was digested with papain in the presence of a reducing agent, cysteine. To determine optimal conditions, pilot fragmentation was carried out, and both the concentration of papain and the time of digestion were varied. After the pilot fragmentation, the fragments were dialyzed and analyzed by PhastSystem SDS-PAGE fast gel electrophoresis (Pharmacia-LKB, Sweden). Optimal conditions were determined according to the gel results. These conditions were used in the large-scale fragmentation of anti-FITC to anti-FITC Fab. 5 ml anti-FITC IgG1 monoclonal antibody (with a concentration of 2 mg/ml) was added to a freshly-mixed digestion buffer (PBS 0.15 M, pH 7.2, 0.02 M EDTA, 0.02 M cysteine), containing 0.1 mg/ml papain. The enzyme-antibody ratio was 1:20. The reaction mixture was well-mixed and incubated in a water bath at 37 ˚C. After six hours, the mixture was removed from the water bath, and 1 ml of 0.3 M iodoacetamide in PBS was added to stop the reaction. The reaction mixture was dialyzed against 2 litres PBS, pH 8.0, for 24 hours at 4 ˚C. The products were analyzed with Pharmacia's PhastSystem SDS-PAGE fast electrophoresis.

A 10 x 200 mm protein A-Sepharose CL-4B (Pharmacia, Sweden) column was made, and the

dialyzed reaction mixture was loaded onto it. Unbound fractions containing the Fab fragment and enzyme were collected and the column was washed with PBS to remove the Fab fragments completely. The mixture was concentrated to 5 ml. A 26 x 900 mm Sephacryl S-200 Superfine column (Pharmacia, Sweden) was made and the concentrated reaction mixture was loaded onto it. Fractions of 50 kD were collected and the purity of the final product was checked using 10% nonreducing SDS-polyacrylamide gel (Pharmacia's PhastSystem). The concentration of the Fab fragments was assessed at A280 and stored in borate buffer (0.015 M sodium borate, 0.15 M NaCl, pH 8.5) at 4 ˚C.

We used monoclonal anti-βhCG antibody (mouse, IgG1) as an isotype (negative) control, which had also been developed at our department earlier. The production, purification, labelling, and preparation of the Fab fragments were carried out as described in case of the anti-FITC IgG1 monoclonal antibody.

Spectrophoto- and fluorimetry, FT-IR spectroscopy:

In order to avoid the so-called "inner filter effect" (this phenomenon can be seen when a solution of a given compound is concentrated enough to absorb an already significant ratio of the exciting light beam, thus reducing light intensity at the centre of the cuvette where the emitted light is detected, consequently interfering with the results), prior to fluorimetric measurements, all samples were diluted in PBS 0.15 M pH 7.2 to a concentration at which the optical density of the solution measured at its absorption and emission peaks was below 0.05. This concentration was 50 ng/ml for free FITC, 5 µg/ml for FITC-BSA, 10 µg/ml for FITC-labelled anti-rat-IgG, and 10 µg/ml for monoclonal antibodies with IgG1 isotype.

Non-diluted protein concentrations were determined by measuring the optical density at 280 nm for all immunoglobulins and by using the dye-binding assay for BSA as described (20, 21).

Spectrophotometric measurements were performed on a UV/VIS photometer (DU-68, Beckman Instruments Inc., USA) using 2 x 10 mm quartz cuvettes, all at room temperature.

Some fluorescence-quenching measurements were done on a steady-state fluorimeter (Locarte, England), in cylindrical cuvettes of 3 mm in diameter, at room temperature. A 330 W Zn arc lamp was used as the excitation light source. 490 nm excitation wavelength was selected using the LF3 monochromatic filter. Emission was monitored through LF4 and LF7 cutoff filters and the 510-570 nm range was therefore selected.

The majority of steady-state and all spectrofluorimetric measurements were performed on a Hitachi-Perkin Elmer (MPF 4) spectrofluorimeter equipped with polarization filters and a thermostated cell holder in 10 x 10 mm quartz cuvettes operated in ratio mode, all at room temperature. The light source was a 300 W Xe arc lamp. Both excitation and emission wavelengths were set by monochromators and the precise values were dependent on the actual fluorescent solution. Slits were 4 and 8 nm, respectively.

Fluorescence polarization measurements were achieved on the Hitachi-Perkin Elmer (MPF 4) spectrofluorimeter. With each sample, four measurements of fluorescence intensity were taken using one pair of polarization filters. The first sample was taken using vertically polarized exciting light and detecting vertically polarized emitted light (Ivv), the second included vertical excitation and horizontal emission (Ivh), the third involved horizontal excitation and vertical emission (Ihv), and the fourth sample included horizontal excitation and horizontal emission (Ihh). Following these measurements, the fluorescence anisotropy of FITC or FITC-labelled proteins could be calculated using an appropriate equation (see below).

Fluorescence life span measurements were taken on an ISS multifrequency phase fluorimeter (ISS Fluorescence Instrumentation, Champaign, Illinois, USA) using the frequency cross-correlation method. A 300 W Xe arc lamp was used as the excitation light source. Excitation light intensity was modulated using a

double-crystal Pockel cell and a two-way polariser. A cross-correlation frequency of 80 Hz was used. The excitation wavelength was set to 493 nm and the emission was also monitored through a monochromator set to 512 or 522 nm. A freshly prepared glycogen (Sigma Chemical Co., USA) solution was used as a reference to correct the instrumental phase delay of the detection equipment. Ten sets of phase and modulation data were collected for each sample. Phase and modulation data were analyzed using the ISS 187 Decay Analysis Software.

Fluorescence anisotropy was calculated using the following equation:

$$r = \frac{(vv - vv_S) - G(vh - vh_S)}{(vv - vv_S) + 2G(vh - vh_S)}$$

where r is fluorescence anisotropy; vv and vh are the fluorescence intensity measured with polarization filters set vertically in the excitation and vertically or horizontally in the emission light beam, respectively; vvs and vhs are the fluorescence intensity of control (FITC) samples measured with polarization filters set vertically in the excitation and vertically or horizontally in the emission light beam, respectively; and G is a correction factor, which is calculated using the following equation:

$$G = \frac{hv - hv_S}{hh - hh_S}$$

where hh and hv are the fluorescence intensity measured with polarization filters set horizontally in the excitation and horizontally or vertically in the emission light beam, respectively; hhs and hvs are the fluorescence intensity of control (FITC) samples measured with polarization filters set horizontally in the excitation and horizontally or vertically in the emission light beam, respectively. (22, 23)

The Perrin equation was applied to analyze fluorescence anisotropy of a given fluorophore depending on its molecular microenvironment:

$$\frac{1}{r} = \frac{1}{r_0}\left(1 + \frac{\tau_F}{\tau_D}\right)$$

where r and r0 are anisotropy and so-called limit anisotropy – the anisotropy extrapolated to 0 K temperature; tF and tD are fluorescence lifetime and rotation correlation time (22, 23).

Fourier-transform infrared spectroscopy (FT-IR) measurements were taken on a Spectra 400 FT-IR spectrometer (Nicolet, USA). 1-mg samples were lyophilized for 24 hours in a Savant Speed Vac lyophilizer (Speed Vac Plus SC210A, Savant, USA). The lyophilized samples were desiccated further for 68 hours in a vacuum desiccator filled with silica crystals. 0.1-0.5 mg of the dehydrated samples were pastillized in KBr. The Fourier-transform infrared transmittance spectrum was measured at a range of 400-4000 cm-1 and studied with a 4 cm-1 resolution. During the investigations of samples, the IR spectra of water vapor, carbon dioxide, and water of potassium bromide were subtracted from the total numeric data before the assignation. The IR bands were identified according to data in the relevant literature (24, 25, 26, 27).

For the analysis of solvent polarity, acetone was used in different dilutions as a non-polar solvent. FITC was dissolved in DMSO, as usual, but afterwards it was diluted in mixtures of acetone and water in various ratios. These samples were measured in cuvettes covered with a lid to prevent the acetone from evaporating. The fluorescence intensity and light absorbency was detected in a thermostatic fluorimeter at 20 °C.

Florescent spectroscopic measurements were repeated from two up to ten times independently and the scattering between the results was under 3% in all cases.

Results

The basic finding was that FITC fluorescence intensity definitely suffers from a fluorescence-quenching effect following pre-incubation with our anti-FITC IgG1 monoclonal antibody (12). Similar observations were made in case of using polyclonal and monoclonal (high affinity IgM) antibodies against FITC (9, 28, 29). Our model permits kinetic studies with different fluorescent

and infrared spectroscopic measurements by the advantageous structure of the mouse IgG1 molecule and its Fab fragment. During the optimization of fluorescence quenching measurements, FITC with anti-FITC antibody were incubated together for 1 - 10 minutes at room temperature in order to let the equilibrium be established, and then the fluorescence intensity of the reaction mixture was quantified. A trial to measure the time needed for anti-FITC to fully achieve its fluorescence-quenching effect was performed. We added a suitable amount of anti-FITC to a cuvette with the FITC solution already inside the fluorimeter and tried to monitor the decline of fluorescence intensity – with the results verifying our assumptions, since there was an instant quenching of fluorescence. According to our pilot study, the optimum incubation time for maximum fluorescence quenching caused by the anti-FITC monoclonal antibody was 10 minutes. No similar fluorescence-quenching effects were found when FITC was preincubated by non-specific monoclonal antibodies with the same isotypes.

We found total (100%) inhibition of FITC fluorescence intensity induced by both anti-FITC monoclonal antibody and its Fab fragment (Figure 1).

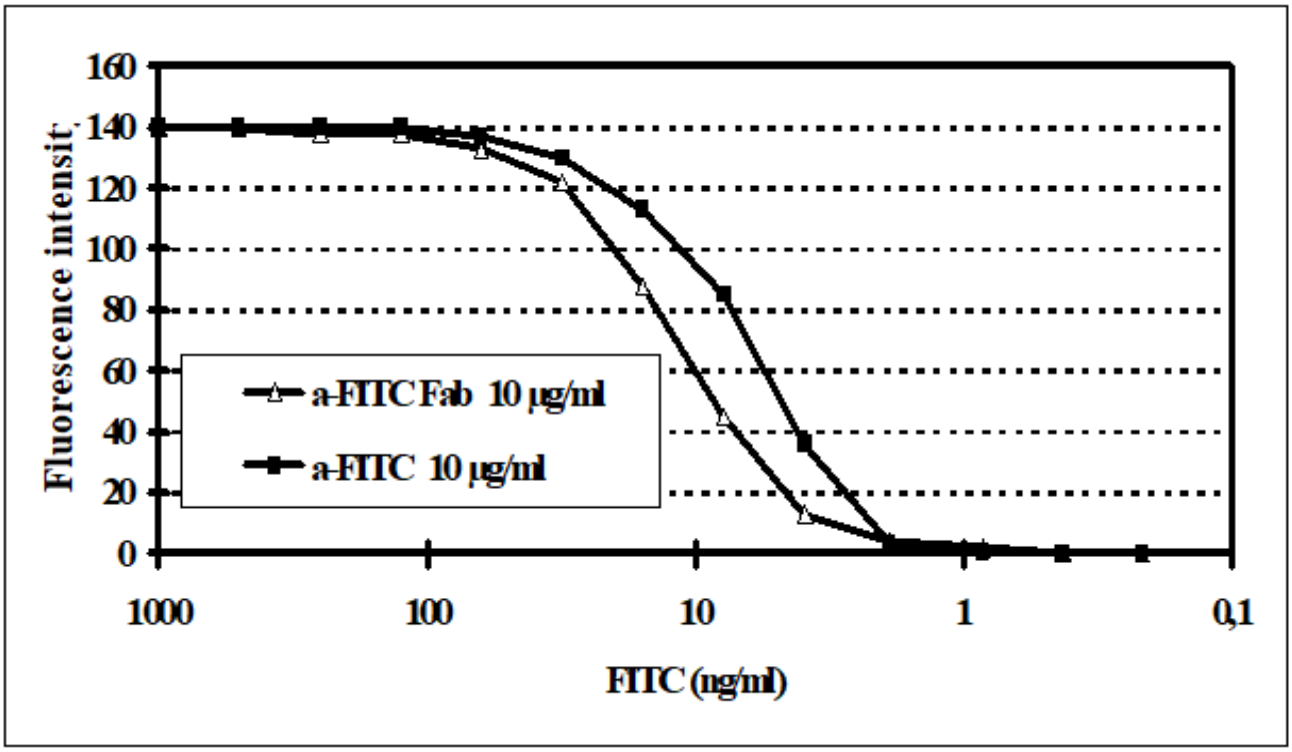

Figure 1. FITC fluorescence quenching by anti-FITC monoclonal antibody and its Fab fragment. Fluorescence intensity presented in relative units of the fluorimeter. Excitation and emission wavelengths were set to 493 and 512 nm. Measurements were taken at pH 7.2 at 21 °C. The figure demonstrates data of one typical measurement. Scattering between five independent assays was under 3%.

In the figure, we demonstrated two separate curves of fluorescence intensity – one for 10 µg/ml anti-FITC antibody and the other for 10 µg/ml anti-FITC Fab – against the concentration of FITC. It is striking that at 15 ng/ml FITC concentration, the fluorescence was quenched by 50% already in the case of anti-FITC Fab. The fluorescence was quenched by 50% in case of anti-FITC at around 5 ng/ml FITC concentration. At the equal paratope and hapten ratio (when the absolute number of hapten molecules theoretically equals the binding sites of the antibody molecules) , total (100%) quenching of fluorescence occurred. At a higher hapten concentration – over 200 ng/ml – a slight inner-filter effect can be seen at the beginning of the

curve. At about the threshold concentration of fluorophore (that is, when the optical density of the solution measured at its excitation peak equals 0.05), the partial quenching effect of a few anti-FITC molecules causes the same phenomenon as dilution. In spite of the lesser quantity of fluorescent compound actually emitting, the fluorescence intensity virtually enhances. Afterwards, with the addition of more antibody, the fluorescence intensity declines quickly to total quenching of fluorescence. This occurs at different hapten and paratope molecular ratios, depending on their total concentration, which is deductible from the law of mass action.

In the following phase of our study, we tried to analyze how this non-covalent molecular interaction – an immune bond – can modify the physico-chemical properties of an antigen molecule to such a fundamental degree.

In general, when the fluorescence intensity of a given fluorescent molecule decreases because of interaction with another molecule, the first interpretation that emerges is spectral shift. We investigated this possibility too, but found no remarkable spectral change if FITC molecules were bound chemically onto the surface of different protein carriers (Figure 2).

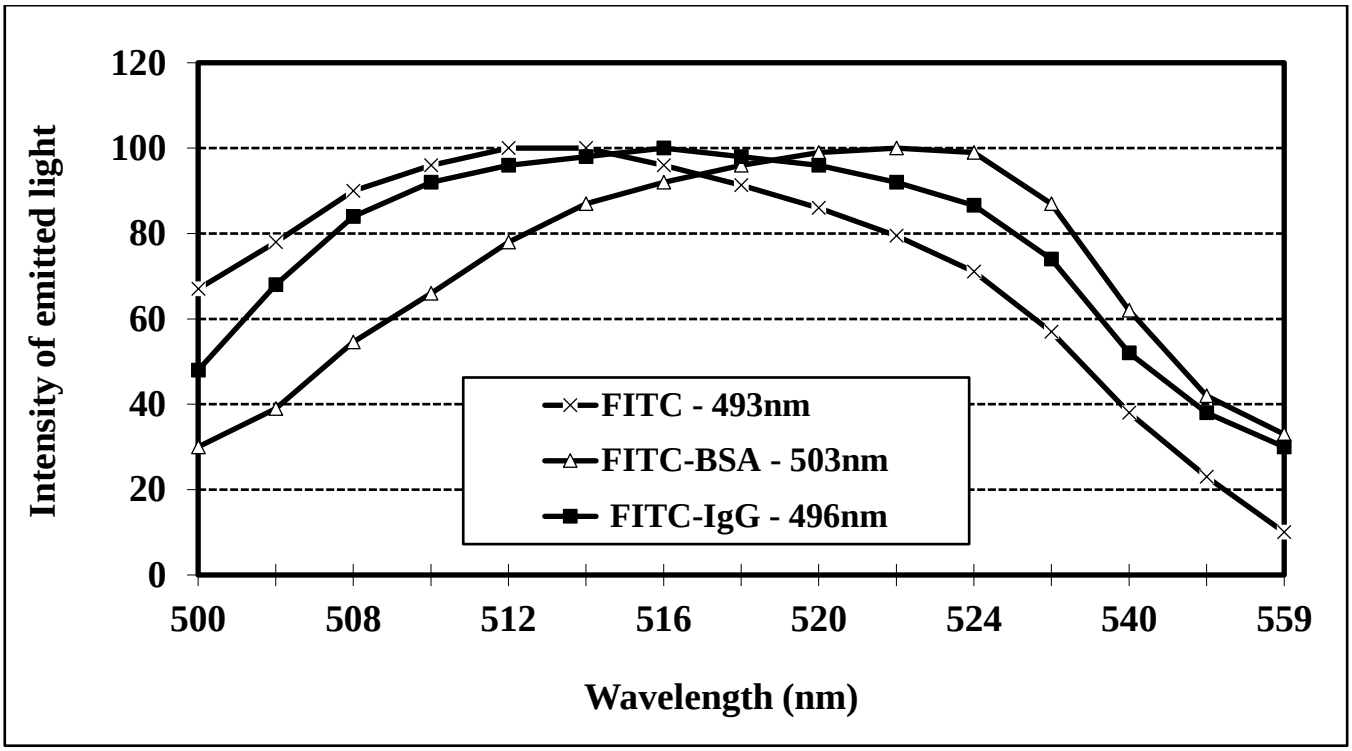

Figure 2. Emission spectrum of FITC covalently bound onto different protein molecules. Excitation wavelengths were set to 493 nm for free FITC, 503 nm for FITC-BSA, 496 nm for FITC-IgG1. Measurements were taken at pH 7.2 at 21 °C. Scattering between three independent measurements was under 5%.

Since covalent binding onto the surface of such big molecules as immunoglobulins or albumin (BSA) did not result in any spectral-shift bigger than 10 nm, it is hard to uphold the assumption that a simple, non-covalent molecular association between the small fluorophore and a relatively big partner molecule (a specific antibody in our model) causes fluorescence quenching. This result suggests that the mechanism of fluorescence quenching caused by anti-FITC monoclonal antibody is different from the covalent chemical binding, because it must be the unique nature of a specific immune bond that causes quenching.

To find a better explanation for this phenomenon, we compared the molecular movement and rotational freedom of free FITC

with FITC molecules covalently bonded to proteins, or with immunologically bonded FITC by anti-FITC or its Fab fragment using fluorescence polarization measurements. Results of these measurements showed further fundamental differences in the physico-chemical nature of covalent (chemical) and non-covalent (immunological) bonds. Using this technique, we were able to quantitatively detect the slightest changes in the rotation and/or flexibility of fluorophore molecules if they were limited in any way by any other molecule. The results of our fluorescent polarization measurements are presented in Figure 3.

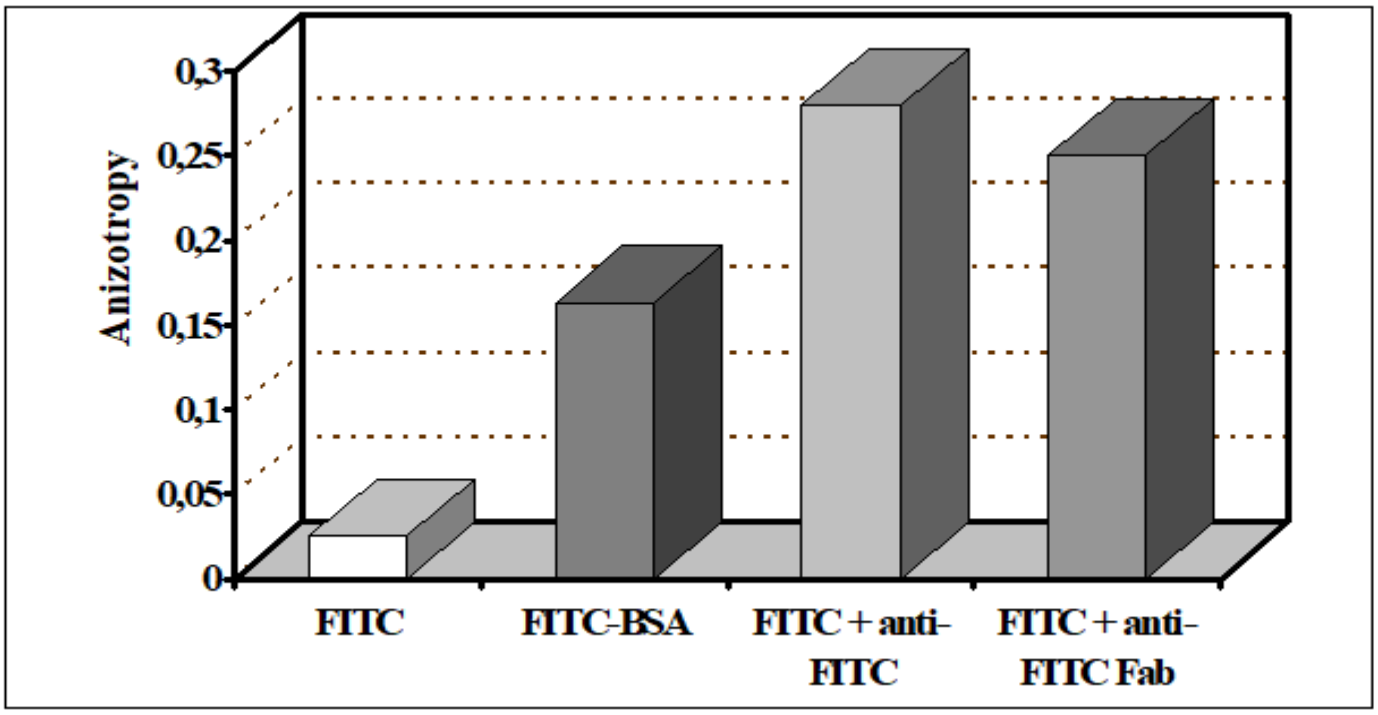

Figure 3. Fluorescence anisotropy of free FITC and FITC bound to proteins chemically or bound by anti-FITC and anti-FITC Fab. Excitation wavelengths were set to 493 nm for FITC, 503 nm for FITC-BSA, 496 nm for FITC-IgG1 and FITC-Fab, while the emission wavelengths were 512 nm for FITC, 522 nm for FITC-BSA, and 515 nm for FITC-IgG1 and FITC-Fab. Measurements were taken at pH 7.2 at 21 °C. The figure demonstrates summarized data of five independent measurements. Scattering was under 3%.

According to the Perrin equation, fluorescence anisotropy of a given fluorophore depends on its molecular microenvironment. This equation says that the bigger the anisotropy, the shorter fluorescence lifetime and the longer rotation correlation. In other words, an increase in anisotropy means that a fluorophore can transmit the energy it absorbs to another molecule in a very short time. This occurs because there is a very close association between the two molecules, which in some cases leads to instant channelling of absorbed energy from the fluorophore to the other molecule; moreover, this interaction can almost totally block the rotation of the little fluorescent molecule.

Based on this equation, we can draw basic conclusions concerning the molecular interactions demonstrated in Figure 3. The free movement and rotation of FITC molecules gets partially restricted after conjugation with higher molecular weight carrier proteins, such as BSA, or an indifferent, mouse IgG, characterized by increased anisotropy. However, the molecular movement of FITC is definitely inhibited after the incubation with specific anti-FITC monoclonal antibody. Immunological binding has a much more dramatic effect on FITC rotation and energy transfer than covalent chemical binding to indifferent proteins, including immunoglobulins with the same isotype (IgG1) the molecules have. The anisotropy was 100% higher in case of immunocomplexes formed by

FITC and anti-FITC (or anti-FITC Fab) than in case of covalent binding to the same isotype (IgG1) the molecule has. Anisotropy difference of only 5% was measured between the whole anti-FITC IgG1 and their Fab fragment during the formation of immunocomplexes with free FITC.

Another proof of a specific molecular movement-inhibiting, "rigidizing" effect of immune binding compared to that of covalent, chemical binding came from fluorescence lifetime measurements. These data are demonstrated in Figure 4.

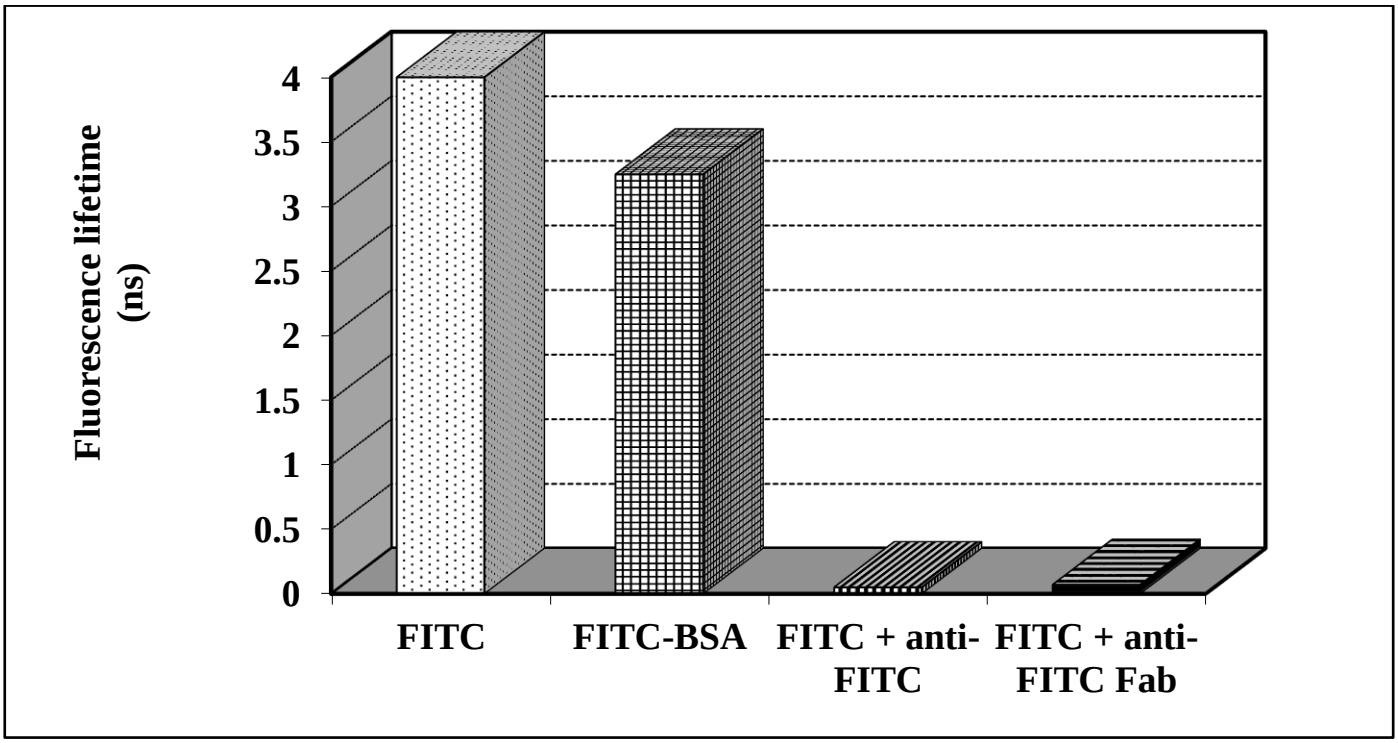

Figure 4. Fluorescence lifetime of free FITC and FITC bound to BSA, bound by anti-FITC IgG1 and anti-FITC Fab. Excitation wavelengths were set to 493 nm for FITC, 503 nm for FITC-BSA, 496 nm for FITC-IgG1 and FITC-Fab. Measurements were taken at pH 7.2 at 21 C. The figure demonstrates summarized data of five independent measurement. Scattering was under 3%.

Fluorescence lifetime gives us valuable information on the milieu surrounding the fluorophore molecule. The shorter the life spans, the quicker the energy transfer between the fluorescent molecule and its environment – that is, the interaction between the two molecules is stronger. It is very well demonstrated that lifetime is greatly affected by the milieu: FITC in PBS has a lifetime of about 4 ns, while BSA-coupled or IgG1-coupled FITC has a bit shorter lifetime, but on the same scale. We practically cannot measure the lifetime of FITC in FITC–anti-FITC (or FITC–anti-FITC Fab) complexes, which is not surprising, since there is practically no fluorescence signal because of quenching. The lifetime of FITC measured was about 4 ns when there was free unbound FITC in the reaction mixture. However, when anti-FITC immunoglobulins or their Fab fragments consumed all free FITC molecules, together they formed a so-called "dark complex". This meant there was no measurable fluorescence signal, so we could determine that lifetime equalled zero.

The "rigidization" of FITC molecules by immunobinding to anti-FITC IgG1, characterized by increased anisotropy and a shorter fluorescence lifetime, is a really striking phenomenon. However, this "high affinity interaction and energy transfer" theory simply cannot explain another astonishing finding that light absorption of FITC is similarly affected – inhibited – by anti-FITC as its fluorescence intensity. This is presented in Figure 5.

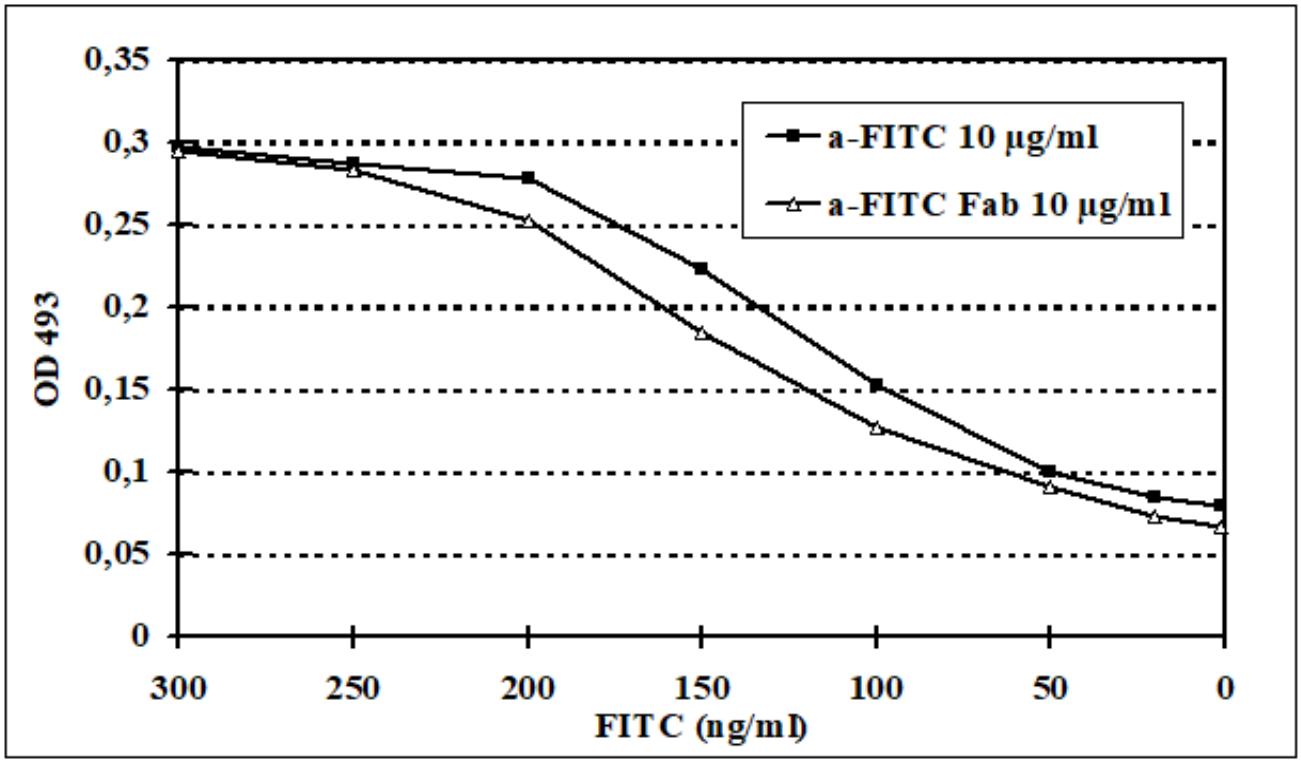

Figure 5. Light absorption of immunocomplexes formed by anti-FITC IgG1 and anti-FITC Fab plotted against the concentration of FITC. Excitation wavelengths were set to 493 nm. Measurements were taken at pH 7.2 at 21 C. Scattering between two independent measurements was under 2%.

Based on these data, it can be said that both fluorescence intensity and light absorption are greatly decreased by anti-FITC IgG1 or its Fab fragment. While the energy transfer from the excited fluorophore molecule can really be responsible for the decreased fluorescence intensity, it cannot explain light absorption at all. No remarkable differences were found between the whole immunoglobulin IgG1 (molecular weight is approximately 150 kD) and its Fab fragment (approximate molecular weight is 45 kD). We did not find any spectral shift caused by anti-FITC monoclonal IgG1 antibody or Fab fragments.

The difference between polar and non-polar microenvironment was analyzed. Figure 6 demonstrates the effect of acetone as a non-polar solvent on FITC fluorescence.

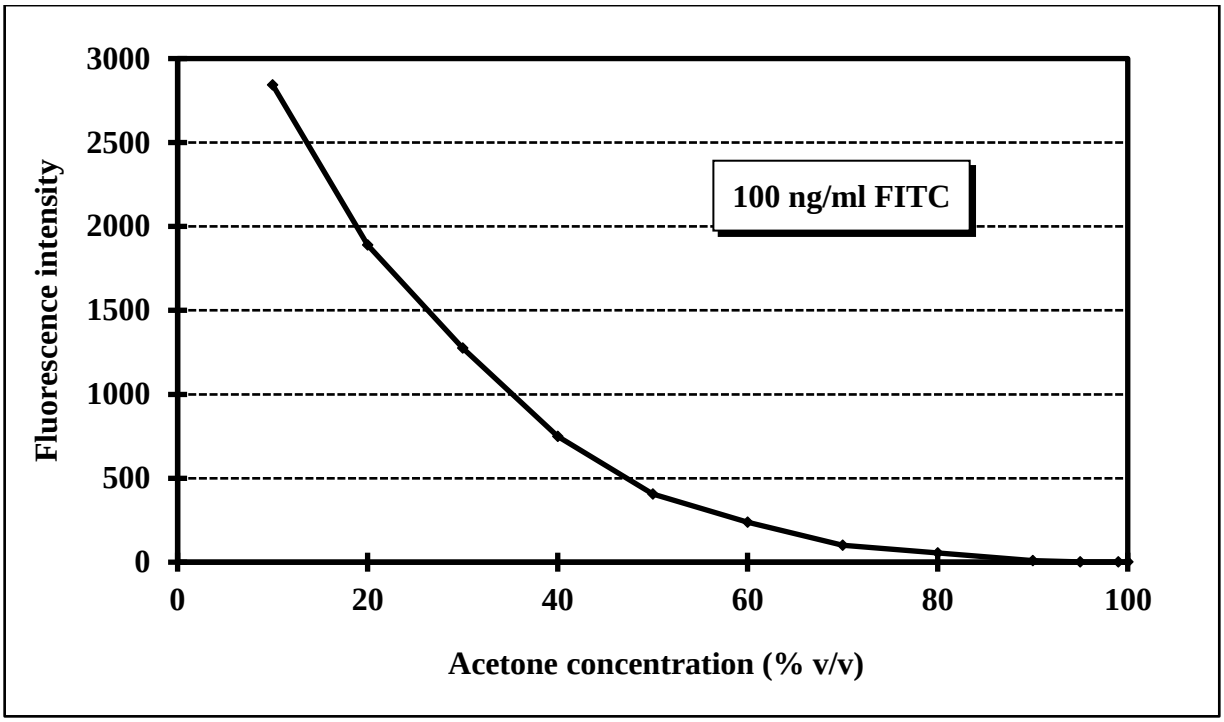

Figure 6. Fluorescence intensity of FITC dissolved in mixtures of acetone and water plotted against the concentration of acetone. Excitation and emission wavelengths were set to 493 and 512 nm, respectively. Fluorescence intensity presented in relative units of the fluorimeter. Measurements were taken at pH 7.2 at 21 C. The figure shows a typical curve. Scattering between three parallel measurements was under 2%.

The data clearly show that acetone has a similar decreasing effect on FITC fluorescence as immunobinding by anti-FITC IgG1 monoclonal antibody.

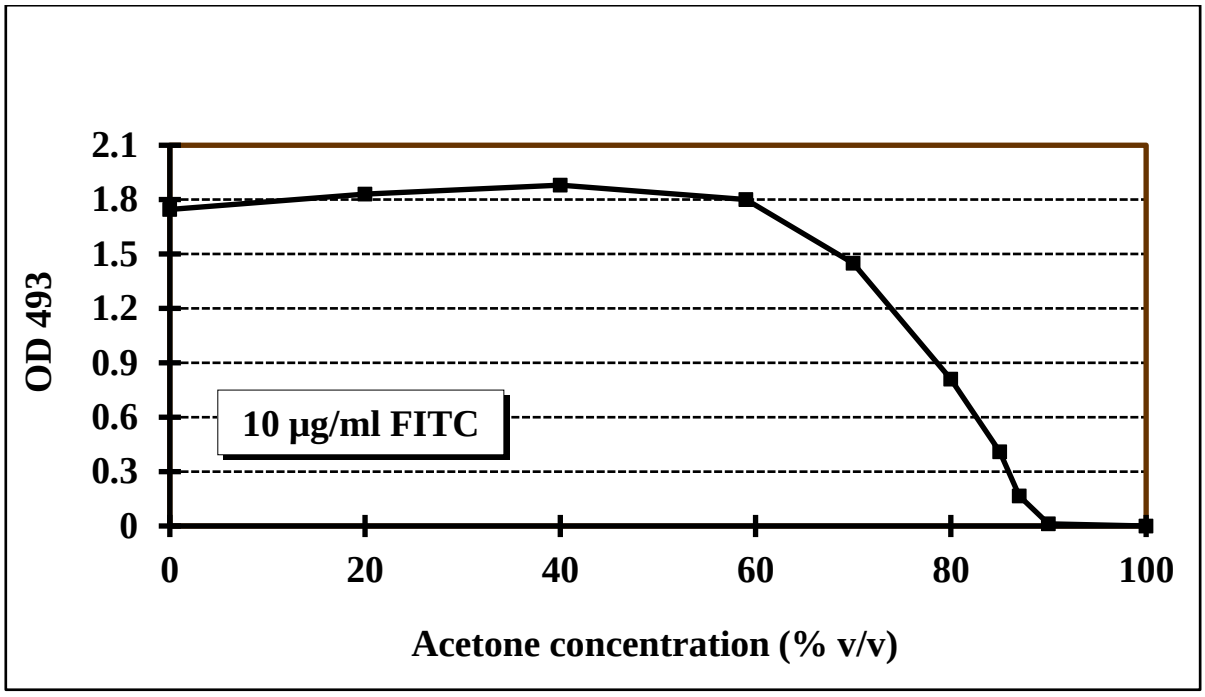

Figure 7. Light absorption of FITC in mixtures of acetone and PBS measured at 493 nm plotted against the concentration of acetone. Measurements were taken at pH 7.2 at 21 C. The figure shows a typical curve. Scattering between three parallel measurements was under 2%.

Table I. Spectrum assignation

FITC		
Position	**Intensity**	**Assignment**
682,303	56,020	C=C
728,317	72,842	=CH
761,780	67,621	=CH
855,877	43,726	=CH
1462,625	33,307	CC_{Ar}
1487,071	54,354	CC_{Ar}
1534,027	35,647	CC_{Ar}
1596,729	13,929	CC_{Ar}
1642,077	65,418	CO
2033,843	36,576	$_{as}N=C=S$
3052,083	80,938	=CH
3071,663	80,675	=CH
Anti-FITC (IgG1) FITC immunocomplex		
Position	**Intensity**	**Assignment**
1332,642	78,635	Amid III
1410,816	65,668	$_{s}CO_2^-$, zwitter-ion
1441,279	81,034	$C=C_{Ar}$*
1508,936	73,703	Amid II, $_{s}NH_3^+$
1632,279	41,895	Amid I, $_{as}NH_3^+$, NH_2 flodsheet
2037,691	86,476	NH_3^+
2964,388	79,044	Aliphatic CH
3069,372	71,81	OH, humidity
3426,762	62,718	OH, humidity
Anti-FITC (IgG1)		
Position	**Intensity**	**Assignment**
1333,148	76,502	Amid III
1411,488	62,640	$_{s}CO_2^-$, zwitter-ion
1508,429	69,217	Amid II, $_{s}NH_3^+$
1632,578	44,031	Amid I, $_{as}NH_3^+$, NH_2 flodsheet
2037,599	84,468	NH_3^+
2964,737	71,120	Aliphatic CH
3090,425	62,214	OH, humidity
3236,178	68,515	OH, humidity
Anti FITC (IgG1) FITC covalent binding (FITC labbeled IgG1)		
Position	**Intensity**	**Assignment**
1289,048	92,069	Amid III
1411,747	86,795	$_{s}CO_2^-$, zwitter-ion
1459,746	86,069	$C=C_{Ar}$*
1510,120	83,004	Amid II, $_{s}NH_3^+$
1534,883	83,579	$C=C_{Ar}$*
1648,909	82,896	Amid I, $_{as}NH_3^+$, NH_2, disorganized protein sequences
1656,884	82,505	Amid I, $_{as}NH_3^+$, NH_2 helix, CO*
2036,716	89,831	NH_3^+
2933,257	96,469	Aliphatic CH
3355,729	93,908	OH, OH, humidity

*FITC

Fluorescence quenching increases proportionally to the concentration of acetone and total (100 %) quenching of fluorescence occurs at 96 % acetone concentration (v/v), when FITC molecules practically have no hydrate wrap. Moreover, the same phenomenon can be observed with respect to light absorption (Figure 7).

Infrared spectroscopy can analyze more precisely the molecular connections between the antigen and antibody structures, including the influence of the microenvironment. According to our Fourier-transform infrared (FT-IR) spectroscopic measurements in case of covalent binding peak 2033 cm-1 of FITC's N-C-S group (which is the covalent binding region) showed remarkable changes; it disappeared. Only the peak 2036 cm-1 of anti-FITC's NH_3^+ groups was present. Figure 8 demonstrates the FT-IR spectrum of free FITC.

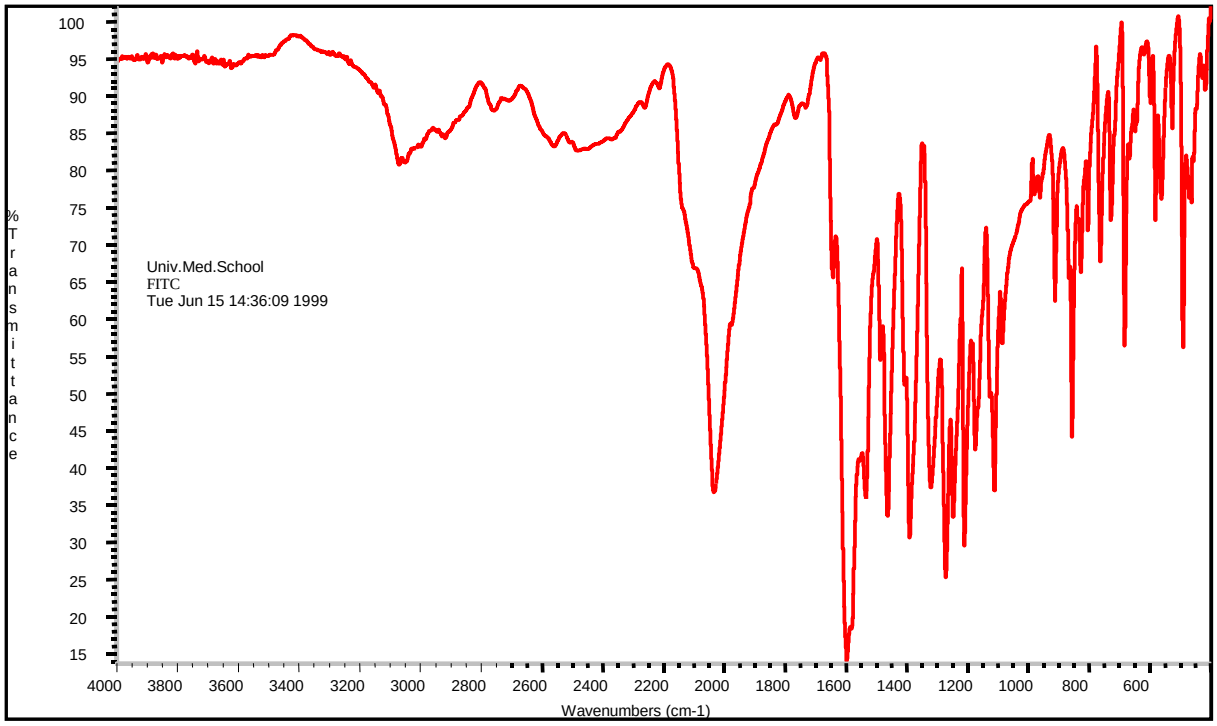

Figure 8. Fourier-transform infrared spectra of free FITC molecules. The 0.2 mg sample was pastillized in KBr at a range of 400-4000 cm-1 and studied with a 4 cm-1 resolution. The details of peak assignations are presented in Table I.

Figure 9 shows the spectrum of free anti-FITC IgG1, and Figure 10 shows the spectrum of FITC covalently bound to monoclonal anti-FITC IgG1.

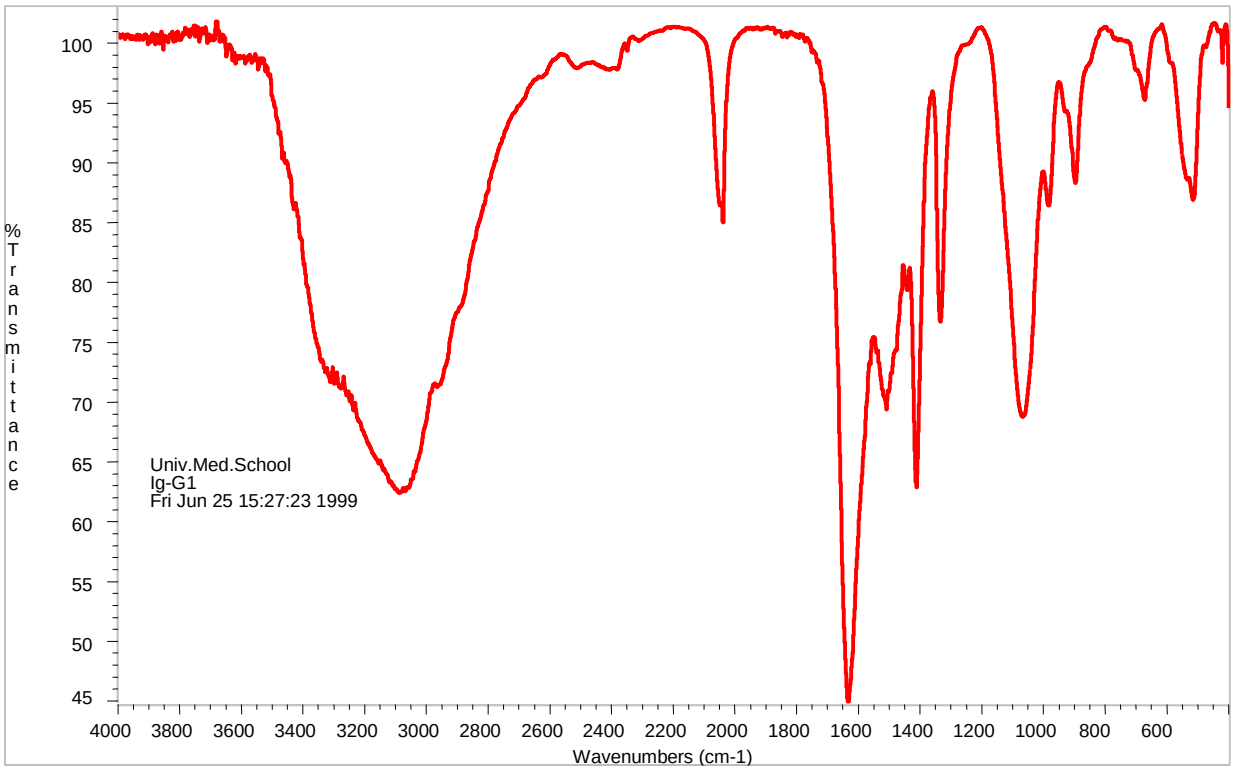

Figure 9. Fourier-transform infrared spectra of anti-FITC IgG1 monoclonal antibody molecules. The 0.5 mg sample was pastillized in KBr at a range of 400-4000 cm-1 and studied with a 4 cm-1 resolution. The details of peak assignations are presented in Table I.

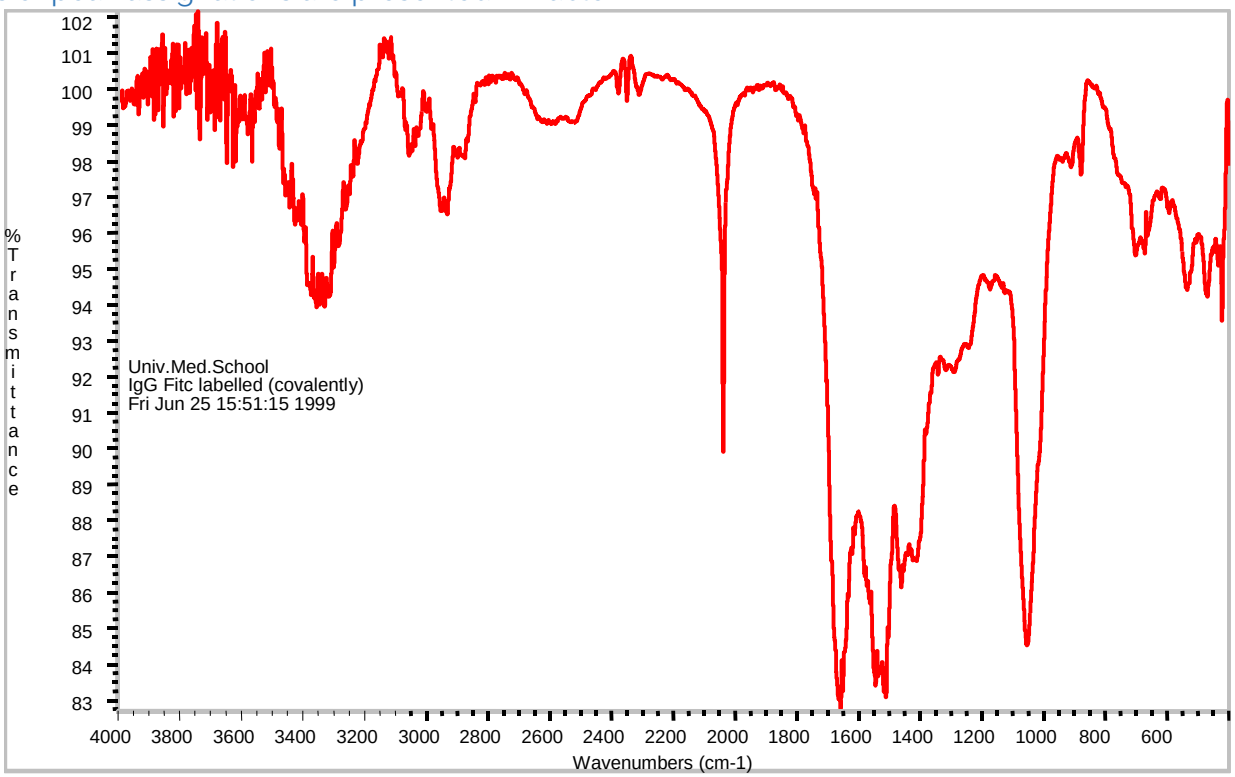

Figure 10. Fourier-transform infrared spectra of IgG1 monoclonal antibody covalently labelled by FITC. The 0.5 mg sample was pastillized in KBr at a range of 400-4000 cm-1 and studied with a 4 cm-1 resolution. The details of peak assignations are presented in Table I. Major characteristics of native FITC and IgG1 molecules can be found in the spectrum of the complex.

Specific binding sites of the anti-FITC IgG1 were blocked before and during the covalent FITC-labelling. The spectrum contains characteristic peaks of both FITC and anti-FITC IgG1. The peaks of poly-aromatic cyclical structures (responsible for fluorescence of FITC molecules) added to the peaks of the anti-FITC IgG1 molecule: peaks 1459 cm-1 and 1534 cm-1 were clearly shown and peak 1642 cm-1 shifted and added to anti-FITC's 1656 cm-1 peak. In case of covalent binding, we did not find hydrophobic interactions between the antigen and antibody molecules: the anti-FITC IgG1's 3236 cm-1 OH peak shifted to 3355 cm-1. In case of immunobinding between the FITC and anti-FITC IgG1, the antigen's N-C-S group was assigned to peak 2033 cm-1, that is, the covalent binding region of FITC. The peak 2033 cm-1 showed no remarkable changes during antigen-antibody reactions, but only shifted and added to the peak 2037 cm-1 of NH_3^+ groups on antibodies. The polyaromatic cyclical structure, which is responsible for fluorescence, showed significant physico-chemical changes: peaks from 1462 cm-1 to 1642 cm-1 disappeared and/or shifted to 1441 cm-1. However, hydrophobic interactions were detected between the antigen and antibody molecules: the antibody's 3090 cm-1 and 3236 cm-1 peaks of OH groups shifted to 3069 cm-1 and 3426 cm-1, and their transmittance decreased (Figure 11).

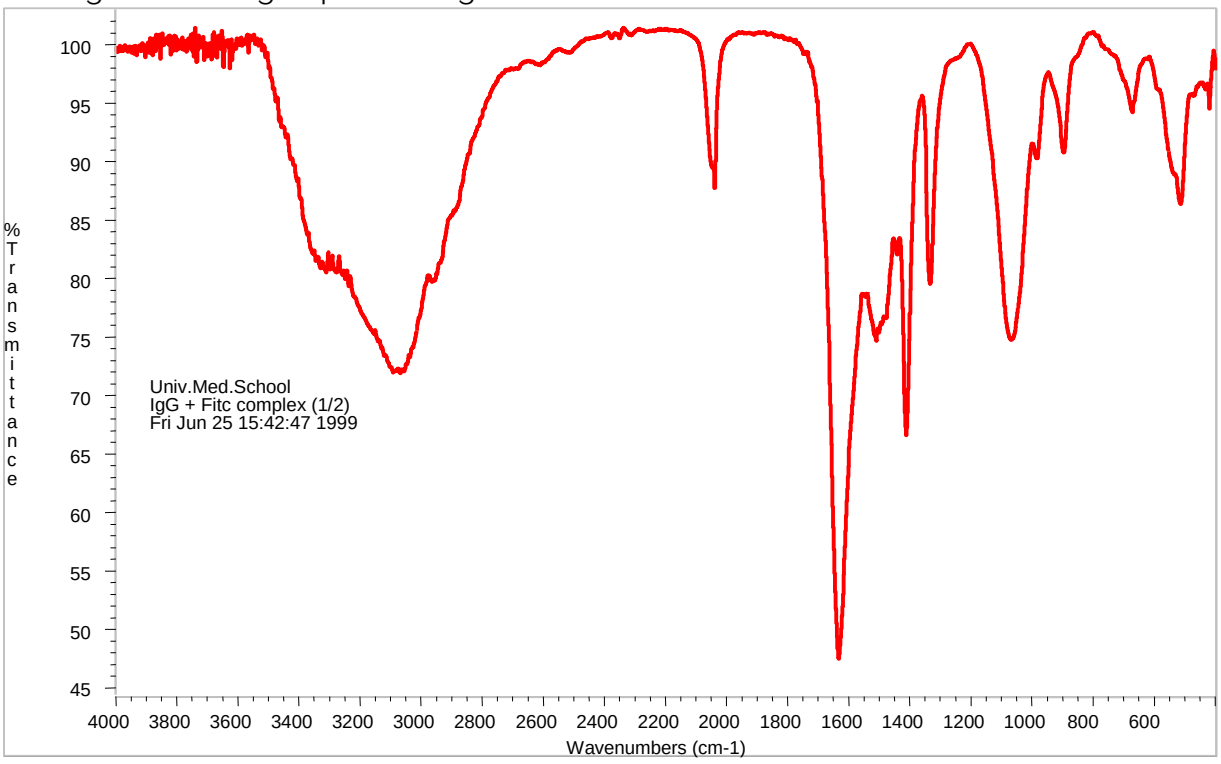

Figure 11. Fourier-transform infrared spectra of immunocomplexes formed by FITC and anti-FITC IgG1. The 0.2 mg sample was pastillized in KBr at a range of 400-4000 cm-1 and studied with a 4 cm-1 resolution. The details of peak assignations are presented in Table I. No polyaromatic peaks of FITC were found (1400-1600 cm-1) and peaks of OH groups of free anti-FITC IgG1 (3000-3400 cm-1) changed remarkably in the immunocomplex.

Discussion

Our conclusion is that immunobinding itself can modify the electron cloud of antigens so dramatically that they could not exhibit the same electrostatic structures anymore. We concluded that this extreme structural modification results from making it impossible for the FITC molecule to get in contact with water. It has been known for a long time that solvents have a basic influence on the fluorescence of fluorescent compounds (30, 31). Considering this, we suspected that this phenomenon is caused by

the lack of water in the microenvironment of FITC bound by anti-FITC IgG1. We tried to model water exclusion by using non-polar solvents for making our samples. The spectral shifts and fluorescence quenching in different acetone (organic solvent) and water mixtures reflect a general effect on the hydrogen-bonding environment of the FITC through water-acetone hydrogen bridges and specific effects due to direct FITC -acetone hydrogen bonding. By increasing acetone concentrations, the FITC-water connections change to FITC-acetone interactions, resulting in basic modifications of hydrogen bonds due to fluorescence quenching. Both the absorption spectra and fluorescence properties (quenching) appear to be dominated by increasing hydrophobicity, indicating that the spectral shifts of the FITC can be used as an indicator of its hydrogen-bonding environment. Application of fluorescein as a probe of hydrogen bonding in the microenvironment immediately surrounding the fluorophore illustrated the effect with reference to the fluorescein-anti-fluorescein antibody complex (30). This finding fits well in our results (as demonstrated in Figure 2, Figure 6, and Figure 7), where it appears that binding sites of our anti-FITC monoclonal antibody and the recognized antigen (FITC) are increasingly dehydrated and become hydrophobic during the immunocomplex formation.

Hydrophobic interactions between the antigen and antibody molecules seem to be essential in the physico-chemical event of antigen-antibody reaction, which is supported both by our fluorescent spectroscopic and fluorescent polarization measurements and other data from the relevant literature (15, 23, 30, 31). Our model experiment, involving non-polar solvent and water mixtures, supported our hypothesis about the importance of hydrophobic interactions in the stabilization of the antigen-antibody ligands. However, further experimental evidence is needed.

The results of the infrared spectroscopic analysis can prove the hydrophobic nature of immunobinding between anti-FITC and FITC. This hydrophobic interaction also perturbed the electron cloud of the polyaromatic cyclical structure. These results can also prove the quenching effect caused by anti-FITC monoclonal antibody.

Our fluorescent and infrared spectroscopic data suggest that the hydrophobic connections not only participate in the stabilization of antigen-antibody complexes, but also modify the physico-chemical nature of participating molecules.

The main ligand-induced conformational changes on the immunoglobulin molecules causing a basic modification of their functions are well-known. However, the same physico-chemical influences on the fine structure of antigens have been less analyzed so far due to technical difficulties (9, 10, 11).

In the original FITC – anti-FITC model, the fluorescence-quenching effect was observed during antigen-antibody reactions (9, 32). The fluorescent activity of FITC molecules as antigens in this model system seems to be beneficial for studying fine structural changes in the antigen after binding with a specific immunoglobulin (9, 33).

Using fluorochrome-labelled anti-idiotypic antibodies and fluorescent spectroscopic measurements, experimental data published suggest the importance of water molecules in the ligand formation (2). Our data, together with previous findings, help understand the molecular dynamics of immunobinding (2, 3, 7). The immunocomplex formed by hydrophobic regions of a specific epitope on the antigen and the recognition part on the antibody molecule stabilized with the surrounding hydrate shell seems to be thermodynamically strong enough for stable molecular binding without a covalent chemical interaction (34, 35).

In our model, direct observations were possible for the physico-chemical changes on the bound antigen because the quenching effect of FITC fluorescence during the immunocomplex formation was analyzed by different and relevant spectroscopic techniques. Our pre-sent fluorescent polarization and infrared spectroscopic measurements reflect a local decrease in the hydration degree in the

submolecular area of a specific ligand between the small antigen (hapten) molecule and the hypervariable region of IgG. This "exclusion" of water molecules from the binding surfaces occurs due to a dramatic modification of the molecular microenvironment. Changes in hydration can influence the functions of the immunoglobulins and the physico-chemical appearance of the antigen at the same time (36). Participation of antigens in immunocomplex formation can cause altered immunoreactivity in further physiological and pathological immune reactions.

Acknowledgement. This paper is a product of our long scientific discussions with Professor Béla Somogyi†. I am grateful for his suggestions and technical help. Many thanks to Gergely Nagy for the initial fluorimetric measurements, to Professor Miklós Nyitrai for the analysis and discussion of the results of fluorescence polarization measurements, and to Dr. Tamás Lóránd for the infrared spectroscopy measurements and their evaluation.

Disclosure

Funding. This paper was realized with the financial support of the University of Pécs, Medical School (Pécs, Hungary), and the following grants: the National Science Foundation of Hungary (OTKA T020661), National Committee for Technical Development of Hungary (OMFB 95-97-48-1028), and by Health Science Committee of Hungary (ETT -06 401/96).

Transparency declaration: We declare that we have no commercial or potential competing interests or any financial and personal relationships with other people or organizations that could inappropriately influence our network.

Conflict of interest: none declared.

References

1. Davies DR, Padlan EA, Sheriff S. Antibody-antigen complexes. Annu Rev Biochem. 1990;59:439-73. doi: 10.1146/annurev.bi.59.070190.002255.

2. Weidner KM, Denzin LK, Voss EW Jr. Molecular stabilization effects of interactions between anti-metatype antibodies and liganded antibody. J Biol Chem. 1992 May 25;267(15):10281-8.

3. Wilson IA, Stanfield RL. Antibody-antigen interactions: new structures and new conformational changes. Curr Opin Struct Biol. 1994 Dec;4(6):857-67. doi: 10.1016/0959-440x(94)90267-4.

4. Edmundson AB, Guddat LW, Shan L, Fan ZC, Hanson BL. Structural aspects of conformational changes in ligand binding by antibody fragments. Res Immunol. 1994 Jan;145(1):56-61. doi: 10.1016/s0923-2494(94)80045-6.

5. Dyson HJ, Wright PE. Antigenic peptides. FASEB J. 1995 Jan;9(1):37-42. doi: 10.1096/fasebj.9.1.7821757.

6. Haaijman JJ, Coolen J, Kröse CJ, Pronk GJ, Ming ZF. Fluorescein and tetramethyl rhodamine as haptens in enzyme immunohistochemistry. Histochemistry. 1986;84(4-6):363-70. doi: 10.1007/BF00482964.

7. Bhat TN, Bentley GA, Boulot G, Greene MI, Tello D, Dall'Acqua W, Souchon H, Schwarz FP, Mariuzza RA, Poljak RJ. Bound water molecules and conformational stabilization help mediate an antigen-antibody association. Proc Natl Acad Sci U S A. 1994 Feb 1;91(3):1089-93. doi: 10.1073/pnas.91.3.1089.

8. Laver WG, Air GM, Webster RG, Smith-Gill SJ. Epitopes on protein antigens: misconceptions and realities. Cell. 1990 May 18;61(4):553-6. doi: 10.1016/0092-8674(90)90464-p. Erratum in: Cell 1990 Aug 10;62(3):following 608

9. Mummert ME, Voss EW Jr. Effects of secondary forces on the ligand binding properties and variable domain conformations of a monoclonal anti-fluorescyl antibody. Mol Immunol. 1996 Sep;33(13):1067-77. doi: 10.1016/s0161-5890(96)00066-1.

10. Roterman I, Konieczny L. Geometrical analysis of structural changes in immunoglobulin domains' transition from native to molten state. Comput Chem. 1995 Sep;19(3):247-52. doi: 10.1016/0097-8485(95)00003-b.

11. Braden BC, Goldman ER, Mariuzza RA, Poljak RJ. Anatomy of an antibody molecule: structure, kinetics, thermodynamics and mutational studies of the antilysozyme antibody D1.3. Immunol Rev. 1998 Jun;163:45-57. doi: 10.1111/j.1600-065x.1998.tb01187.x.

12. Nemeth P, Horvath G., Balogh P. Hapten-immunoglobulin molecular interaction analysed in a FITC - anti-FITC model. 1994. 12th European Immunology Meeting, Barcelona (Abstr. No.: W13/29)

13. Herron JN, Kranz DM, Jameson DM, Voss EW Jr. Thermodynamic properties of ligand binding by monoclonal anti-fluorescyl antibodies. Biochemistry. 1986 Aug 12;25(16):4602-9. doi: 10.1021/bi00364a022.

14. Balogh P, Szekeres G, Németh P. Hapten-mediated identification of cell membrane antigens using an anti-FITC monoclonal antibody. J Immunol Methods. 1994 Feb 28;169(1):35-40. doi: 10.1016/0022-1759(94)90122-8.

15. Li Z, He Y, Wong L, Li J. Progressive dry-core-wet-rim hydration trend in a nested-ring topology of protein binding interfaces. BMC Bioinformatics. 2012 Mar 27;13:51. doi: 10.1186/1471-2105-13-51.

16. Lane D (ed.). Antibodies: A laboratory Manual. 2nd Edition. Cold Spring harbor N.Y: Cold Spring Harbor Press; 1988.

17. Mason DW, Penhale WJ, Sedgwick JD. Preparation of lymphocyte subpopulations. In: Klaus GB (ed), Lymphocytes: A Practical Approach. Oxford: IRL Press, 1987; p. 35.

18. Jobbágy A, Király K. Chemical characterization of fluorescein isothiocyanate-protein conjugates. Biochim Biophys Acta. 1966 Jul 27;124(1):166-75. doi: 10.1016/0304-4165(66)90325-4.

19. Parham P. Preparation and purification of active fragments from mouse monoclonal antibodies. In: Weir DM (ed) Handbook of experimental immunology. Blackwell, Edinburgh; 1986, p 14.1–14.23.

20. Bradford MM. A rapid and sensitive method for the quantitation of microgram quantities of protein utilizing the principle of protein-dye binding. Anal Biochem. 1976 May 7;72:248-54. doi: 10.1006/abio.1976.9999.

21. Zor T, Selinger Z. Linearization of the Bradford protein assay increases its sensitivity: theoretical and experimental studies. Anal Biochem. 1996 May 1;236(2):302-8. doi: 10.1006/abio.1996.0171.

22. Fox E, Chanon J (eds.). Photoinduced electron transfer. Part a, 1st Edition. Elsevier Science, Oxford; 1989, pp. 19-21., 53-73., 115-202.

23. Work TS, Work E (eds). Laboratory techniques in Biochemistry and Molecular Biology. Vol. 11. Oxford: Elsevier Science; 1982. p. 37-41, 94-96.

24. Holly S, Sohár P. Infrared spectroscopy. 3rd edition. Budapest: Műszaki Kiadó; 1968.

25. Wong PPT, Mantsch HH. Infrared spectroscopy. In: Bridge RR, Mantsch HH (eds). Biomolecular Spectroscopy. Vol. 1057. 1989. pp. 49-56.

26. Yang WJ, Griffiths PR, Byler MD, Susi H. Proteins Conformation by Infrared Spectroscopy: Resolution Enhancement by Fourier Self-Deconvolution. Applied Spectroscopy. 1985 39:469-487.

27. Wong PT, Heremans K. Pressure effects on protein secondary structure and hydrogen deuterium exchange in chymotrypsinogen: a Fourier transform infrared spectroscopic study. Biochim Biophys Acta. 1988 Aug 31;956(1):1-9. doi: 10.1016/0167-4838(88)90291-9.

28. Mummert ME, Voss EW Jr. Effects of secondary forces on a high affinity monoclonal IgM anti-fluorescein antibody possessing cryoglobulin and other cross-reactive properties. Mol Immunol. 1998 Feb;35(2):103-13. doi: 10.1016/s0161-5890(98)00017-0.

29. Mummert ME, Voss EW Jr. Secondary force-mediated perturbations of antifluorescein monoclonal antibodies 4-4-20 and 9-40 as determined by circular dichroism. J Protein Chem. 1998 Apr;17(3):237-44. doi: 10.1023/a:1022532618038.

30. Müller JD, Nienhaus GU, Tetin SY, Voss EW. Ligand binding to anti-fluorescyl antibodies: stability of the antigen binding site. Biochemistry. 1994 May 24;33(20):6221-7. doi: 10.1021/bi00186a023.

31. Klonis N, Clayton AH, Voss EW Jr, Sawyer WH. Spectral properties of fluorescein in solvent-water mixtures: applications as a probe of hydrogen bonding environments in biological systems. Photochem Photobiol. 1998 May;67(5):500-10.

32. Watt RM, Voss EW Jr. Mechanism of quenching of fluorescein by anti-fluorescein IgG antibodies. 1977. Immunochemistry. Jul;14(7):533-51. doi: 10.1016/0019-2791(77)90308-1. PMID: 303233

33. Omelyanenko VG, Jiskoot W, Herron JN. Role of electrostatic interactions in the binding of fluorescein by anti-fluorescein antibody 4-4-20. Biochemistry. 1993 Oct 5;32(39):10423-9. doi: 10.1021/bi00090a018.

34. Howlett JR, Ismail AA, Armstrong DW, Wong PT. Pressure-induced conformational changes in an antigen and an antibody and the implications on their use for hyperbaric immunoadsorption. Biochim Biophys Acta. 1992 Oct 20;1159(3):227-36. doi: 10.1016/0167-4838(92)90049-j.

35. Sii D, Sadana A. Bioseparation using affinity techniques. J Biotechnol. 1991 Jun;19(1):83-98. doi: 10.1016/0168-1656(91)90076-8.

[1] **Author contribution.** single author

Original article

Fractionation of *Vipera berus berus* Snake Venom and Detection of Bioactive Compounds Targeted to Blood Coagulation System

Eldar Iskandarov [1,2*], Volodymyr Gryshchuk [1], Oleh Platonov [1], Yevhenii Kucheriavyi [1], Oleksandr Slominskyi [1], Yevhenii Stohnii [1], Volodymyr Vartanov [1], Volodymyr Chernyshenko [1]

[1] Palladin Institute of Biochemistry, NAS of Ukraine, Ukraine
[2] Biology and Medicine Institute Science Educational Center of Taras Shevchenko National University of Kyiv, Ukraine

*Corresponding author: Eldar Iskandarov, iskandarov.e.sh@gmail.com

Abstract

Introduction. The performed research focused on a search for new biologically active compounds acting on blood coagulation system proteins and cells. To achieve this goal, we fractionated Vipera berus berus snake venom and studied the action of the separated fractions on human blood plasma, fibrinogen, platelets or red cells.

Methods. Crude venom was fractionated using ion-exchange chromatography. Protein composition of fractions was studied using SDS-PAGE. The ability of fractions to prolong or initiate blood plasma clotting was studied using the prothrombin time test with thromboplastin. Fibrinogen-specific proteases were detected using enzyme-electrophoresis. Action on red cells was estimated using the hemolysis test. Aggregometry was used for the detection of action on platelets. All experiments in this study were performed in vitro.

Results. We obtained fractions containing phospholipase and a protease that is able to hydrolyze fibrinogen, leading to the loss of its ability to polymerize and to maintain platelet aggregation.
Conclusion. Further purification and study of these components can be a promising research direction for biotechnological as well as for biomedical use.

(Iskandarov E*, Gryshchuk V, Platonov O, Kucheriavyi Y, Slominskyi O, Stohnii Y, Vartanov V, Chernyshenko V. Fractionation of *Vipera berus berus* Snake Venom and Detection of Bioactive Compounds Targeted to Blood Coagulation System. SEEMEDJ 2022; 6(2); 20-31)

Received: Sep 21, 2022; revised version accepted: Oct 24, 2022; published: Nov 28, 2022

KEYWORDS: snake venoms, blood coagulation, fibrinogen, hemolysis, platelet aggregation

Introduction

Snake venoms are complex mixtures of bioactive components, particularly proteins, nucleic acids, and organic compounds. The venom's main purpose is to immobilize or kill prey, usually small mammals, reptiles, birds or amphibians. The venom's components get into the prey's blood during the bite, and are instantly distributed through its body via blood flow.

Evolutionary, venomous reptiles have developed different routes to hit the prey, one or a few of which appeared to be more successful and thus started to prevail. Most snake venoms have neurotoxic action [1]; however, some snakes kill their prey by inducing generalized inflammatory tissue response, or by using blood coagulation activators, which cause massive coagulation or conversely cause hemolysis, inability of the blood to clot, destroy blood vessels and lead to internal hemorrhages [2].

In any case, if one way of immobilizing a preferable type of prey prevails, other venom components do not vanish from the venom instantly. Instead, their effects are masked by the more active components. This is why venoms of some snakes simultaneously contain, for instance, enzymes hydrolyzing fibrinogen, which decrease blood coagulation ability, and fibrinogen activators, which stimulate thrombus production, in different proportions.

Since venom comes into contact primarily with the prey's blood, the action of many of its components is aimed at the circulatory system. In particular, the proteases destroying fibrinogen, platelet aggregation inhibitors, activators of blood coagulation factors, phospholipases, etc. were found in snake venoms [2]. Obtaining and describing these components led to the discovery of unique enzymes, used nowadays in medicine and laboratory diagnostics. That is why the study of snake venom composition is a current issue of modern biotechnology [3].

Functionally active components of snake venoms may also be used in fundamental research on the features of certain elements of the hemostasis system. In particular, fibrinogenases (enzymes capable of selectively hydrolyzing fibrinogen) appear to be useful tools for studying the role of certain molecule sites [4].

In our research, we focused on the venom of a snake from Ukrainian fauna, which made our object available for analysis, as well as for potential further biotechnological production. The purpose of the study was to search for Vipera berus berus venom proteins, which can be used as effectors of the blood coagulation system.

Materials and methods

Materials

a) Vipera berus berus *venom*

Crystalline venom of Vipera berus berus was provided by the Laboratory of Experimental Herpetology of the Trypillia Biochemical Factory (Trypillia, Ukraine).

b) Human blood plasma

Blood was taken from the vein using a sharp dry needle with a large diameter without a syringe (to prevent hemolysis), discarding the first 5–6 blood drops. During blood taking, neither a tourniquet nor a massage was applied in order to prevent blood coagulation activation and fibrinolysis. Blood collection was performed under fasting conditions.

A 3.8% sodium citrate solution was introduced into the polyethylene tube using a dispenser and further admixed with blood in a 1:9 ratio. Next, the tube was tightly closed and gently mixed using slow hand movements, without shaking.

Platelet-rich plasma (PRP) was obtained by centrifugation at 200 g for 30 min [5]. During centrifugation, the tubes were open so as not to prevent oxygen access to the platelets.

Platelet-poor plasma was obtained by centrifugation at 450 g for 20 min at a temperature lower than 20 ˚C.

This study was approved by the ethical committee of the Palladin Institute of Biochemistry of NAS of Ukraine, on 9 December 2021, N12. Volunteers signed informed consent forms prior to blood sampling, in accordance with the Declaration of Helsinki.

c) Human fibrinogen

Fibrinogen was obtained from human blood plasma by salt extraction using 16% Na2SO4. The content of protein coagulated by thrombin was 96–98%. To remove vitamin K dependent proteins – prothrombin, factors IX and X of the blood coagulation system, and protein C – plasma was cooled to +4 ˚C and, under constant mixing, admixed with BaSO4 (30 g/L of blood), then centrifuged at 1300 g for 10 min. The BaSO4 addition procedure was repeated twice.

In the next step, blood plasma was heated to room temperature, and 1 M glycine buffer (glycine and 1 M NaOH, pH 9) was added at a 1:10 ratio to the entire volume. After that, one fraction was precipitated using 16% Na2SO4 (slowly adding a small portion thereof with constant mixing). The resulted precipitate was spun-down at 1300 g for 30 min at ambient temperature. Supernatant was carefully discarded, and then fibrinogen precipitation was performed using 16% Na2SO4. After that, fibrinogen was spun-down for 30 min at 1300 g at a temperature of 10–15 ˚C. The precipitate was then diluted in 0.2 M NaCl – 250 mL of solvent was used for solving the precipitate from 1 L blood plasma.

The obtained fibrinogen was re-precipitated by an equal volume of 16% Na2SO4, and then the precipitate was diluted in 0.2 M NaCl (150–200 mL for 1 L blood plasma). After that, the fibrinogen solution was added with 0.5 M phosphate buffer (KH2PO4 and NaOH, pH 6.5) at a 1:5 ratio to the entire fibrinogen solution volume, and then again re-precipitated by equal volume of 16% Na2SO4. The order of steps is analogous with the first precipitation, but re precipitated fibrinogen was diluted with 0.15 M NaCl (70–150 mL of solvent for 1 L blood plasma).

Re-precipitated fibrinogen was placed on ice with a temperature of +4 ˚C for the night in order to separate the cryoforms of fibrinogen. The expected concentration of fibrinogen while cryoforms were separating was 10–12.5 mg/mL. Then, the fibrinogen solution was centrifuged for 30 min at 1300 g, the supernatant liquid was carefully discarded, and another re precipitation by 16% Na2SO4 was performed. The precipitated fibrinogen was diluted in 0.15 M NaCl, after which the solution was frozen and stored at -20 ˚C [6].

d) Reagents

The following materials and reagents were used in the present experiments: acrylamide, bis-acrylamide, molecular mass markers for electrophoresis (Fermentas, EU), tris (Merck, USA), SDS (Bio-Rad Laboratories), Q Sepharose (Pharmacia, Sweden), PD-10 columns. The thromboplastin (Thromborel) was bought from Siemens, Germany. Molecular weight markers SM0671 (250; 130; 100; 70; 55; 35; 25 та 10 kDa) were purchased from Fermentas (EU). BluEye molecular weight markers (245; 180; 100; 75; 63; 48; 35; 25; 20; 17 та 11 kDa) were purchased from Sigma-Aldrich (USA).

Methods

a) Ion-exchange chromatography

Q Sepharose is the anion-exchange agent, which allows efficient fractioning of the protein mixture under alkaline pH [7]. To fraction the venom, Q Sepharose was balanced with 0.05 M tris-HCl buffer, pH 8.9. The column volume was 12.5 mL, and flow speed was 1 mL/min. The adsorbed proteins were eluted with the same buffer in staged gradient: 0.1, 0.2, 0.5 and 2 M NaCl, pH 8.9. For fractioning, the Acta Prime (Acta, USA) chromatographic system was used.

The obtained material was described using SDS-PAGE.

b) Protein concentration identification

Protein concentration in obtained fractions was approximately identified through spectrophotometry, by optic absorbency under 280 nm subtracting the absorbency under 320 nm using the Optizen POP (Optizen, Korea) spectrophotometer. The Bradford method was used for quantitative identification of protein concentrations [8].

c) Electrophoresis in polyacrylamide gel

Electrophoresis in polyacrylamide gel (PAGE) with SDS was performed according to the Laemmli method, where the tris-glycine system is used in the device for vertical gel electrophoresis in the plates [9].

Samples for electrophoresis were prepared in accordance with the following algorithm: the 1 mg/mL protein solution was added with a sample buffer that contained 5% sucrose or glycerin, 2% SDS and bromophenol (bromophenol is added until coloration appearance).

To identify the sites containing proteins, gel-plates were developed by staining it in a solution (0.125% Coomassie G-250 in 25% isopropanol and 10% acetic acid) for 10 minutes. To discard the staining remains, we used a 3–9% acetic acid solution. The method resolution was 1 μg of protein.

To establish the molecular mass of studied proteins, molecular markers were used (Fermentas, EU): SM0671 (250; 130; 100; 70; 55; 35; 25 та 10 kDa).

d) Enzyme-electrophoresis with fibrinogen as substrate

Enzyme-electrophoresis was performed using the Laemmli method in 15% PAAG [9]. The 0.5 mg/mL fibrinogen was put into the separating gel before polymerization. After electrophoresis, SDS was removed from the gel through trice washing with 2.5% Triton X-100 for 30 min. The gel was incubated in 0.1 M glycine buffer, pH = 8.3, for 12 hours. After that, the gel was stained with Coomassie G-250, and the sites of proteolytic activity were identified by uncolored spots on the gel [9].

To establish the molecular mass of studied proteins, molecular markers were used (Sigma-Aldrich, USA): BluEye (245; 180; 100; 75; 63; 48; 35; 25; 20; 17 та 11 kDa).

e) Prothrombin time (PT)

This method consists of measuring the coagulation time of citrate plasma after thromboplastin and Ca^{2+} addition. Normal prothrombin time is 12–17 s. Elongation of prothrombin time may be linked to deterioration of vitamin K-dependent factor synthesis, which are involved in the external pathway of blood coagulation – VII, X, II – and also to indirect anticoagulant therapy. Shortening of prothrombin time is linked to anticoagulant content decrease in the blood, or to pathological activation of the procoagulant chain of the hemostasis system [10]. To perform the test, 80 μL of blood plasma was added with 20 μL of examined fraction (or equal volume of 0.05 M tris-HCl buffer, pH 8.9, in control), and with 100 μL of 0.025 M $CaCl_2$ solution, and then polymerization was initiated by adding 100 μL of thromboplastin (Thromborel, Siemens, Germany). The time of clot formation was controlled.

f) Establishing hemolytic activity

Red blood cells were obtained from citrate blood via centrifugation for 20 min at 125 g and a temperature of 20 ˚C. The precipitated erythrocytes were washed by trice re-suspending in 10 mM HEPES buffer, pH 7.4, containing 0.15 M NaCl, 5 mM KCl, 1 mM $MgSO_4$, and 10 mM sucrose, with following precipitation at 125 g and a temperature of 20 ˚C.

The suspension of washed human red blood cells obtained using this method [11] was diluted in a 1:8 ratio with 10 mM HEPES buffer, pH 7.4, containing 0.15 M NaCl, 5 mM KCl, 1 mM $MgSO_4$, and 10 mM sucrose. The amount of 50 μ L of the suspension was added with the studied sample (total volume – 1 mL), mixed, and incubated at 37 ˚C for 30 min.

After incubation, the red blood cells were precipitated through centrifugation at 1000 g for 10 min and examined the supernatant's absorbency at 543 nm against the buffer. Hemolysis caused by 50 μL of 1% Triton-X100 was treated as 100%.

Absorbance was measured using the Optizen POP spectrophotometer (Korea).

g) Platelet aggregation study

Platelet aggregation was studied using the SOLAR AP2110 aggregometer (Belarus). The 0.2 mL blood platelet-rich plasma (PRP) was put into the spectrophotometer cuvette and added with 50 μL of studied fraction, or the equal volume of 0.05 M tris-HCl buffer, pH 8.9, in control. The mixture was incubated for 3 min, then 0.025 mL of 0.025 M CaCl2 was added and it was again incubated in the cuvette for 3 min. After that, 0.025 mL of 25 μM ADP was added to the cuvette [12]. The entire aggregation process was recorded, and the aggregation level was estimated.

h) Statistical analysis

Statistical analysis was performed using Microsoft Excel (Microsoft package). All analyses were conducted in the series of three replicates; standard deviation was considered in data analysis. Student's T-test was used. Results are presented as mean ± standard deviation. Data were considered significant when $p < 0.05$.

Results

Fractionation of V. berus berus *venom*

For fractionation, 50 mg of crude Vipera berus berus venom was diluted in 1 mL of 0.05 M tris-HCl buffer, pH 7.4. Before injection, the venom solution was centrifuged at 200 g for 15 min. Using the Akta Prime chromatographic system, the venom was fractionated at a speed of 4 mL/min using the column, filled with chromatographic sorbent Q Sepharose of 15 mL volume.

After we collected the fraction, which did not bond with the sorbent under present conditions, the column was washed with 0.05 M tris-HCl buffer, pH 7.4. Elution was performed using stepping gradient of NaCl: 0.1, 0.2, 0.3, 0.5 M of NaCl in 0.05 M tris-HCl buffer, pH 8.9. Finally, the sorbent was washed with a buffer of 1 M NaCl. The chromatogram is presented in Figure 1.

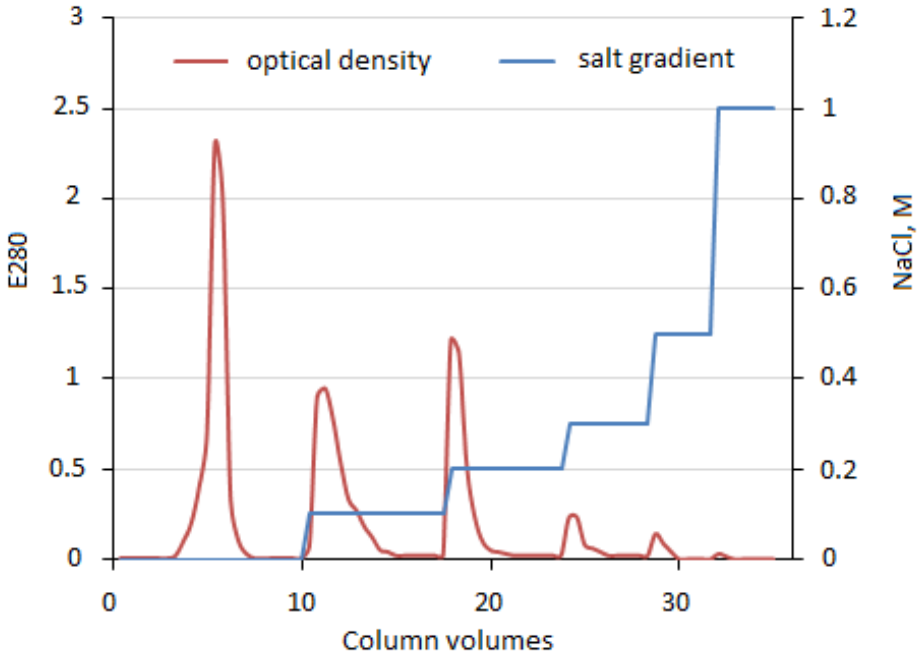

Figure 1. Separation of crude Vipera berus berus venom on Q Sepharose. Speed of elution was 4 mL/min (elution by stepping gradient of NaCl (0.1, 0.2, 0.3, 0.5, 1 M) in 0.05 M tris-HCl buffer, pH = 7.4).

The obtained fractions were de-salted and concentrated using centrifuge microconcentrators Amicon Ultra 3K. For detection of fractions' protein composition, gel-electrophoresis was used.

SDS-PAGE

It was demonstrated that all obtained fractions had different protein compositions and contained proteins of molecular mass from 120 to 10 kDa (Figure 2). This was important for describing each fraction, and for revealing their potential unique physiological effects.

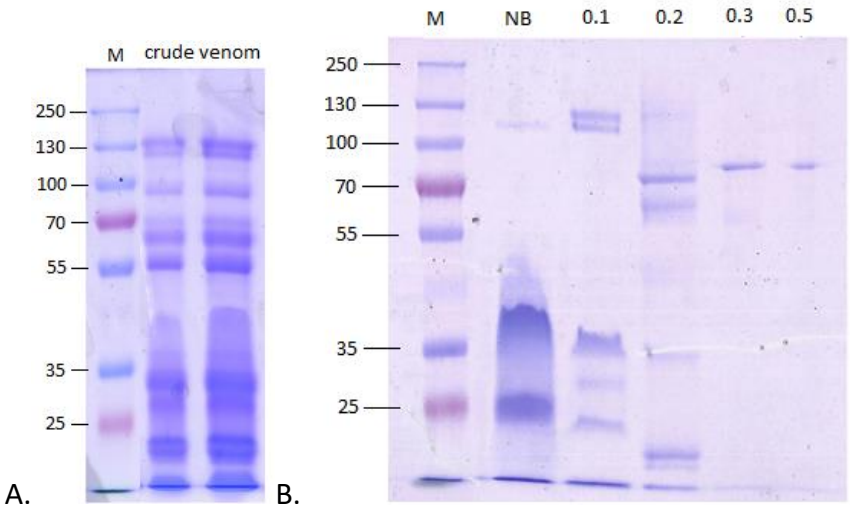

Figure 2. A. – electrophoregram of crude Vipera berus berus venom. B. – electrophoregram of Vipera berus berus venom fractions obtained on Q Sepharose. M – molecular mass markers (250-10 kDa). NB – fraction which did not bind to the sorbent under present conditions. 0.1, 0.2, 0.3, 0.5 – fractions eluted by 0.1, 0.2, 0.3, 0.5 M NaCl, respectively.

Fractions' impact on fibrinogen and fibrin polymerization

To estimate the ability of obtained fractions to inhibit fibrin polymerization, we detected the coagulation time prolongation for blood plasma in the prothrombin time test in the presence of studied fractions. For this purpose, 80 µL of blood plasma was incubated with 20 µL of the fraction at the final concentration of 0.05 o.u./mL (or equal quantity of buffer) for 5 min. The coagulation was initiated by adding 100 µL of 0.025 M CaCl2, and 100 µL of thromboplastin solution. It showed prolongation of the coagulation time for blood plasma of up to 60 s (compared to 40 s in control) in the presence of the fraction eluted by 0.2 M NaCl. Such prolongation may be linked to the presence of the enzyme which can hydrolyze fibrinogen, and which was found in this fraction and in the crude venom. Other fractions did not have such ability (Figure 3).

Identification of proteolytic action toward fibrinogen in the chosen fraction was performed using enzyme-electrophoresis with fibrinogen as the substrate. The enzyme-electrophoresis method combines electrophoretic separation and enzymography.

In particular, it was proved that the fraction eluted by 0.2 M NaCl contained the enzyme capable of hydrolyzing fibrinogen. Its approximate molecular mass was 50 kDa (Figure 4). We concluded that the presence of this enzyme explains the ability of this fraction to slow down fibrin polymerization.

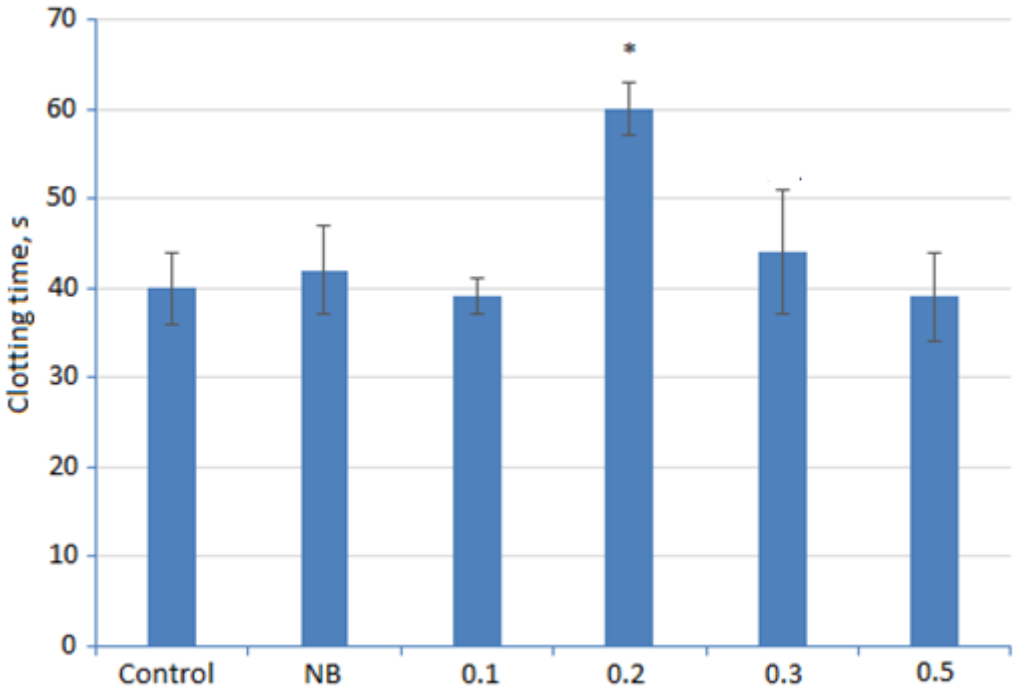

Figure 3. Time of thromboplastin-induced blood plasma coagulation after 5 minutes of incubation with Vipera berus berus venom fractions, obtained on Q Sepharose. NB – fraction which did not bind to the sorbent under present conditions. 0.1, 0.2, 0.3, 0.5 – fractions eluted by 0.1, 0.2, 0.3, 0.5 M NaCl, respectively. * – the result is significant in comparison to control at p < 0.05. The diagram is based on the results of three independent experiments.

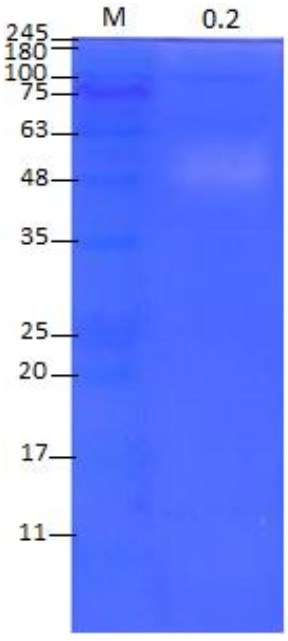

Figure 4. The enzymogram of Vipera berus berus venom fraction obtained on Q Sepharose and eluted with 0.2 M NaCl. M – molecular mass markers (245-11 kDa); 0.2 – fraction.

Hemolytic activity

To reveal phospholipases in the obtained fractions, their ability to provoke red blood cell hemolysis was studied. For this purpose, a homogeneous suspension of human red blood cells was prepared. As the positive control, the hemolytic agent Triton X-100 was used. The samples were incubated at 37 ˚C for 60 min, then the red blood cells were precipitated by centrifugation, and relative hemolytic activity was estimated by absorbance under 543 nm.

Red blood cell hemolysis was observed in the presence of the Vipera berus berus venom fraction eluted by 0.5 M NaCl. It is curious that the gel-electrophoretic data showed the presence of a single protein component of 70 kDa mass in this fraction.

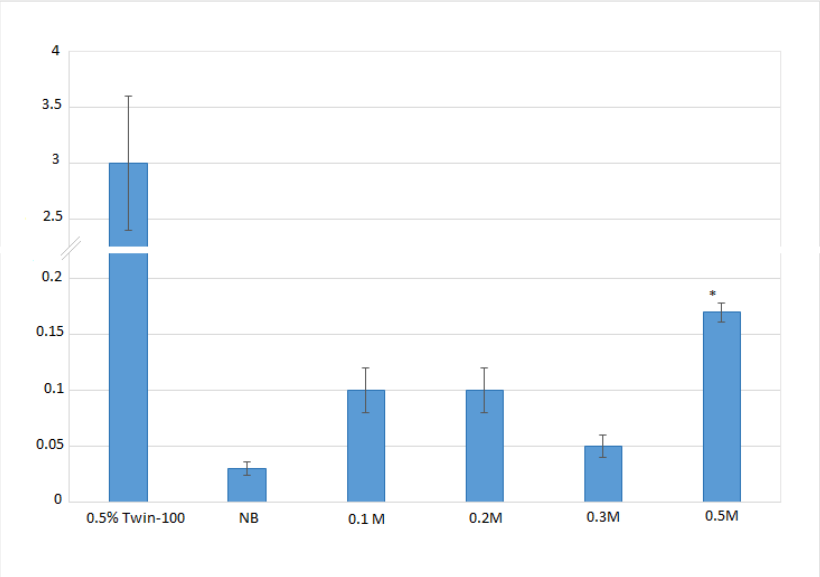

Figure 5. Time of erythrocyte hemolysis under previous incubation with Vipera berus berus venom fractions. Extinction of supernatant after hemolysis was estimated under the 543 nm light wave. As the control, extinction of supernatant of erythrocyte solution with PBS buffer was taken. 0.5% Twin-100 – erythrocyte solution with 0.5% Twin-100 detergent (positive control). NB – fraction which did not bind to the sorbent under present conditions. 0.1, 0.2, 0.3, 0.5 – fractions eluted by 0.1, 0.2, 0.3, 0.5 M NaCl, respectively.

*** – the result is significant at $p < 0.05$. The diagram is based on the results of three independent experiments.**

Impact on platelets

To estimate the impact of obtained fractions on hemostasis, we used the original approach with modified aggregometry, which allowed us to consider the ability of fractions to activate the platelets, initiate blood coagulation, or inhibit platelet aggregation.

For this purpose, 50 mL of the fraction (in the final quantity of 0.05 o.u./mL) was added to 200 µL of platelet-rich blood plasma and incubated in the aggregometer cuvette for 3 min, recording the platelet aggregation process. After that, 25 µL of 0.025 M CaCl2 was added, and recording was continued for another 3 min. Then, 25 µL of 25 µM ADP was added, and platelet aggregation was recorded. Decrease of the platelet aggregation level at this stage of measurement may indicate inhibition of aggregation or the damaging of platelets after contact with the studied fractions.

The analysis of aggregation curves presented in Figure 6 allowed us to conclude that the fraction, which did not bond to the sorbent, and the fraction eluted by 0.1 M NaCl were able to activate the platelets moderately.

At the same time, the platelet aggregation inhibitor was found in the fraction eluted with 0.2 M NaCl. The ADP addition did not cause platelet aggregation. It is important to underline that the same fraction had the fibrinogen-specific protease, according to our data. Fibrinogen hydrolysis may be one of the causes of inhibition of platelet aggregation, since this process is mediated by fibrinogen.

The fraction eluted with 0.5 M NaCl did not have an intense impact on the platelets. Apparently, 6 minutes of incubation of fractions with platelets was not enough for a manifestation of phospholipase activity, which was predicted by the results of red blood cell hemolysis (60 min incubation).

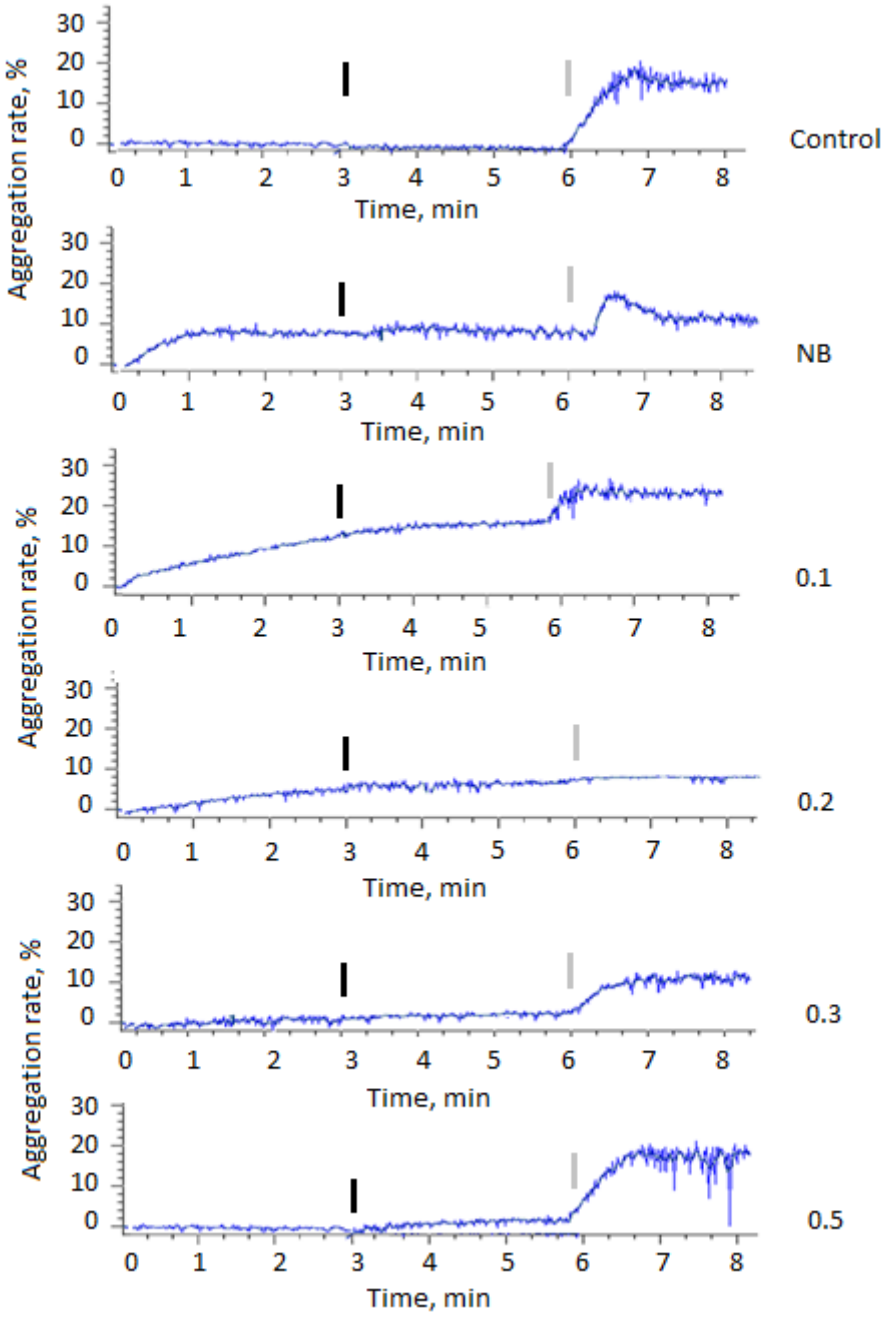

Figure 6. The plot of platelet aggregation in platelet-rich blood plasma after incubation with Vipera berus berus venom fractions. Control – under the equal buffer volume. NB – fraction which did not bind to the sorbent under present conditions. 0.1, 0.2, 0.3, 0.5 – fractions eluted by 0.1, 0.2, 0.3, 0.5 M NaCl, respectively. Typical curves for three independent experiments are shown.

Black lines – points of addition of 25 mkl of 0.025 M CaCl2; Grey lines – points of addition of 25 µl of 25 µM ADP.

Discussion

The fractioning of Vipera berus berus venom allowed us to obtain separate fractions, which differ in their protein compositions and in their action on the hemostasis system. In particular, we obtained the fractions containing phospholipase. We also found a protease capable of hydrolyzing fibrinogen, leading to the

loss of its ability to maintain platelet aggregation. The presence of components capable of moderately activating the platelets is expected for some venom fractions. Further purification and study of these components may represent a promising research direction.

Phospholipases, the enzymes that selectively destroy phospholipids, have been obtained from a few snake venoms. In particular, the phospholipases of 12.5, 13.9 and 14.2 kDa were obtained from the Crotalus molossus nigrescens venom. Authors suggest that they should be used in oncological medicine due to their potential as anticancer agents and their lower neurotoxic effects compared to conventional drugs [13]. Phospholipases were also found in the Naja sumatrana and Bothrops alternatus venoms, and methods for their purification were suggested [14,15]. We expect that the application of newly purified phospholipase may be useful for researching the structural-functional features of lipid membranes.

Recent studies have discussed the practical application of phospholipases. In particular, by inducing Treg cells, these enzymes can be effective as potential therapeutic agents in atherosclerosis [16]. Antibacterial activity is another promising feature of phospholipases [17,18]. Targeting the cell membrane, phospholipases can disrupt the cellular integrity of bacteria. In addition to their potential biomedical use, phospholipases can be applied in studying liposomes and lipid rafts [19].

Further study of the fibrinogen-specific protease from the Vipera berus berus venom will let us establish its specificity concerning certain chains of the fibrinogen molecule. Enzymes capable of selectively hydrolyzing fibrinogen are used in studying its structure and function [20] and obtaining partly hydrolyzed fibrinogen forms [21]. The possibility of fibrinogenase use for thrombolysis is also being discussed [22]. For this purpose, several recombinant analogs for certain fibrinogenases were obtained [23,24].

The mechanism of anticoagulant action of fibrinogen-specific proteases is obvious – cleaving of fibrinogen chains by these enzymes decreases its ability to polymerize [25]. In contrast to other anticoagulants that inhibit coagulation factors (mainly thrombin or factor Xa), fibrinogen-specific proteases act in the final step of the clotting process, preventing the formation of a clot [26]. Likewise, these enzymes can often effectively cleave polymerized fibrin, thus promoting the dissolution of intravascular thrombus [27]. cardiovascular and renal disease in non-diabetic individuals with arterial hypertension remains a question to be answered.

Conclusion

Proteins from vipers' venoms do not only cause death; they can also be used for treatment of thrombosis, arthritis, cancer and many other diseases [ ]. As snake venom contains a wide spectrum of biological compounds, research conducted for the purpose of identifying their structure, biological activity, and pharmaco-clinical application is now of great significance [28].

We have developed a novel method of fractionation of Vipera berus berus venom, which enabled us to obtain fractions with different action on the human blood coagulation system. Our data corresponded to the recently summarized results presented in [2]. Further purification of bioactive proteins that we found in Vipera berus berus venom will allow the performance of their full characterization. These molecular effectors can be used for studying regulatory mechanisms of blood coagulation system regulation.

Acknowledgement. None.

Disclosure

Funding. This research was carried out within the framework of the basic theme of the Palladin Institute of Biochemistry of the National Academy of Sciences of Ukraine N° 0119U002512 «Interactions of the components of the hemostasis system at the cellular and molecular level in the process of thrombus formation and elimination» (2019–2023).
Competing interests. None to declare.

References

1. Nițescu GV, Ulmeanu CE, Crăciun MD, Ciucă AM, Ulici A, Ghira I, Lonati D. Neurotoxicity and Other Clinical Manifestations of a Common European Adder (Vipera berus) Bite in Romania. Toxins (Basel) 2022; 18;14(7):500.
2. Siigur J, Siigur E. Biochemistry and toxicology of proteins and peptides purified from the venom of Vipera berus berus. Toxicon X 2022 Jun 12;15:100131. doi: 10.1016/j.toxcx.2022.100131
3. Op den Brouw B, Ghezellou P, Casewell NR, Ali SA, Fathinia B, Fry BG, Bos MHA, Ikonomopoulou MP. Pharmacological Characterisation of Pseudocerastes and Eristicophis Viper Venoms Reveal Anticancer (Melanoma) Properties and a Potentially Novel Mode of Fibrinogenolysis. Int J Mol Sci. 2021; 22(13):6896. doi: 10.3390/ijms22136896.
4. Cortelazzo A, Guerranti R, Bini L, Hope-Onyekwere N, Muzzi C, Leoncini R, Pagani R. Effects of snake venom proteases on human fibrinogen chains. Blood Transfus 2010 Jun;8 Suppl 3(Suppl 3):s120-5. doi: 10.2450/2010.019S.
5. Chernyshenko V, Shteinberg K, Lugovska N, Ryzhykova M, Platonova T, Korolova D, Lugovskoy E. Preparation of highly-concentrated autologous platelet-rich plasma for biomedical use. Ukr. Biochem. J. 2019; 91:2.
6. Varetska T, Microheterogeneity of fibrinogen. Cryofibrinogen Ukr. Biochem. J. 1960; 32:13-24.
7. Cummins PM, Rochfort KD, O'Connor BF. Ion-Exchange Chromatography: Basic Principles and Application. Methods Mol Biol. 2017; 1485:209-223.
8. Bradford MM. A rapid and sensitive method for quantities of utilizing the principle of protein binding. Analytical Biochemistry 1976; 86:193-200.
9. Ostapchenko L, Savchuk O, Burlova-Vasilieva N. Enzyme electrophoresis method in analysis of active components of haemostasis system. ABB 2011 ;2:20-26.
10. Koroleva DS, Vynogradova RP, Chernyshenko TM, Platonova TM, Volkov GL. The use of ekamulin - a prothrombin activator from the poison of the Echis multisquamatus in clinical laboratory diagnostics. Laboratory diagnostics 2006; 3:18-21.
11. Kozynets GI, Makarov VA. Blood system research in clinical practice. Triada-X 1997: 480.
12. Born GV. Changes in the distribution of phosphorus in platelet-rich plasma during clotting. Biochem J. 1958; 68(4):695-704.
13. Lazcano-Pérez F, Rangel-López E, Robles-Bañuelos B, Franco-Vásquez AM, García-Arredondo A, Navarro-García JC, Zavala-Moreno A, Gómez-Manzo S, Santamaría A, Arreguín-Espinosa R. Chemical structure of three basic Asp-49 phospholipases A2 isolated from Crotalus molossus nigrescens venom with cytotoxic activity against cancer cells. Toxicon 2022; 210:25-31.
14. Abdullah NAH, Rusmili MRA, Zainal Abidin SA, Shaikh MF, Hodgson WC, Othman I. Isolation and Characterization of A2-EPTX-Nsm1a, a Secretory Phospholipase A2 from Malaysian Spitting Cobra (Naja sumatrana) Venom. Toxins (Basel) 2021; 13(12):859.
15. Dias EHV, Dos Santos Paschoal T, da Silva AP, da Cunha Pereira DF, de Sousa Simamoto BB, Matias MS, Santiago FM, Rosa JC, Soares A, Santos-Filho NA, de Oliveira F, Mamede CCN. BaltPLA2: A New Phospholipase A2 from Bothrops Alternatus Snake Venom with Antiplatelet Aggregation Activity. Protein Pept Lett. 2018; 25(10):943-952.
16. Kang GH, Lee S, Choi DB, Shin D, Kim J, Yang H, Bae H. Bee Venom Phospholipase A2 Ameliorates Atherosclerosis by Modulating Regulatory T Cells. Toxins (Basel). 2020; 12(10):609. doi: 10.3390/toxins12100609.
17. Nunes E, Frihling B, Barros E, de Oliveira C, Verbisck N, Flores T, de Freitas Júnior A, Franco O, de Macedo M, Migliolo L, Luna K. Antibiofilm Activity of Acidic

Phospholipase Isoform Isolated from Bothrops erythromelas Snake Venom. Toxins (Basel). 2020; 12(9):606. doi: 10.3390/toxins12090606.
18. Corrêa EA, Kayano AM, Diniz-Sousa R, Setúbal SS, Zanchi FB, Zuliani JP, Matos NB, Almeida JR, Resende LM, Marangoni S, da Silva SL, Soares AM, Calderon LA. Isolation, structural and functional characterization of a new Lys49 phospholipase A2 homologue from Bothrops neuwiedi urutu with bactericidal potential. Toxicon. 2016; 115:13-21. doi: 10.1016/j.toxicon.2016.02.021.
19. Staneva G, Angelova MI, Koumanov K. Phospholipase A2 promotes raft budding and fission from giant liposomes. Chem Phys Lipids. 2004; 129(1):53-62. doi: 10.1016/j.chemphyslip.2003.11.005.
20. Weisel JW, Litvinov RI. Fibrin Formation, Structure and Properties. Subcell Biochem 2017; 82:405-456.
21. Mihalyi E. Kinetics and molecular mechanism of the proteolytic fragmentation of fibrinogen. Ann N Y Acad Sci. 1983; 408:60-70.
22. Kumar SS, Sabu A. Fibrinolytic Enzymes for Thrombolytic Therapy. Adv Exp Med Biol. 2019; 1148:345-381.
23. He J, Chen S, Gu J. Identification and characterization of Harobin, a novel fibrino(geno)lytic serine protease from a sea snake (Lapemis hardwickii). FEBS Lett. 2007; 581(16):2965-73.
24. Wagstaff AJ, Gillis JC, Goa KL. Alteplase. A reappraisal of its pharmacology and therapeutic use in vascular disorders other than acute myocardial infarction. Drugs 1995; 50(2):289-316.
25. Gardiner EE, Andrews RK. The cut of the clot(h): snake venom fibrinogenases as therapeutic agents. J Thromb Haemost. 2008; 6(8):1360-2. doi: 10.1111/j.1538-7836.2008.03057.x.
26. Chernyshenko V. O, Lugovska N. E. Molecular mechanisms of intravascular inhibition and stimulation of extravascular thrombosis. Biotechnologia Acta. 2021, 14(6), pp. 5–22. https://doi.org/10.15407/biotech14.06.005
27. Altaf F, Wu S, Kasim V. Role of Fibrinolytic Enzymes in Anti-Thrombosis Therapy. Front Mol Biosci. 2021; 8:680397. doi: 10.3389/fmolb.2021.680397.
28. Pal SK, Gomes A, Dasgupta SC, Gomes A. Snake venom as therapeutic agents: from toxin to drug development. Indian J Exp Biol. 2002; 40(12):1353-8.
29. Cristina RT, Kocsis R, Tulcan C, Alexa E, Boldura OM, Hulea CI, Dumitrescu E, Radulov I, Muselin F. Protein structure of the venom in nine species of snake: from bio-compounds to possible healing agents. Braz J Med Biol Res. 2020; 53(1):e9001.

Author contribution. Acquisition of data: EI, VG, OP, YK, OS, YS, VV, VC
Administrative, technical or logistic support: EI, VG, OP, YK, OS, YS, VV, VC
Analysis and interpretation of data: EI, VG, OP, YK, OS, YS, VV, VC
Conception and design: EI, VG, OP, YK, OS, YS, VV, VC
Critical revision of the article for important intellectual content: EI, VG, OP, YK, OS, YS, VV, VC
Drafting of the article: EI, VG, OP, YK, OS, YS, VC
Final approval of the article: EI, VG, OS, YS, VC
Guarantor of the study: VC
Obtaining funding: OS, VV, VC
Provision of study materials or patients: EI, VG, OP, YK, OS, YS, VV, VC
Statistical expertise: EI, VG, OP, OS, YS, VV, VC

Original article

The Effect of Submaximal Exercise on Cutaneous Blood Flow, Thermoregulation and Recovery Hemodynamics Following Endurance Exercise

Nejka Potočnik

Institute of Physiology, Medical Faculty, University of Ljubljana, Slovenia

*Corresponding author: Nejka Potočnik, nejka.potocnik@mf.uni-lj.si

Abstract

Aim. There are numerous reports of attenuation of cutaneous blood flow (CBF) during the recovery period after a single bout of exercise, but no one has investigated the CBF response to consecutive short-lasting aerobic exercise (SLAE) sessions following exhaustive endurance exercise (EEE) on daily basis, although this is a commonly used training regime in recreational athletes and could cause a cumulative increase in CBF that may be important for wound healing. This study examined the effects of EEE on forearm skin blood flow (LDF), cutaneous vascular conductance (CVC), and mean arterial pressure (MAP) in response to SLAE sessions performed for 7 days after EEE, as well as the correlation between cutaneous blood flow and indices associated with heart rate (HR) to examine the role of thermoregulation in post-exercise HR regulation.

Methods. In 19 recreational runners, LDF, MAP, HR, heart rate recovery (HRR), and HR variability indices (lnRMSSD, lnHF, and lnLF/ HF) were measured after SLAE in the form of submaximal graded cycling performed on consecutive days after EEE in the form of a half marathon and compared with baseline values before EEE. A significant time effect was observed for all measured parameters throughout the study period.

Results. Postexercise LDF increased 24 hours after EEE compared with baseline (77.814 AU compared with 54.712 AU). Postexercise hypotension was significantly more pronounced immediately after EEE compared with baseline (88.95.3 mmHg compared with 99.33.2 mmHg). However, postexercise CVC showed a progressive increase compared with baseline both immediately and 24 hours after EEE (0.53 0.07 AU/mmHg, 0.66 0.09 AU/mmHg compared with 0.4 0.09 AU/mmHg). A small negative correlation between LDF and HRR was observed throughout the experimental protocol.

Conclusion. These results suggest that EEE strongly influences cutaneous and systemic hemodynamics and cardiac autonomic response during recovery after SLAE. Our most important finding was that EEE improved cutaneous perfusion 24 hours after completion of EEE, which may be important for wound healing. The results of our study are potentially applicable for patients with chronic wounds who should be encouraged to exercise moderately on daily basis and to include endurance exercises occasionally, as this strategy potentiates postexercise cutaneous perfusion.

(Potočnik N. The Effect of Submaximal Exercise on Cutaneous Blood Flow, Thermoregulation and Recovery Hemodynamics Following Endurance Exercise. SEEMEDJ 2022; 6(2); 32-43)

Received: Oct 28, 2022; revised version accepted: Nov 6, 2022; published: Nov 28, 2022

KEYWORDS: postexercise cutaneous blood flow, endurance exercise, short-lasting aerobic exercise, postexercise hypotension

Introduction

Recreational athletes often include exercises of varying intensity and duration in their daily training schedule. During several consecutive training sessions and subsequent recovery, a complex interplay of many physiological processes, such as thermoregulation, autonomic nervous system adaptation, and nitric oxide production (NO), establishes a dynamic state that may be reflected in cutaneous blood flow (CBF) as the integration site of all the above processes. The term "training recovery" was introduced by Bishop et al. as recovery between successive exercise sessions (1). It can be assumed that the CBF response in training recovery is the cumulative result of recovery and exercise, especially when exhaustive endurance exercise (EEE), with its long-term effects on cardiovascular function (2), is included in the training process. There are numerous reports of CBF in the recovery phase after a single exercise session (3–7) but no one has investigated the CBF response to successive submaximal, short-lasting aerobic exercise (SLAE) sessions following exhaustive exercise on daily basis, although this is a commonly used training regime in recreational athletes. Knowledge of the CBF response to cumulative exercise could be useful in planning exercise strategies for patients with chronic wounds.

During exercise, cutaneous blood flow increases in hairy skin (5), as it is mainly controlled by sympathetic vasodilator fibers. In addition, vasodilation is provoked in an attempt to achieve thermal equilibrium and thus stable core body temperature to allow heat dissipation (8). However, during the recovery phase after exercise, with a sudden decrease in metabolic demand, loss of muscle pump activity, and significant change in autonomic nervous system activity (ANS), cutaneous blood flow rapidly decreases to near baseline levels (5). Nevertheless, core (9,10) and muscle (9) temperatures remain elevated 60-90 min after exercise cessation. Cutaneous blood vessels in non-glabrous skin are innervated by two branches of sympathetic nerves: noradrenergic vasoconstrictor and cholinergic vasodilator fibers. Consequently, the rapid decrease in cutaneous blood flow after cessation of exercise could be caused by increased vasoconstriction, active vasodilation, or a combination of both. Because nitric oxide mediates 30-45% of active cutaneous vasodilation (11), it could potentially contribute to the modulation of cutaneous blood flow after exercise.

After exercise, heart rate (HR) decreases to pre-exercise levels. The initial, rapid phase of HR recovery caused by parasympathetic reactivation is followed by a secondary, slow decline mediated by continued parasympathetic reactivation and sympathetic withdrawal (2). Several studies have examined the mechanisms underlying these post-exercise autonomic responses and have suggested that exercise-induced thermoregulatory demands play an important role (12). There is evidence for the role of thermoregulation in post-exercise HR recovery (13). A possible link between thermoregulation and HR recovery after exercise could be related to thermoregulatory-induced changes in systemic (mean arterial pressure (MAP)) and/or skin hemodynamics (4).

Recently, it has been shown that HR recovery after a short SLAE in response to EEE differs significantly (2), synchronous with changes in ANS activity. Thus, it can be assumed that cutaneous blood flow is simultaneously affected.

Therefore, the aim of this study was to investigate the effects of EEE on cutaneous blood flow in hairy skin after subsequent SLAEs and the relationship between the changes in HR and cutaneous hemodynamic responses to exercise. Therefore, heart rate, arterial blood pressure, and cutaneous blood flow in the volar forearm were measured simultaneously during recovery from SLAE, repeated sequentially before and immediately, 24 hours, 48 hours, and 7 days after EEE. We hypothesized that EEE provokes an increase in cutaneous perfusion and that skin blood flow correlates with concomitant heart rate changes after exercise.

Methods

Subjects

Nineteen recreational runners (13 men) aged 40.4 ± 15.2 years with a body mass index of 23.0 ± 2.7 were recruited to participate voluntarily in this study, which was in accordance with the Declaration of Helsinki and approved by the National Ethics Committee of the Republic of Slovenia (on 10/ 19/2021/No. 0120-126/2021/10). Written informed consent was obtained from all subjects participating in the study. Physical examination and medical history revealed no autonomic dysfunction, chronic diseases, medication use, or smoking. Their ECG and arterial blood pressure were normal. Individual maximum heart rate (HRmax) was determined according to the formula (14).

Procedure

The study was conducted in an air-conditioned laboratory room between 2 pm and 6 pm. Subjects refrained from physical exertion at least three days before the first exercise test and were asked not to perform any other physical activity during the experimental period. They were not allowed to consume alcohol, caffeine, or tobacco for at least 2 hours before the start of each exercise test and were asked to eat a light meal 1 hour before visiting the laboratory. Each participant visited the laboratory 4 times a week for 5 measurements. On the first visit, EEE was performed in the form of a 21-km run on the predefined outdoor track, on partly sunny days with temperatures between 17˚C and 20˚C and humidity between 55% and 65%.

Experimental sessions. SLAE was repeated at 5 different time points: before, one hour (day 0), 24 hours (day 1), 48 hours (day 2), and 7 days (day 7) after EEE, as shown in Figure 1A. Values recorded in the "before" session are referred to as baseline values. SLAE consisted of a 5-minute rest in a seated position followed by a graded exercise test on the Ergoselect 100 (Ergoline, Germany) cycloergometer, starting at 40 W for 3 minutes and continuing with a load increase of 50 W every 3 minutes until the target heart rate (HRpeak), defined as 85% of the individual HRmax, was reached (Fig. 1B). Immediately thereafter, subjects terminated exercise and remained in a seated position for an additional 15 min to passively recover from SLAE.

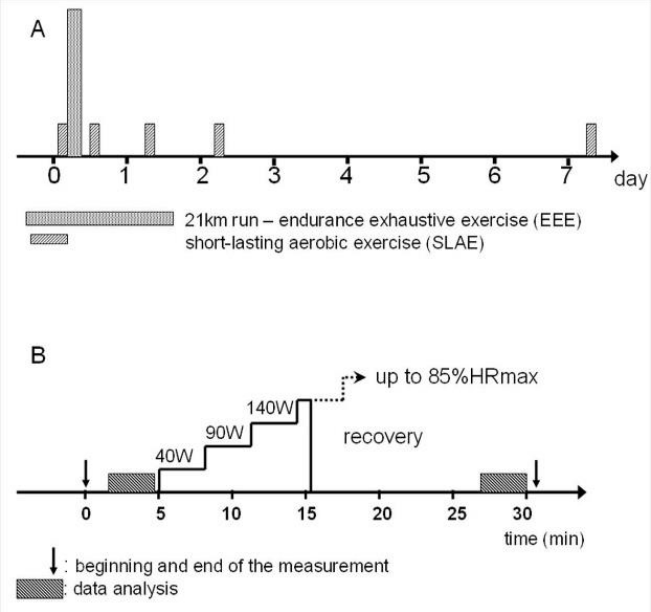

Figure 1. Experimental protocol: schedule of successive exercise bouts (A); short-lasting graded cycling protocol (B)

Measurements

ECG and arterial blood pressure on the middle finger of the right hand were measured continuously (Finometer, Amsterdam, Netherlands). During the measurement, the right arm and hand were placed in an arm rest when sitting on the cycle ergometer that was adjusted to the height of the heart and equipped with hemodynamic sensors. Cutaneous blood flow was measured by laser Doppler (LDF) perfusion monitoring (PeriFlux System 5000, Perimed, Stockholm, Sweden) on the right volar forearm. The principles of LDF monitoring are described elsewhere (15). All signals were recorded simultaneously at 500 Hz using WinDaq data acquisition software (DataQInstruments Inc., Ohio, ZDA). At each SLAE, a time interval of 180 s between the 12th and 15th minutes after cessation of cycling was selected for further analysis. Averaged LDF and MAP were determined using Nevrokard software

(Nevrokard, Slovenia). CVC was calculated as the ratio of LDF to MAP.

Heart rate analysis. RR interval duration was determined beat by beat from ECG using aHRV_file_preparation software (Nevrokard, Slovenia), with artefacts and premature beats corrected. Heart rate (HR) and root mean square of successive differences (RMSSD) as time-domain markers of parasympathetic modulation (Task Force of the European Society of Cardiology) were calculated from RR interval time series using aHRV_analysis_software (Nevrokard), and the natural logarithm of RMSSD (lnRMSSD) was calculated. The following frequency-domain parameters were determined using the autoregressive method (Nevrokard, Slovenia): the power of the high-frequency band (HF; 0.15-0.40 Hz), a marker of parasympathetic modulation, and the LF/HF ratio, which is considered a marker of sympathovagal balance, where LF denotes the power of the low-frequency band (0.04-0.15 Hz) (16). HF and LF/HF were expressed in the natural logarithmic scale (lnHF)

Heart rate recovery in 30 (HRR30) and 60 s (HRR60) was defined as the differences between HRpeak and HR, measured 30 and 60 s after termination of SLAE for each SLAE session.

Statistical analysis

Statistical analysis was performed using IBM SPSS Statistics, version 27 (IBM, New York, USA). Data were tested for normality and log transformed if they were not normally distributed. We compared the mean differences between the measured parameters over time (before, day 0, day 1, day 2, and day 7) with a one-way repeated-measures analysis ANOVA (rANOVA). The assumption of sphericity was checked with the Mauchly's test; Greenhouse-Geisser or Huynh-Feldt corrections were applied when the sphericity assumption was violated, as published elsewhere (17). When a significant time effect was detected, appropriate contrast tests were used to detect differences between mean values at day 0, day 1, day 2, and day 7 compared with the corresponding baseline (before) values. For post hoc comparisons, the least significant difference test was applied and Bonferroni correction was used to eliminate type I errors in multiple comparisons.

Pearson's product-moment correlation coefficients (r) were used to estimate bivariate correlations between each index of cardiac autonomic activity (HRR30, HRR60, lnRMSSD, lnHF, and lnLF/ HF) and subsequent LDF. SSE performance indices (Pmax, HRstmax, RPE) were combined over the entire experimental period. The following criteria were used to interpret the magnitude of correlations: $r \leq 0.1$ - trivial; $r > 0.1$-0.3 - small; $r > 0.3$-0.5 - moderate; $r > 0.5$-0.7 - large; $r > 0.7$-0.9 - very large (17). Data are presented as mean ± standard deviation, and a confidence level $p < 0.05$ was chosen.

Results

LDF, CVC and MAP

In recovery from subsequent SLAE, there was a significant time effect found in LDF ($F=2.9$; $p=0.026$; $\eta 2=0.08$), CVC ($F=4.5$; $p=0.003$; $\eta 2=0.11$) and MAP ($F=2.8$; $p=0.030$; $\eta 2=0.10$), as displayed on Figures 2B, 2C and 2A, respectively.

LDF was significantly augmented 24 hours after EEE compared to baseline (Fig. 2B), while CVC was enhanced already one hour after EEE cessation and even more 24 hours after EEE compared to baseline conditions (Fig. 2C). MAP was significantly decreased one hour after EEE cessation (Fig. 2A) regarding to baseline.

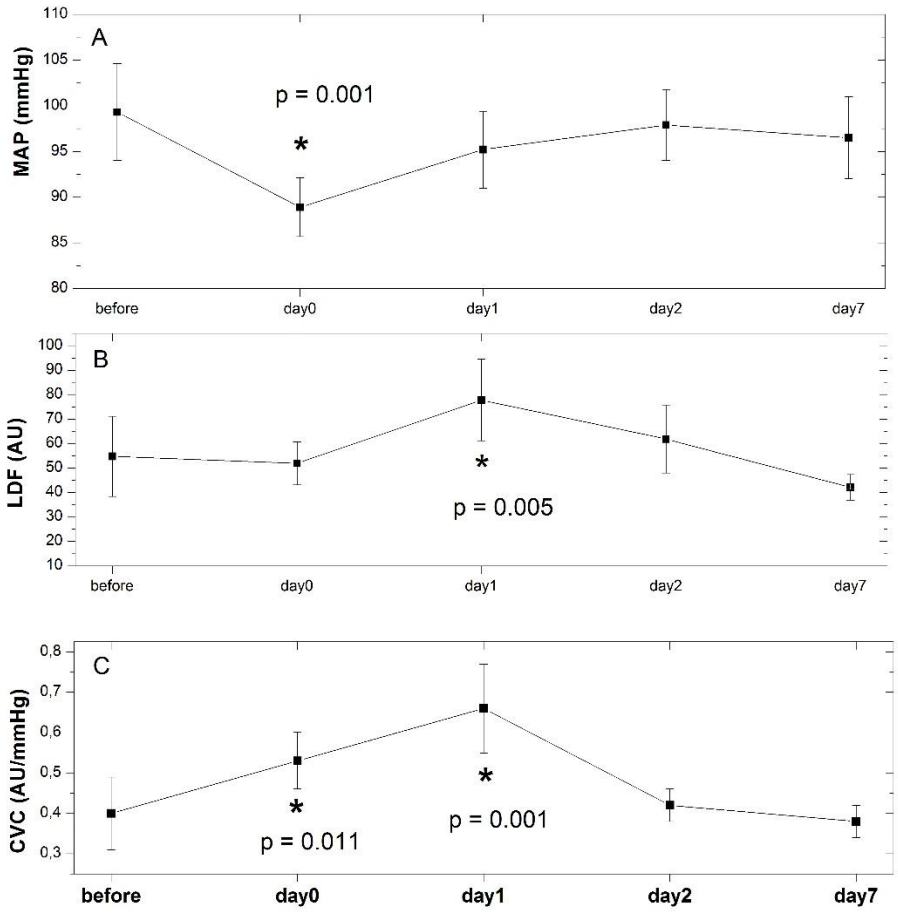

Figure 2: Changes in mean arterial pressure (MAP) (A), laser Doppler flow in the forearm (LDF) (B) and cutaneous vascular conductance (CVC) (C) during experimental protocol (before – before exhausting endurance exercise (EEE); day 0 – 1 hour after EEE; day 1 – 24 hours after EEE; day 2 – 48 hours after EEE, day 7 – 1 week after EEE).

*** - statistically significant compared to baseline (before)**

p – p value according to rANOVA

HR and HR-derived measures

There was a significant time effect found in HR after SLAE ($F=45.6$; $p<0.001$; $\eta 2=0.38$), HRR30 ($F=16.2$; $p<0.001$; $\eta 2=0.20$) and HRR60 ($F=19.6$; $p<0.01$; $\eta 2=0.16$) across all measuring points as displayed in Figure 3. All three parameters exhibited a biphasic change compared to baseline: HR was significantly higher at day 0 and significantly lower at day 1 compared to baseline (Fig. 3), yet HRR30 and HRR60 were significantly lower at day 0 and significantly higher at day 1 compared to baseline (Fig. 3). Additionally, HR after SLAE was decreased also at day 2 compared to baseline (Fig. 3).

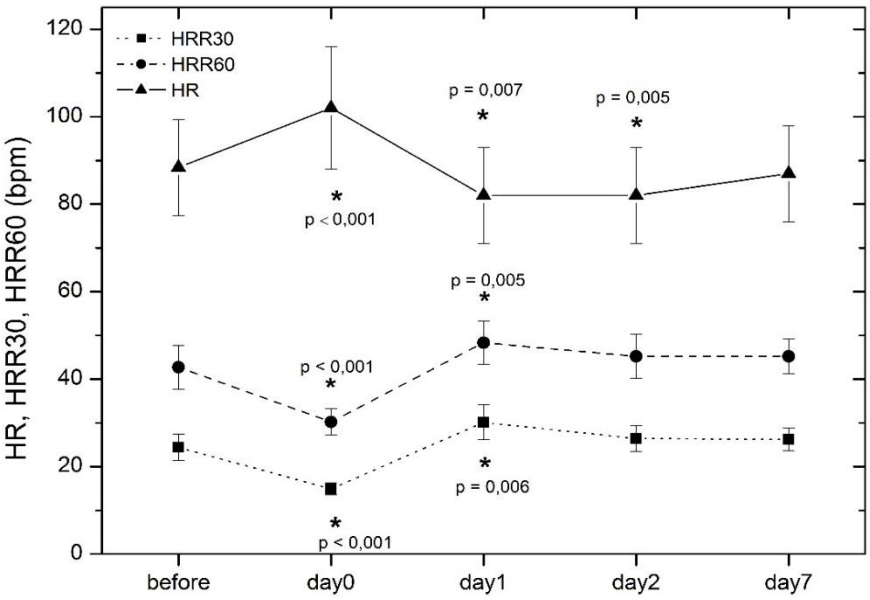

Figure 3: Changes in heart rate (HR) after short-lasting aerobic exercise, heart rate recovery in 30 s (HRR30) and heart rate recovery in 60 s (HRR60) during experimental protocol (before – before exhausting endurance exercise (EEE); day 0 – 1 hour after EEE; day 1 – 24 hours after EEE; day 2 – 48 hours after EEE, day 7 – 1 week after EEE).

*** - statistically significant compared to baseline (before)**

p – p value according to rANOVA

The parameters of heart rate variability, lnRMSSD ($F=10.1$; $p<0.001$; $\eta^2=0.19$), lnHF ($F=7.3$; $p<0.001$; $\eta^2=0.13$) and lnLF/HF ($F=7.6$; $p=0.011$; $\eta^2=0.22$) exhibited significant time effect along measuring protocol (Fig. 4). lnRMSSD behaved biphasically compared to baseline, while lnHF and lnLF/HF differed significantly from baseline only at the day 0 (Fig. 4).

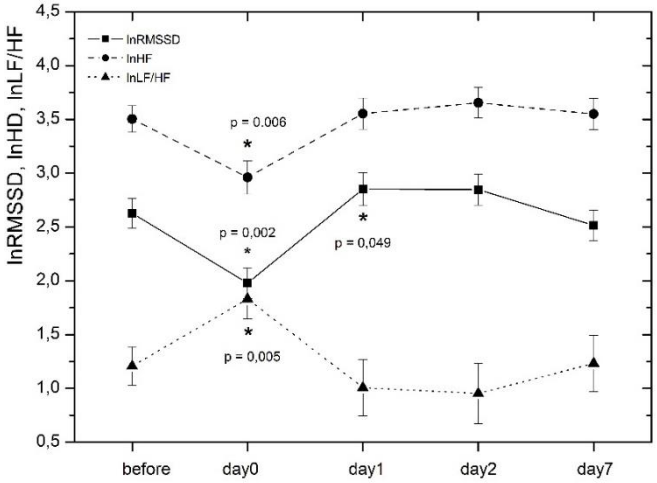

Figure 4: Changes in natural logarithm of root mean square of successive differences (lnRMSSD), the power of high-frequency band (lnHF) and the relationship between the power of low-frequency band to high frequency band (lnLF/HF) during the measuring protocol.

*** - statistically significant compared to baseline (before)**

p – p value according to rANOVA

Bivariate correlations

When all data were pooled there were no clear correlations neither between LDF and HR

(p=0.93), lnRMSSD (p=0.66), lnHF (p=0.17) and lnLF/HF (p=0.34) nor between CVC and HR (p=0.17), lnRMSSD (p=0.78), lnHF (p=0.42), lnLF/HF (p=0.65), HRR30 (p=0.09) and HRR60 (p=0.18), respectively. A small negative correlation was observed between LDF and HRR30 (p=0.036, r= -0.229) as well as between LDF and HRR60 (p=0.032, r= -0.233), as seen in Figures 5A and 5B.

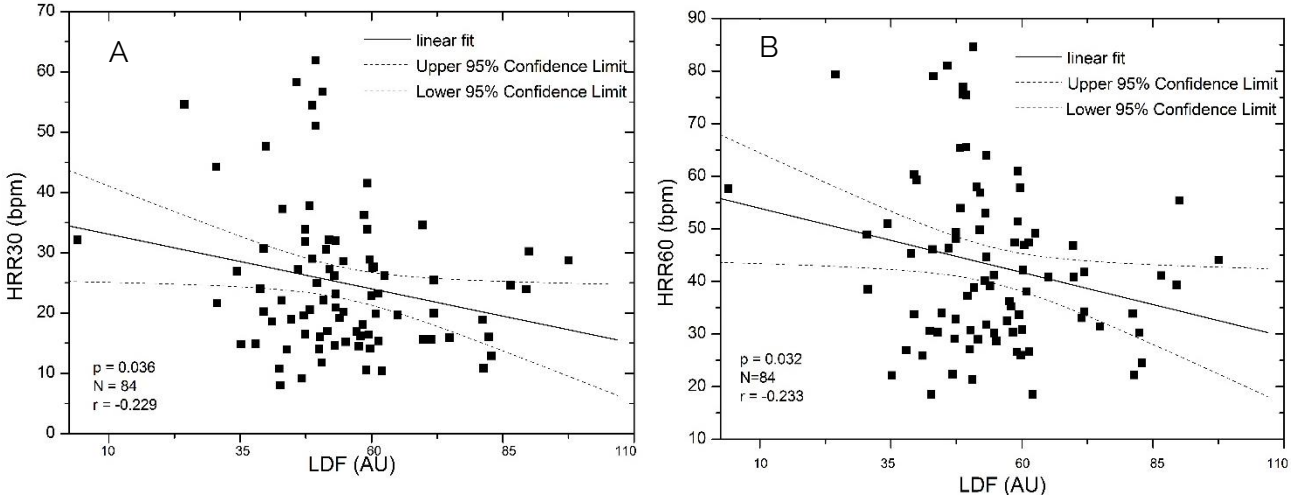

Figure 5: Linear fit between laser-Doppler flow (LDF) in the forearm during recovery from short-lasting aerobic exercise and heart rate recovery in 30 s (HRR30) (A) and heart rate recovery in 60 s (HRR60) (B); 95% confidence limits are indicated by a dashed line. p – p value according to rANOVA; r – Pearson's coefficient; N – number of correlated points

Discussion

In the present study, we investigated the response of cutaneous blood flow in hairy skin in the recovery phase after short lasting aerobic exercise at different time points after exhaustive endurance exercise and compared it with concomitant changes in cardiac autonomic activity in recreational runners. The aim of this study was to contribute to the understanding of the control of cutaneous blood flow in relation to training history. We found that training history has a strong influence on cutaneous (LDF and CVC) and systemic hemodynamics (MAP), as well as on cardiac autonomic (HR, HR derived indices) response during recovery from SLAE. Our most important finding was that exhaustive endurance exercise as part of the training history improved cutaneous perfusion 24 hours after completion of EEE, which may be important for wound healing.

The results of the present study are as follows:

- LDF in the recovery phase at SLAE after exhaustive endurance training was significantly increased 24 hours after EEE compared with baseline, which might be important for wound healing,

- A progressive increase in CVC after training was observed during the first 24 hours after exhaustive endurance training,

- Post-exercise hypotension was significantly increased immediately after exhaustive endurance training, and

- A small bivariate correlation between LDF and HRR30(60) was observed throughout the experimental protocol, indicating the role of thermoregulation in post-exercise regulation HR

To our knowledge, this is the first study to report time-dependent changes in LDF during exercise recovery after exhaustive endurance training. Accordingly, we can only speculate about the mechanisms controlling these changes. During the recovery phase after exercise, there is a rapid decrease in cutaneous perfusion despite a

significant residual heat load (18–21). It has been suggested that both centrally mediated (sympathetic adrenergic and cholinergic innervation) and peripheral endothelium-dependent and independent factors may modulate the control of cutaneous blood flow after exercise (9,22) and that either enhanced vasoconstriction or attenuated active vasodilation may play the role (18). Since nitric oxide mediates 30-45% of active cutaneous vasodilation (18), it seems likely that the bioavailability of NO may additionally influence post-exercise vasodilation. However, the time-dependent contributions of all potentially involved mechanisms during recovery after exhaustive endurance training remain unclear.

According to the literature, postexercise hypotension is caused by at least two mechanisms: increased vasodilation due to thermoregulatory challenges and/or impairment of baroreceptor reflex (23). The predominant mechanism was found to depend on exercise intensity and duration (24). Liu et al. reported that prolonged endurance exercise induces significant postexercise hypotension regardless of exercise intensity (24), and it has been shown that, at least in males, reduced cardiac baroreflex sensitivity triggers postexercise hypotension (25) after a half marathon. In addition, McGinn et al. (26) found decreased baroreflex sensitivity as a major cause of postexercise hypotension after 90 minutes of graded dynamic exercise.

Surprisingly, LDF, CVC, and MAP did not change synchronously during the measurement protocol, although this was generally expected. Based on CVC, which was increased immediately and 24 hours after EEE compared with baseline, one would expect increased postexercise hypotension and skin vasodilation at the same measuring points. However, MAP was significantly decreased only immediately after EEE and LDF was significantly decreased only 24 hours after EEE, suggesting that different mechanisms are involved in the regulation of MAP and LDF. The main cause of the postexercise increase in CVC immediately after EEE appears to be a decreased MAP, whereas its further increase 24 hours after EEE is due to an increased LDF at that measurement time point.

Response immediately after exhaustive endurance exercise

Immediately after EEE, the postexercise decrease of MAP observed in our study compared with baseline (Fig. 2) can be attributed to an impairment of the baroreflex, as suggested by Mourot et al.

After endurance exercise, core body temperature and mean muscle temperature remain elevated for up to 24 hours (20). Therefore, increased cutaneous blood flow during recovery from short lasting aerobic exercise performed immediately after EEE, compared with baseline before endurance exercise, would be expected to eliminate the additional heat load generated during EEE. However, in our study, postexercise LDF was not increased after EEE compared with baseline. The concomitant observed dominance of the cardiac sympathetic nervous system activity over the parasympathetic activity (Fig. 4) suggests that the simultaneously increased adrenergic vasoconstrictor nerve activity affecting the skin may prevent vasodilation.

Another possible explanation would be increased oxidative stress immediately after endurance exercise. Numerous data show that a decreased ability to release NO in the skin microcirculation is associated with increased oxidative stress (19,27). Interestingly, a biphasic response of exhaled NO, a potent surrogate for oxidative stress (28), was reported after endurance exercise (29). More specifically, exhaled NO increased significantly immediately after endurance exercise and decreased 24 hours after endurance exercise compared with the level before endurance exercise. Consequently, we can probably assume that increased oxidative stress immediately after EEE induces endothelial dysfunction with the impairment of NO availability. Immediately after a half marathon, the response of the cardiovascular system to short lasting aerobic exercise has been shown to mimic the response found in cardiovascular dysfunction (2). Thus,

subsequent endothelial dysfunction could be due to cardiovascular dysfunction at that time point.

Dehydration after endurance exercise could lead to decreased MAP and affect cutaneous blood flow. However, concurrent measurements of total body water showed that water volume was preserved after endurance exercise in our study, as reported elsewhere (2).

Response 24 hours after exhaustive endurance exercise

Postexercise MAP was decreased 24 hours after cessation of endurance training compared with baseline, although not to a statistically significant extent (Fig. 2). These results are consistent with the findings of other authors who report that post-exercise hypotension can persist for up to 24 hours (23,30,31).

The main finding of our study was that both LDF and CVC increased significantly at SLAE 24 hours after endurance training compared to baseline (Fig. 2). Since increased skin blood flow accelerates the wound healing process (32), these results support the use of endurance training in wound healing. This finding of our study can be applied in practice by encouraging patients with chronic wounds to include occasional endurance exercise in their regular moderate training schedule to increase skin blood flow and accelerate wound healing. We can only suggest a few possible mechanisms responsible for the improvement in cutaneous blood flow 24 hours after EEE: increased sympathetic cholinergic vasodilation as the main mechanism to eliminate excessive heat, increased NO bioavailability due to suppressed oxidative stress 24 hours after EEE (29), the involvement of adenosine receptors that have been shown to prevent the decrease in skin blood flow after exercise (18), or a complex interplay of many physiological processes leading to cardiovascular supercompensation, which probably includes improved skin blood flow observed by many authors after endurance training (2,33,34). Further studies need to be conducted to substantiate these assumptions.

No significant changes in measured parameters were observed on day 2 and day 7, suggesting that the effect of EEE on cutaneous blood flow diminishes after two days.

Bivariate correlations

We found a small negative correlation between postexercise LDF and HRR30 and HRR60 when data were pooled across the entire measurement protocol (Fig. 5). A correlation of this magnitude requires careful interpretation. However, this correlation suggests that improved cutaneous blood flow delays recovery of HR after SLAEs regardless of endurance exercise. These results are consistent with the conclusions of Pecanha et al. (4), who found that heat stress delays heart rate recovery and highlighted the role of thermoregulation in post-exercise regulation of the HR. They suggested that thermally induced redirection of blood flow to cutaneous vessels, as evidenced by increased LDF, may involve reduced central blood volume and ventricular filling during recovery, resulting in compensatory sympathetic activation and parasympathetic deactivation after exercise (4).

Limitations of our study and perspectives

Our cohort consists of recreational runners, so results are limited to physically active, healthy individuals. Further studies are needed to prove that endurance exercise accelerates wound healing in patients prone to developing chronic wounds, such as those with type 2 diabetes.

Gender and age differences of cutaneous blood flow and postexercise hypotension after endurance exercise described by Stapelton (20) and Mourot et al. (25) were not examined in our study. The analysis of our data should be repeated separately for men and women to identify possible gender differences that could influence our conclusions.

Measurement of core temperature during the study protocol would be helpful to determine the magnitude of heat stress induced by endurance exercise compared with short-lasting exercise.

The proposed mechanisms underlying our results could be better determined if different substances such as bretylium tosylate, an inhibitor of noradrenergic vasoconstriction, and a NO synthase inhibitor (L- NAME) were applied to the skin during the measurement protocol.

Furthermore, spectral analysis based on the fast Fourier or wavelet transform of the periodic oscillations of the LDF after exercise could be used to analyze the periodic oscillations of different frequencies representing the influence of heartbeat, respiration, intrinsic myogenic activity, and neurogenic factors, respectively, on cutaneous blood flow after exercise (3,7). Additional analysis of LDF should be performed according to spectral analysis guidelines.

Conclusion

We measured the response of cutaneous blood flow in the forearm during recovery after short lasting aerobic exercise at different time points after exhaustive endurance exercise and compared it with concomitant changes in cardiac autonomic activity in recreational runners. We aimed to contribute to the understanding of the control of cutaneous blood flow in relation to training history. We found that training history has a strong influence on cutaneous and systemic hemodynamics as well as on cardiac autonomic response during recovery to SLAE. Our most important finding was that exhaustive endurance exercise as a part of the training history improved cutaneous perfusion 24 hours after completion of EEE, which may be important for wound healing. The results of our study are potentially applicable for patients with chronic wounds, who should be encouraged to exercise moderately on daily basis and to occasionally include endurance exercises, as this strategy potentiates postexercise cutaneous perfusion.

Acknowledgement. This research work was funded by the Slovenian Research Agency (core research funding no. P3-0019). The author declares no conflict of interests.

Disclosure

Funding. This research work was funded by the Slovenian Research Agency (core research funding no. P3-0019).
Competing interests. None to declare.

References

1. Bishop PA, Jones E, Woods AK. Recovery from training: A brief review. J Strength Conditioning Research. 2008; 22(3):1015-1024 doi: 10.1519/JSC.0b013e31816eb518

2. Špenko M, Potočnik I, Edwards I, Potočnik N. Training History, Cardiac Autonomic Recovery from Submaximal Exercise and Associated Performance in Recreational Runners. Int J Environ Res Public Health. 2022; 19(16):9797. doi: 10.3390/ijerph19169797

3. Kvernmo HD, Stefanovska A, Bracic M, Kirkebøen KA, Kvernebo K. Spectral analysis of the laser Doppler perfusion signal in human skin before and after exercise. Microvasc Res 1998; 56(3):173-82. doi: 10.1006/mvre.1998.2108.

4. Peçanha T, Forjaz CL d. M, Low DA. Passive Heating Attenuates Post-exercise Cardiac Autonomic Recovery in Healthy Young Males. Front Neurosci. 2017; 11:727. doi: 10.3389/fnins.2017.00727.

5. Potocnik N, Lenasi H. The responses of glabrous and nonglabrous skin microcirculation to graded dynamic exercise and its recovery. Clin Hemorheol Microcirc 2016; 64(1):65-75. doi: 10.3233/CH-162045

6. Reynes C, Beaume JB, Latil-Plat F, Ennaifer H, Rocher L, Antoine-Jonville S, et al. Concomitant Peripheral Neuropathy and Type 2 Diabetes Impairs Postexercise Cutaneous Perfusion and Flowmotion. J Clin Endocrinol Metab 2021; 106(10):e3979-e3989. doi: 10.1210/clinem/dgab414.

7. Rossi M, Santoro G, Maurizio S, Carpi A. Spectral analysis of skin blood flowmotion before and after exercise in healthy trained and in sedentary subjects. Int J Sports Med 2006; 27(7):540-5. doi: 10.1055/s-2005-865825.

8. Gagge AP, Gonzalez RR. Mechanisms of Heat Exchange: Biophysics and Physiology. Compr Physiol. 1996 Dec;45–84. DOI: 10.1002/cphy.cp040104

9. Kenny GP, Webb P, Ducharme MB, Reardon FD, Jay O. Calorimetric measurement of postexercise net heat loss and residual body heat storage. Med Sci Sports Exerc 2008; 40(9):1629-36. doi: 10.1249/MSS.0b013e31817751cb.

10. Wilkins BW, Minson CT, Halliwill JR. Regional hemodynamics during postexercise hypotension. II. Cutaneous circulation. J Appl Physiol (1985). 2004; 97(6):2071-6. doi: 10.1152/japplphysiol.00466.2004.

11. Kellogg DL, Crandall CG, Liu Y, Charkoudian N, Johnson JM. Nitric oxide and cutaneous active vasodilation during heat stress in humans. J Appl Physiol (1985). 1998; 85(3):824-9. doi: 10.1152/jappl.1998.85.3.824.

12. Michael S, Graham KS, Davis GM. Cardiac Autonomic Responses during Exercise and Post-exercise Recovery Using Heart Rate Variability and Systolic Time Intervals—A Review. Front Physiol. 2017 May 29;8.

13. Leicht AS, Sinclair WH, Patterson MJ, Rudzki S, Tulppo MP, Fogarty AL, Winter S. Influence of postexercise cooling techniques on heart rate variability in men. Exp Physiol 2009; 94(6):695-703. doi: 10.1113/expphysiol.2009.046714.

14. Danieli A, Lusa L, Potočnik N, Meglič B, Grad A, Bajrović FF. Resting heart rate variability and heart rate recovery after submaximal exercise. Clin Auton Res 2014; 24(2):53-61. doi: 10.1007/s10286-014-0225-2.

15. Shepherd AP. History of Laser-Doppler Blood Flowmetry. 1990;1–16.

16. Malik M, Camm AJ, Bigger JT, Breithardt G, Cerutti S, Cohen RJ, et al. Heart rate variability. Standards of measurement, physiological interpretation, and clinical use. Task Force of the European Society of Cardiology and the North American Society of Pacing and Electrophysiology. Eur Heart J 1996; 17(3):354-81.

17. Hopkins WG, Marshall SW, Batterham AM, Hanin J. Progressive statistics for studies in sports medicine and exercise science. Med Sci Sports Exerc 2009; 41(1):3-13. doi: 10.1249/MSS.0b013e31818cb278.

18. Mcginn R, Fujii N, Swift B, Lamarche DT, Kenny GP. Adenosine receptor inhibition attenuates the suppression of postexercise cutaneous blood flow. J Physiol 2014; 592(12):2667-78. doi: 10.1113/jphysiol.2014.274068.:

19. Cracowski JL, Roustit M. Human skin microcirculation. Compr Physiol. 2020; 10(3):1105–54. doi: 10.1002/cphy.c190008.

20. Stapleton JM, Fujii N, McGinn R, McDonald K, Kenny GP. Age-related differences in postsynaptic increases in sweating and skin blood flow postexercise. Physiol Rep 2014; 2(7):e12078. doi: 10.14814/phy2.12078.

21. Wong BJ, Hollowed CG. Current concepts of active vasodilation in human skin. Temp (Austin, Tex) 2016; 4(1):41-59. doi: 10.1080/23328940.2016.1200203. 4

22. Jay O, Reardon FD, Webb P, DuCharme MB, Ramsay T, Nettlefold L, et al. Estimating changes in mean body temperature for humans during exercise using core and skin temperatures is inaccurate even with a correction factor. J Appl Physiol 2007; 103(2):443-51. doi: 10.1152/japplphysiol.00117.2007

23. Farinatti P, Pescatello LS, Crisafulli A, Taiar R, Fernandez AB. Editorial: Post-Exercise Hypotension: Clinical Applications and Potential Mechanisms. Front Physiol. 2022 Apr 12;13:720.

24. Liu S, Thomas SG, Sasson Z, Banks L, Busato M, Goodman JM. Blood pressure reduction following prolonged exercise in young and middle-aged endurance athletes. Eur J Prev Cardiol 2013; 20(6):956-62. doi: 10.1177/2047487312454759.

25. Mourot L, Fornasiero A, Rakobowchuk M, Isacco L, Brighenti A, Stella F, Zignoli A, Pellegrini B, Tarperi C, Schena F. Post-Exercise Hypotension and Reduced Cardiac Baroreflex after Half-Marathon Run: In Men, but Not in Women. Int J Environ Res Public Health 2020; 17(17):6337. doi: 10.3390/ijerph17176337.

26. McGinn R, Carter MR, Barrera-Ramirez J, Sigal RJ, Flouris AD, Kenny GP. Does type 1 diabetes alter post-exercise thermoregulatory and cardiovascular function in young adults? Scand J Med Sci Sports 2015; 25(5):e504-14. doi: 10.1111/sms.12344370

27. Holowatz LA, Thompson-Torgerson C, Kenney WL. Aging and the control of human skin blood flow. Front Biosci (Landmark Ed 2010; 15(2):718-39. doi: 10.2741/3642.

28. Pavord ID, Beasley R, Agusti A, Anderson GP, Bel E, Brusselle G, Cullinan P, Custovic A, Ducharme FM, Fahy JV, Frey U, Gibson P, Heaney LG, Holt PG, Humbert M, Lloyd CM, Marks G, Martinez FD, Sly PD, von Mutius E, Wenzel S, Zar HJ, Bush A. After asthma: redefining airways diseases. Lancet. 2018; 391(10118):350–400.

29. Sierra AP, Oliveira-Junior MC, Almeida FM, Benetti M, Oliveira R, Felix SN, Santos Genaro I, Mangueira Saraiva Romanholo B, Ghorayeb N, Peduti Dal Molin Kiss MA, Cury-Boaventura MF, Pesquero JB, Vieira RP. Impairment on Cardiopulmonary Function after Marathon: Role of Exhaled Nitric Oxide. Oxid Med Cell Longev 2019; 2019:5134360. doi: 10.1155/2019/5134360.

30. Pescatello LS, Buchner DM, Jakicic JM, Powell KE, Kraus WE, Bloodgood B, et al. Physical Activity to Prevent and Treat Hypertension: A Systematic Review. Med Sci Sports Exerc 2019; 51(6):1314-1323. doi: 10.1249/MSS.0000000000001943.

31. Day C, Wu Y, Pescatello LS. Evaluating the Methodological Quality of Postexercise Hypotension Aerobic Exercise Interventions. Front Physiol. 2022; 13:407.

32. Raposio E, Bertozzi N, Moretti R, Grignaffini E, Grieco MP. Laser Doppler Flowmetry and Transcutaneous Oximetry in Chronic Skin Ulcers: A Comparative Evaluation. Wounds a Compend Clin Res Pract 2017; 29(7):190-195.

33. Buchheit M, Laursen PB, Al Haddad H, Ahmaidi S. Exercise-induced plasma volume expansion and post-exercise parasympathetic reactivation. Eur J Appl Physiol 2009; 105(3):471-81. doi: 10.1007/s00421-008-0925-1.

34. Hautala A, Tulppo MP, Mäkikallio TH, Laukkanen R, Nissilä S, Huikuri H V. Changes in cardiac autonomic regulation after prolonged maximal exercise. Clin Physiol. 2001; 21(2):238–45..

Author contribution. Single author

Review article

Trefoil Factor 3 Protein and Sepsis – A Review

Iva Bazina [1], Mirela Baus Lončar [1]

[1] Department of Molecular Medicine, Ruđer Bošković Institute, Zagreb, Croatia

*Corresponding author: Iva Bazina; ibazina@irb.hr

Abstract

Sepsis is one of the most common causes of death in hospitalized patients. Disruption of intestinal barrier homeostasis is one of its main hallmarks. Trefoil factor family proteins are known for their role in protecting and repairing the intestinal mucosa. It has been repeatedly shown that the TFF3 protein is involved in maintaining the intestinal barrier. For that reason, it has been studied in the search for objective measures to predict the onset or outcome of sepsis. Several studies have been performed on rodent sepsis models and on sepsis patients, both children and adults. From the limited research available to date, it appears that TFF3 is involved in the pathogenesis of sepsis, but the exact mechanism is not yet clear. Its potential as a sepsis biomarker has so far been low, but more extensive studies on its role in predicting disease severity and outcome, as well as organ dysfunction, may lead to finding specific patient groups or sepsis stages for which it would be suitable.

(Bazina I, Baus Lončar M. Trefoil Factor 3 Protein and Sepsis. SEEMEDJ 2022; 6(2); 44-53)

Received: Jul 26, 2022; revised version accepted: Nov 1, 2022; published: Nov 28, 2022

KEYWORDS: sepsis, trefoil factor 3 (TFF3), biomarker, intestinal mucosal barrier disruption, serum TFF3

Sepsis

Sepsis is one of the leading causes of death in hospitalized patients worldwide [1]. Sepsis is a "life-threatening organ dysfunction caused by a dysregulated host response to infection", as defined by the Third International Consensus Definitions for Sepsis and Septic Shock (Sepsis-3) in 2016 [2]. Since most of the research presented here was conducted before 2016, it is important to note the changes made by Sepsis-3. Earlier definitions stated that sepsis is a consequence of the host's systemic inflammatory response syndrome (SIRS) to infection. When this is complicated by organ dysfunction, it is referred to as severe sepsis, which can progress to septic shock. Sepsis-3 considers this continuum misleading, the criteria of SIRS nonspecific, the term severe sepsis redundant, and defines septic shock as a subset of sepsis in which the underlying circulatory and cellular/metabolic abnormalities are so profound as to significantly increase mortality [2].

Septic conditions can be caused by or lead to alterations in intestinal homeostasis [3]. The gastrointestinal tract is under perpetual pressure from potentially destructive agents, such as chemicals, drugs, bacteria, and their products [4]. The intestinal epithelium, a single layer of cells, forms a selective barrier to the external environment, and is critical in protecting the intestinal mucosa from luminal contents [4]. Alterations in homeostasis of the intestinal barrier can lead to increased production of proteolytic enzymes in the intestine, changes in composition of the mucus layer, epithelial apoptosis, increased permeability of epithelial cells, and inflammatory signaling [5–7]. Gut barrier dysfunction in combination with disturbed balance of the microbiome and immune response can lead to remote injury and the development of multiple organ dysfunction syndrome (MODS), and eventually death [3,8–10].

Trefoil factor family proteins

The trefoil factor family owes its name to a characteristic trefoil-like structure consisting of six disulfide-linked cysteine residues in a 38- or 39-amino-acid sequence [11–13]. There are three members of the family: TFF1, formerly known as pS2 [14], and TFF3, formerly ITF [15], have a single trefoil domain, while TFF2, formerly PSP [16], has two. The trefoil domain enables their resistance to digestion by proteases [15–17], which is important because they are secreted by goblet cells into the hostile environment of the intestine.

Minor disruptions of epithelial integrity are common and require prompt intervention in order to restore homeostasis [18]. Trefoil factor family proteins play a role in maintaining mucosal integrity, which is supported by the fact that their accumulation has been shown to be increased after a gastrointestinal tract injury [19–22]. Normal repair of the epithelium requires restitution and regeneration, with restitution being the critical first phase required to reestablish epithelial continuity [23]. Trefoil factor family proteins have been shown to be important for intestinal epithelial restitution [18,24], with TFF3 even being essential [23]. Mice lacking TFF3 fail to restitute the intestinal mucosal barrier after injury, which makes even minor injuries lethal [23]. The TFF3 protein is involved in maintaining the intestinal barrier by reducing intestinal permeability [25–31]. TFF3 preserves the integrity of the intestinal barrier by inhibiting apoptosis induced by inflammatory stress [32]. It is possible that TFF3 protects the gastrointestinal mucosa through its interaction with mucins [24,33].

Sepsis and its course depend on many factors, including the site and type of infection, genetic predisposition, demographic characteristics, underlying conditions, immune system status, disease progression, treatment, etc., which inherently makes sepsis a very heterogeneous disease [34–37]. In search of objective measures that could predict the onset or outcome of such a complex disease, some research, summarized in this article, has been conducted on proteins belonging to the trefoil factor family [38–47], in particular the TFF3 protein [38–42,45–47].

TFF3 in rodent models of sepsis

Since intestinal barrier disruption has a major impact on the development of sepsis, Jiang et al. studied the changes in the intestinal mucosal immune barrier in septic rats induced by cecal ligation and puncture (CLP) [38]. CLP is the most widely used technique for inducing sepsis in animals [48]. The intestinal mucosa of septic rats exhibited lower TFF3 mRNA expression compared with control groups. The expression levels decreased with time, namely 3, 6, or 12 hours after induction of sepsis. In parallel with the gradual decrease in TFF3 expression, apoptosis increased with time and was higher than in control animals. Under these conditions, bacterial DNA in the blood was increased, i.e., bacterial translocation increased [38].

Later, a group from the same hospital performed the CLP experiment on mice [39]. This time, they divided the animals into 6-hour, 24-hour, and 48-hour groups, depending on how long after induction of sepsis they were sacrificed, and they measured TFF3 protein accumulation. Interestingly, the TFF3 protein level was slightly increased at the 6-hour time point compared with the control group, while the other two time groups showed a significant decrease in the TFF3 protein level. In addition, a significantly lower number of goblet cells was observed in all three groups of treated animals compared with the control group. The researchers did not observe rapid repair of intestinal disruption, which they suggest could be explained by the reduction of TFF3, along with a reduction in goblet cell migration to the site of injury and TGF- β 1 accumulation, as well as an increase in pro-inflammatory cytokines and pro-apoptotic caspase-3 protein levels [39].

Using an LPS (bacterial lipopolysaccharide) induced sepsis model in rats, Shi et al. [40] demonstrated a delay in intestinal mucosal repair during sepsis. They focused on the molecular mechanism through which protein disulfide isomerase a1 (PDIA1) affects the formation of TFF3 dimers and how they change during sepsis; they hypothesized that PDIA1 and TFF3 dimer levels are important contributors to intestinal mucosal destruction and lack of repair, and that PDIA1 is the critical catalyst for TFF3 dimerization. They confirmed a close correlation between PDIA1 and TFF3 dimerization using several methods, including protein modeling. They indicated that TFF3 monomers are unlikely to dimerize in the absence of PDIA1. They noted a decreasing trend in the expression of TFF3 (monomer and dimer) and PDIA1, as well as impaired PDIA1 function in both rat and cell models of sepsis, suggesting that a lack of both may be an important factor in intestinal mucosal damage and impaired repair in sepsis, as impaired PDIA1 function may lead to decreased formation of TFF3 dimers, ultimately resulting in more intestinal damage and less repair.

TFF3 in pediatric patients with sepsis

In search of a new objective diagnostic marker for gastrointestinal failure, a pediatric intensive care unit in China studied serum TFF3 levels of children with MODS, where one group had gastrointestinal failure (GIF), and the other did not [41]. TFF3 levels were associated with both GIF and mortality. Serum TFF3 levels were nearly ten times higher in children with MODS and GIF than in children with MODS and without GIF, and they increased over time. In the group without GIF, serum TFF3 levels remained the same over time and were similar to those of the healthy control group. A total of 71% of the children with MODS, GIF, and high TFF3 died, compared with 32% of the children with normal TFF3 and without GIF. This suggests that early measurement of serum TFF3 levels in hospitals may serve as a prognostic factor, but, as the authors themselves note, the levels should be measured over a longer period in order to see exactly how they change. It should also be noted that this study was conducted in only one hospital in China; it would need to be confirmed in other facilities.

A group from Brno [42] found that the serum TFF3 protein level can distinguish children with SIRS, sepsis, severe sepsis, septic shock, and MODS (according to the 2005 International Pediatric Sepsis Consensus Conference [49]) from control subjects, but the TFF3 level was not adequate for distinguishing between the stages

of septic state prior to the development of severe organ dysfunction. In all patients, the TFF3 level was significantly higher compared with the control group, and in MODS patients, it was significantly higher compared with the rest of the patients. No temporal effect on TFF3 protein level was observed.

The same group also examined TFF1 [43] and TFF2 [44] protein levels in the serum of septic children. They found that TFF1 levels did not discriminate between different septic states up to the development of significant septic shock and organ dysfunction, and TFF2 levels up to organ dysfunction, but the discriminatory power is too low to serve as a diagnostic tool. Both could be used to distinguish septic patients from controls, and TFF2 could additionally differentiate survivors from non-survivors, as its levels were significantly higher in non-survivors [43].

Interestingly, in a study focusing on biomarkers for distinguishing necrotizing enterocolitis (NEC) from septic bowel manifestations, no difference was found between preterm infants with sepsis and control groups [46]. NEC patients had significantly higher TFF3 levels than septic patients, and no association was found between TFF3 and nonspecific systemic inflammation indicators, which suggests that there exists only an association with intestinal damage, rather than the systemic inflammatory response [46]. In addition, TFF3 has been proposed as a potential new therapy for NEC because it was shown that treatment of rat NEC models with TFF3 alleviated the intestinal tissue injury [45].

TFF3 in adult patients with sepsis

A study was conducted on adult intensive care unit (ICU) patients diagnosed with sepsis [47]. The severity of the condition was determined using the APACHE II (acute physiology and chronic health evaluation) score [50], and the extent of organ dysfunction was determined using the SOFA (Sequential Organ Failure Assessment) score [51]. The ELISA assay was used for measurement of septic patients' TFF3 protein levels; they were measured on admission to the ICU and after 3 days of treatment in the ICU. Serum TFF3 levels were significantly higher in septic patients than in control subjects, and they increased with time. Patients with higher APACHE II scores had increased TFF3 concentrations, as did patients with higher SOFA scores. Patients with septic shock, which is defined as severe sepsis complicated with refractory arterial hypotension requiring fluid replacement and vaso¬pressors, had higher TFF3 levels than those with uncomplicated sepsis. While serum TFF3 levels on admission were only slightly higher in patients with a fatal outcome, TFF3 levels were significantly higher three days later in non-survivors compared with survivors. High TFF3 levels correlated with renal dysfunction, systemic inflammation, long ICU stay, and higher mortality. Overall, these results suggest that high serum TFF3 levels are associated with the severity of organ dysfunction and a worse prognosis for the septic patient. The researchers suggest that TFF3 could serve as a prognostic biomarker in the early stages of sepsis, but a larger-scale study is needed first.

In a different study [52], serum TFF3 protein levels were determined in patients with abdominal sepsis, postoperative gastrointestinal patients, and healthy volunteers. TFF3 levels were elevated in patients with abdominal sepsis compared with healthy volunteers, as well as postoperative gastrointestinal patients (no differences were found in the latter two). In contrast to the study presented above [47], TFF3 protein levels were maintained for four days in sepsis patients. Meanwhile, serum TFF3 levels in the postoperative group increased on day 2 and reached sepsis patients' levels on day 4 post-op, suggesting that plasma TFF3 levels increase in response to GI injury of a larger extent or longer duration. TFF3 was higher in patients belonging to both the sepsis and the post-op group who were admitted with shock than those without shock. They found markedly increased TFF3 levels in patients with three or more organs in failure, and a correlation with renal dysfunction. TFF3 levels were higher in abdominal sepsis patients with a fatal outcome; however, TFF3 levels at admission were not a good predictor of survival.

Studies conducted on human subjects are summarized in Table 1.

Table 1. Summary of studies regarding TFF3 in the context of sepsis conducted so far on human subjects

Patient subgroups	Controls	Method	Main findings of the study	Biomarker potential	Ref.
			Pediatric patients		
MODS patients with or without GIF	Healthy controls	ELISA of serum TFF3	Higher serum TFF3 was associated with GIF and with mortality.	Early measurement of serum TFF3 levels may prove useful as a prognostic factor.	[41]
Patients with sepsis, severe sepsis, septic shock, and MODS	Patients undergoing surgery without signs of infection	quantitative enzyme immunoassay of serum TFF3	All septic patients had higher serum TFF3 levels compared to controls with no signs of infection. MODS patients had higher TFF3 levels than other patient groups. Higher TFF3 levels were associated with higher mortality.	TFF3 levels could not differentiate between various septic conditions in patients until a marked organ dysfunction developed.	[42]
			Adult patients		
Patients with sepsis and septic shock	Healthy blood donors	ELISA of serum TFF3	TFF3 concentrations were much higher in sepsis patients than in healthy controls. High serum TFF3 levels were associated with the severity of sepsis and mortality. TFF3 levels were higher in septic shock than uncomplicated sepsis patients.	Serum TFF3 might serve as a potential prognostic biomarker in the early phase of sepsis.	[47]
Abdominal sepsis, postoperative gastrointestinal patients	Healthy volunteers	Luminex multiplex assay of serum TFF3	TFF3 levels were elevated in patients with abdominal sepsis compared with healthy volunteers, as well as postoperative gastrointestinal patients. TFF3 was higher in patients belonging to both the sepsis and the post-op group who were admitted with shock than those without shock. TFF3 levels were higher in abdominal sepsis patients with a fatal outcome.	TFF3 levels at admission were not a good predictor of patient survival.	[52]

The potential of TFF3 as a biomarker for sepsis

Research to date has only scratched the surface of the issue of TFF3 in the context of sepsis. Although the exact mechanisms and details remain to be elucidated, it is evident from both rodent and human data that TFF3 is involved in the pathophysiology of sepsis. In rodent models, lower intestinal TFF3 levels were associated with septic conditions and decreased intestinal repair, while in humans, higher serum TFF3 levels correlated with disease severity. It is difficult to compare the currently available human and rodent data since they are scarce, describe different things, and so far do not offer any mechanistic explanations. A link between TFF3 and sepsis possibly lies in sepsis-induced dysfunction of the intestinal barrier. Intestinal permeability and apoptosis [9], as well as both pro- and anti-inflammatory cytokine production [53] are the hallmarks of sepsis. TFF3 is essential for intestinal epithelial restitution [23], and it preserves the integrity of the intestinal barrier by inhibiting apoptosis induced by inflammation [32]. The expression of TFF3 can be regulated by inflammatory signals and vice versa [54]. The association between TFF3 activation and some known interleukins produced in sepsis, such as IL-6 [55,56], IL-10 [57], IL-8 [58,59], TNF α [60], IFN γ, and IL-12 [61], was previously reported. Perhaps a balance between cytokine and TFF3 activation in sepsis determines the progression and outcome of the disease.

The major limitation of sepsis research conducted so far were the small and demographically homogeneous patient groups for such a heterogeneous disease. Further and more extensive studies are needed to explore the molecular role of TFF3 in the pathogenesis of sepsis, the mechanisms of intestinal damage and repair, the immune response, apoptosis, and the temporal evolution of its effect. It remains to be seen whether sepsis promotes TFF3 production or whether TFF3 promotes sepsis progression, and at what stage of the disease it makes the greatest contribution. Based on the information available to date, TFF3 is not a good biomarker for sepsis in general, but further research into its potential for predicting disease severity and outcome, as well as organ dysfunction, may lead to finding specific patient populations or stages of sepsis for which it is appropriate.

Acknowledgement. This paper was supported by the Croatian Science Foundation grant IP-06-2016-2717 and the European Structural Fund 2014–2020 as financial support for the PhD student I. Bazina.

Disclosure

Funding. None.

Competing interests. None to declare.

References

1. Rudd KE, Johnson SC, Agesa KM, Shackelford KA, Tsoi D, Kievlan DR, Colombara D V., Ikuta KS, Kissoon N, Finfer S, Fleischmann-Struzek C, Machado FR, Reinhart KK, Rowan K, Seymour CW, Watson RS, Eoin West T, Marinho F, Hay SI, Lozano R, Lopez AD, Angus DC, Murray CJL, Naghavi M. Global, Regional, and National Sepsis Incidence and Mortality, 1990–2017: Analysis for the Global Burden of Disease Study. Lancet 2020; 395: 200–211. doi:10.1016/S0140-6736(19)32989-7.

2. Singer M, Deutschman CS, Seymour W, Shankar-Hari M, Annane D, Bauer M, Bellomo R, Bernard GR, Chiche J-D, Coopersmith CM, Hotchkiss RS, Levy MM, Marshall JC, Martin GS, Opal SM, Gordon D Rubenfeld GD, van der Poll T, Vincent J-L, Angus DC. The Third International Consensus Definitions for Sepsis and Septic Shock (Sepsis-3) Clinical Review & Education Special Communication | CARING FOR THE CRITICALLY ILL PATIENT. JAMA 2016; 315: 801–810. doi:10.1001/jama.2016.0287.

3. Haussner F, Chakraborty S, Halbgebauer R, Huber-Lang M. Challenge to the Intestinal Mucosa during Sepsis. Front Immunol 2019;

10: 891. doi:10.3389/FIMMU.2019.00891/BIBTEX.

4. Podolsky DK. V. Innate Mechanisms of Mucosal Defense and Repair: The Best Offense Is a Good Defense*. 1999https://doi.org/10.1152/ajpgi.1999.277.3.G495

5. Wells JM, Brummer RJ, Derrien M, MacDonald TT, Troost F, Cani PD, Theodorou V, Dekker J, Méheust A, De Vos WM, Mercenier A, Nauta A, Garcia-Rodenas CL. Homeostasis of the Gut Barrier and Potential Biomarkers. Am J Physiol - Gastrointest Liver Physiol 2017; 312: G171–G193. doi: 10.1152/ajpgi.00048.2015.

6. Altshuler AE, Lamadrid I, Li D, Ma SR, Kurre L, Schmid-Schönbein GW, Penn AH. Transmural Intestinal Wall Permeability in Severe Ischemia after Enteral Protease Inhibition. PLoS One 2014; 9: e96655. doi:10.1371/JOURNAL.PONE.0096655.

7. Chang M, Alsaigh T, Kistler EB, Schmid-Schönbein GW. Breakdown of Mucin as Barrier to Digestive Enzymes in the Ischemic Rat Small Intestine. PLoS One 2012; 7: e40087. doi:10.1371/JOURNAL.PONE.0040087.

8. Mittal R, Coopersmith CM. Redefining the Gut as the Motor of Critical Illness. Trends Mol Med 2014; 20: 214–223. doi:10.1016/J.MOLMED.2013.08.004.

9. Fay KT, Ford ML, Coopersmith CM. The Intestinal Microenvironment in Sepsis. Biochim Biophys Acta - Mol Basis Dis 2017; 1863: 2574–2583. doi:10.1016/J.BBADIS.2017.03.005.

10. Clark JA, Coopersmith CM. Intestinal Crosstalk: A New Paradigm for Understanding the Gut as the "Motor" of Critical Illness. Shock 2007; 28:384–393. doi:10.1097/SHK.0B013E31805569DF.

11. Thim L. A New Family of Growth Factor-like Peptides 'Trefoil' Disulphide Loop Structures as a Common Feature in Breast Cancer Associated Peptide (PS2), Pancreatic Spasmolytic Polypeptide (PSP), and Frog Skin Peptides (Spasmolysins). FEBS Lett 1989; 250: 85–90. doi:10.1016/0014-5793(89)80690-8.

12. Carr MD. Proton NMR-Based Determination of the Secondary Structure of Porcine Pancreatic Spasmolytic Polypeptide: One of a New Family of "Trefoil" Motif Containing Cell Growth Factors. Biochemistry 1992; 31: 1998–2004. doi:10.1021/BI00122A015/SUPPL_FILE/BI00122A015_SI_001.PDF.

13. De A, Brown DG, Gorman MA, Carr M, Sanderson MR, Freemont PS. Crystal Structure of a Disulfide-Linked "trefoil" Motif Found in a Large Family of Putative Growth Factors. Proc Natl Acad Sci U S A 1994; 91: 1084–1088. doi:10.1073/PNAS.91.3.1084.

14. Masiakowski P, Breathnach R, Bloch J, Gannon F, Krust A, Chambon P. Cloning of CDNA Sequences of Hormone-Regulated Genes from the MCF-7 Human Breast Cancer Cell Line. Nucleic Acids Res 1982; 10: 7895–7903. doi:10.1093/NAR/10.24.7895.

15. Suemori S, Lynch-Devaney K, Podolsky DK. Identification and Characterization of Rat Intestinal Trefoil Factor: Tissue- and Cell-Specific Member of the Trefoil Protein Family. Proc Natl Acad Sci U S A 1991; 88: 11017–11021. doi:10.1073/PNAS.88.24.11017.

16. Jørgensen KH, Thim L, Jacobsen HE. Pancreatic Spasmolytic Polypeptide (PSP): I. Preparation and Initial Chemical Characterization of a New Polypeptide from Porcine Pancreas. Regul Pept 1982; 3:207–219. doi:10.1016/0167-0115(82)90126-4.

17. Kinoshita K, Taupin DR, Itoh H, Podolsky DK. Distinct Pathways of Cell Migration and Antiapoptotic Response to Epithelial Injury: Structure-Function Analysis of Human Intestinal Trefoil Factor. Mol Cell Biol 2000; 20: 4680–4690.

18. Taupin D, Podolsky DK. TREFOIL FACTORS : INITIATORS OF MUCOSAL HEALING. 2003; 4: doi:10.1038/nrm1203.

19. Hanby AM, Poulsom R, Elia G, Singh S, Longcroft JM, Wright NA. The Expression of

the Trefoil Peptides PS2 and Human Spasmolytic Polypeptide (HSP) in 'Gastric Metaplasia' of the Proximal Duodenum: Implications for the Nature of 'Gastric Metaplasia.' J Pathol 1993; 169: 355–360. doi:10.1002/PATH.1711690313.

20. Podolsky DK, Lynch-Devaney K, Stow JL, Oates P, Murgue B, DeBeaumont M, Sands BE, Mahida YR. Identification of Human Intestinal Trefoil Factor. Goblet Cell-Specific Expression of a Peptide Targeted for Apical Secretion. J Biol Chem 1993; 268: 6694–6702. doi:10.1016/S0021-9258(18)53305-6.

21. Wright NA, Poulsom R, Stamp GWH, Hall PA, Jeffery RE, Longcroft JM, Rio M -C, Tomasetto C, Chambon P. Epidermal Growth Factor (EGF/URO) Induces Expression of Regulatory Peptides in Damaged Human Gastrointestinal Tissues. J Pathol 1990; 162: 279–284. doi:10.1002/PATH.1711620402.

22. Nakov R. New Markers in Ulcerative Colitis. Clin Chim Acta 2019; 497:141–146. doi:10.1016/J.CCA.2019.07.033.

23. Mashimo H, Wu DC, Podolsky DK, Fishman MC. Impaired Defense of Intestinal Mucosa in Mice Lacking Intestinal Trefoil Factor. Science (80-) 1996; 274:262–265. doi:10.1126/SCIENCE.274.5285.262.

24. Dignass A, Lynch-Devaney K, Kindon H, Thim L, Podolsky DK. Trefoil Peptides Promote Epithelial Migration through a Transforming Growth Factor β -Independent Pathway. J Clin Invest 1994; 94:376–383. doi:10.1172/JCI117332.

25. Beck PL, Wong JF, Li Y, Swaminathan S, Xavier RJ, Devaney KL, Podolsky DK. Chemotherapy- and Radiotherapy-Induced Intestinal Damage Is Regulated by Intestinal Trefoil Factor. Gastroenterology 2004; 126: 796–808. doi:10.1053/j.gastro.2003.12.004.

26. Carrasco R, Pera M, May FEB, Westley BR, Martinez A, Morales L. Trefoil Factor Family Peptide 3 Prevents the Development and Promotes Healing of Ischemia-Reperfusion Injury in Weanling Rats. J Pediatr Surg 2004; 39: 1693–1700. doi:10.1016/J.JPEDSURG.2004.07.017.

27. Meyer zum Büschenfelde D, Tauber R, Huber O. TFF3-Peptide Increases Transepithelial Resistance in Epithelial Cells by Modulating Claudin-1 and -2 Expression. Peptides 2006; 27: 3383–3390. doi:10.1016/J.PEPTIDES.2006.08.020.

28. Xu LF, Teng X, Guo J, Sun M. Protective Effect of Intestinal Trefoil Factor on Injury of Intestinal Epithelial Tight Junction Induced by Platelet Activating Factor. Inflammation 2012; 35: 308–315. doi:10.1007/S10753-011-9320-X/FIGURES/8.

29. Buda A, Jepson MA, Pignatelli M. Regulatory Function of Trefoil Peptides (TFF) on Intestinal Cell Junctional Complexes. http://dx.doi.org/103109/154190612012748326 2012; 19: 63–68. doi:10.3109/15419061.2012.748326.

30. Wang Y, Liang K, Kong W. Intestinal Trefoil Factor 3 Alleviates the Intestinal Barrier Function Through Reducing the Expression of TLR4 in Rats with Nonalcoholic Steatohepatitis. Arch Med Res 2019; 50: 2–9. doi:10.1016/J.ARCMED.2019.03.004.

31. Lin N, Xu L fen, Sun M. The Protective Effect of Trefoil Factor 3 on the Intestinal Tight Junction Barrier Is Mediated by Toll-like Receptor 2 via a PI3K/Akt Dependent Mechanism. Biochem Biophys Res Commun 2013; 440: 143–149. doi:10.1016/J.BBRC.2013.09.049.

32. Podolsky DK, Gerken G, Eyking A, Cario E. Colitis-Associated Variant of TLR2 Causes Impaired Mucosal Repair Because of TFF3 Deficiency. Gastroenterology 2009; 137: 209–220. doi:10.1053/j.gastro.2009.03.007.

33. Thim L, Madsen F, Poulsen SS. Effect of Trefoil Factors on the Viscoelastic Properties of Mucus Gels. Eur J Clin Invest 2002; 32: 519–527. doi:10.1046/J.1365-2362.2002.01014.X.

34. Fohner AE, Greene JD, Lawson BL, Chen JH, Kipnis P, Escobar GJ, Liu VX. Assessing Clinical Heterogeneity in Sepsis through Treatment Patterns and Machine Learning. J Am Med Informatics Assoc 2019; 26: 1466–1477. doi:10.1093/JAMIA/OCZ106.

35. Prescott HC, Calfee CS, Taylor Thompson B, Angus DC, Liu VX. Toward Smarter Lumping and Smarter Splitting: Rethinking Strategies for Sepsis and Acute Respiratory Distress Syndrome Clinical Trial Design. Am J Respir Crit Care Med 2016; 194:147–155. doi:10.1164/RCCM.201512-2544CP/SUPPL_FILE/DISCLOSURES.PDF.

36. Cohen J, Vincent JL, Adhikari NKJ, Machado FR, Angus DC, Calandra T, Jaton K, Giulieri S, Delaloye J, Opal S, et al. Sepsis: A Roadmap for Future Research. Lancet Infect Dis 2015; 15: 581–614. doi:10.1016/S1473-3099(15)70112-X.

37. Hotchkiss RS, Sherwood ER. Getting Sepsis Therapy Right. Science (80-) 2015; 347:1201–1202. doi:10.1126/SCIENCE.AAA8334.

38. Jiang L, Zhang M, Zhou T, Yang Z, Wen L, Chang J. Changes of the Immunological Barrier of Intestinal Mucosa in Rats with Sepsis. World J Emerg Med 2010; 1: 138.

39. Chang R, Wen L, Chang J, Fu Y, Jiang Z, Chen S. Repair of Damaged Intestinal Mucosa in a Mouse Model of Sepsis. World J Emerg Med 2013; 4:223. doi:10.5847/WJEM.J.ISSN.1920-8642.2013.03.012.

40. Shi Y, Wang C, Wu D, Zhu Y, Wang ZE, Peng X. Mechanistic Study of PDIA1-Catalyzed TFF3 Dimerization during Sepsis. Life Sci 2020; 255:117841. doi:10.1016/J.LFS.2020.117841.

41. Fujikawa T, Fujikawa T, Yoshimoto Y, Kawamura Y, Kawamoto H, Yamamoto T, Tanaka A. Association between Trefoil Factor 3 and Gastrointestinal Failure in Critically Ill Children. J Gastroenterol Hepatol Res 2013; 2: 765–768. doi:10.6051/.

42. Žurek J, Kỳr M, Vavřina M, Fedora M. Trefoil Factor 3 as a Marker of Intestinal Cell Damage during Sepsis. Open Med 2015; 10: 261–266. doi:10.1515/MED-2015-0020/MACHINEREADABLECITATION/RIS.

43. Žurek J, Fedora M. Trefoil Factor 1 as a Marker of Mucosal Damage of the Gastrointestinal Tract in Children with Sepsis. https://doi.org/103109/1354750X201378311 6 2013; 18: 338–342. doi:10.3109/1354750X.2013.783116.

44. Žurek J, Kýr M, Vavřina M, Fedora M. Trefoil Factor 2 Expression and Its Significance as a Predictor of Severity of Sepsis in Children. Peptides 2013; 46: 1–5. doi:10.1016/J.PEPTIDES.2013.04.011.

45. Shi L, Zhang BH, Yu HG, Yu JP, Xi JL. Intestinal Trefoil Factor in Treatment of Neonatal Necrotizing Enterocolitis in the Rat Model. J Perinat Med 2007; 35: 443–446. doi:10.1515/JPM.2007.096/MACHINEREADABLECITATION/RIS.

46. Ng EWY, Poon TCW, Lam HS, Cheung HM, Ma TPY, Chan KYY, Wong RPO, Leung KT, Lam MMT, Li K, et al. Gut-Associated Biomarkers L-FABP, I-FABP, and TFF3 and LIT Score for Diagnosis of Surgical Necrotizing Enterocolitis in Preterm Infants. Ann Surg 2013; 258: 1111–1118. doi:10.1097/SLA.0B013E318288EA96.

47. Sun W, Qin J, Shan R-F, Zhu Y-A, Zhu H-Y. Elevated Serum Levels of Trefoil Factor 3 Are Correlated with Severity of Sepsis Patients. Int J Clin Exp Pathol 2016; 9: 8122–8131.

48. Dejager L, Pinheiro I, Dejonckheere E, Libert C. Cecal Ligation and Puncture: The Gold Standard Model for Polymicrobial Sepsis? Trends Microbiol 2011; 19: 198–208. doi:10.1016/J.TIM.2011.01.001.

49. Goldstein B, Giroir B, Randolph A. International Pediatric Sepsis Consensus Conference: Definitions for Sepsis and Organ Dysfunction in Pediatrics. Pediatr Crit Care Med 2005; 6: doi:10.1097/01.PCC.0000149131.72248.E6.

50. Knaus WA, Draper EA, Wagner DP, Zimmerman JE. APACHE II: A Severity of Disease Classification System. Crit Care Med 1985; 13: 818–829. doi:10.1097/00003246-198510000-00009.

51. Vincent JL, De Mendonça A, Cantraine F, Moreno R, Takala J, Suter PM, Sprung CL,

Colardyn F, Blecher S. Use of the SOFA Score to Assess the Incidence of Organ Dysfunction/Failure in Intensive Care Units: Results of a Multicenter, Prospective Study. Working Group on "Sepsis-Related Problems" of the European Society of Intensive Care Medicine. Crit Care Med 1998; 26: 1793–1800. doi:10.1097/00003246-199811000-00016.

52. Meijer MT, Uhel F, Cremer OL, Scicluna BP, Schultz MJ, van der Poll T. Elevated Trefoil Factor 3 Plasma Levels in Critically Ill Patients with Abdominal Sepsis or Non-Infectious Abdominal Illness. Cytokine 2020; 133: 155181. doi:10.1016/J.CYTO.2020.155181.

53. Chaudhry H, Zhou J, Zhong Y, Ali MM, Mcguire F, Nagarkatti PS, Nagarkatti M. Role of Cytokines as a Double-Edged Sword in Sepsis. In Vivo 2013; 27: 669.

54. Hoffmann W. Trefoil Factor Family (Tff) Peptides and Their Links to Inflammation: A Re-Evaluation and New Medical Perspectives. Int. J. Mol. Sci. 2021; , 22, 4909.

55. Jiang GX, Zhong XY, Cui YF, Liu W, Tai S, Wang ZD, Shi YG, Zhao SY, Li CL. IL-6/STAT3/TFF3 Signaling Regulates Human Biliary Epithelial Cell Migration and Wound Healing in Vitro. Mol Biol Rep 2010; 37: 3813–3818. doi:10.1007/s11033-010-0036-z.

56. Barrera GJ, Sanchez G, Gonzalez JE. Trefoil Factor 3 Isolated from Human Breast Milk Downregulates Cytokines (IL8 and IL6) and Promotes Human Beta Defensin (HBD2 and HBD4) Expression in Intestinal Epithelial Cells HT-29. Bosn J Basic Med Sci 2012; 12: 256–264. doi:10.17305/bjbms.2012.2448.

57. Belle NM, Ji Y, Herbine K, Wei Y, Park JH, Zullo K, Hung LY, Srivatsa S, Young T, Oniskey T, et al. TFF3 Interacts with LINGO2 to Regulate EGFR Activation for Protection against Colitis and Gastrointestinal Helminths. Nat Commun 2019; 10: 1–13. doi:10.1038/s41467-019-12315-1.

58. Lau WH, Pandey V, Kong X, Wang XN, Wu Z, Zhu T, Lobie PE. Trefoil Factor-3 (TFF3) Stimulates De Novo Angiogenesis in Mammary Carcinoma Both Directly and Indirectly via IL-8/CXCR2. PLoS One 2015; 10: e0141947. doi:10.1371/JOURNAL.PONE.0141947.

59. Barrera Roa GJ, Sanchez Tortolero G. Trefoil Factor 3 (TFF3) from Human Breast Milk Activates PAR-2 Receptors, of the Intestinal Epithelial Cells HT-29, Regulating Cytokines and Defensins. Bratislava Med J 2016; 117: 332–339. doi:10.4149/BLL_2016_066.

60. Baus Loncar M, Al-Azzeh ED, Sommer PSM, Marinovic M, Schmehl K, Kruschewski M, Blin N, Stohwasser R, Gött P, Kayademir T. Tumour Necrosis Factor α and Nuclear Factor κB Inhibit Transcription of Human TFF3 Encoding a Gastrointestinal Healing Peptide. Gut 2003; 52: 1297–1303. doi:10.1136/gut.52.9.1297.

61. Fu T, Znalesniak EB, Kalinski T, Möhle L, Biswas A, Salm F, Dunay IR, Hoffmann W. TFF Peptides Play a Role in the Immune Response Following Oral Infection of Mice with Toxoplasma Gondii. Eur J Microbiol Immunol 2015; 5: 221–231. doi:10.1556/1886.2015.00028..

Author contribution.
Conception and design: IB, MBL
Critical revision of the article for important intellectual content: IB, MBL
Drafting of the article: IB, MBL
Final approval of the article: IB, MBL

Original article

Comorbidity of Somatic Illnesses on People With Treated Mental Disorders – A New Challenge in Medicine

Romana Marušić [1,2], Adriana Levaković [2], Dunja Degmečić [2,3], Tatjana Bačun [2,4*]

1 Department of Internal Medicine, National Memorial Hospital Vukovar, Croatia
2 Faculty of Medicine, J.J. Strossmayer University, Osijek, Croatia
3 Department of Psychiatry, University Hospital Centre, Osijek, Croatia
4 Division of Endocrinology, Department of Internal Medicine, University Hospital Centre, Osijek; Croatia

*Corresponding author: Tatjana Bačun, tbacun@gmail.com

Abstract

Aim. Comorbidities pose a major challenge for 21st century medicine. The mutual pathophysiological effect of one disease on another can significantly affect their course and prognosis. The aims of this study were to examine the frequency of comorbidities and the most common psychiatric and somatic comorbidities and to determine the difference in the incidence of certain diseases by gender and age.

Methods. Data were recorded in several groups: demographic characteristics, psychiatric and somatic diagnoses classified according to gender, age, and the legally determined ability to work, and correlations of somatic and psychiatric diagnoses.

Results. The most common psychiatric diagnoses in men were post-traumatic stress disorder (PTSD) (25%) and alcoholism (23%), while in women these were recurrent depressive disorder (19%) and psychosis (10%). A statistically significant difference was found in the incidence of alcoholism and PTSD, which are more common in men than in women. The most common somatic diseases in both sexes were arterial hypertension (M = 33%, F = 46%) and diabetes mellitus (M = 18%, F = 32%). Statistically significant differences were found in the frequency of hypertension ($p = 0.03$) and epilepsy ($p = 0.002$), which are more common in men. The ratio alcoholism-hypertension ($p = 0.03$), alcoholism-diabetes ($p < 0.0001$), alcoholism-COPD ($p < 0.001$) was statistically significant.

Conclusion. It is extremely important to improve the multidisciplinary approach and cooperation in treatment in order to reduce the number of hospitalizations, emergency interventions and suicides and to improve the patients' quality of life and life expectancy.

(Marušić R, Levaković A, Degmečić D, Bačun T*. Comorbidity of Somatic Illnesses on People With Treated Mental Disorders – A New Challenge in Medicine. SEEMEDJ 2022; 6(2); 54-66)

Received: Apr 12, 2022; revised version accepted: Oct 20, 2022; published: Nov 28, 2022

KEYWORDS: chronic diseases, comorbidity, mental disorders

Introduction

Comorbidity indicates the presence of two or more different diseases or disorders simultaneously and poses a major challenge for 21st century medicine (1). People with a chronic physical illness are 1.5 to 2 times more likely to develop a mental disorder (2).

It is estimated that 25% of the general population has some form of mental disorder. Of these, as many as 68% have one or more physical comorbidities (3). Due to the extended average lifespan, the prevalence of multimorbidity is increasing; in Australia, it is 75% for people aged 65 to 74 and over 80% for people aged 75 and above. A study conducted in Ontario showed a multimorbidity of 7 to 35 % in people between the ages of 18 and 65 (4). In Croatia, the prevalence of multimorbidity is 79.8 % for people over 65 (5).

Mental disorders are a major public health problem that has a significant impact on the health of people with chronic diseases and can change the course of their illness and their prognosis. Depression is present in 40% of people with hypertension; the prevalence is 36.6% in men and as much as 63.4% in women. In somatically healthy individuals with depressive disorder, the risk of coronary heart disease is increased 1.5- to 2-fold, while in individuals with coronary heart disease, the risk of myocardial infarction is increased 1.5- to 4.5-fold (2). Some studies show that the prevalence of depressive disorders in people with diabetes ranges from 8 to 15% (6). Only 25% to 50% of people with diabetes who suffer from depression get diagnosed and treated (7). The risk of complications of the disease is increased as much as 4 times due to the reduced ability to regulate glucose metabolism (1, 8). Other studies show that as many as 47.6% of young people with insulin-dependent diabetes develop a mental disorder after ten years, most often one year after diagnosis (2).

The cost of hospital treatment of patients with comorbid depression was increased 1.5-fold compared with other patients. The positive correlation of psychological comorbidities with the length of hospital stays, doctor visits, and longer sick leave has also been proven, which leads to a reduced quality of life and higher treatment costs (2). One study showed that every fifth person in physical rehabilitation suffers from a comorbid mental disorder. This has an adverse effect on the outcome of rehabilitation due to the patient's reduced motivation, cooperation, and active participation in the rehabilitation process (9).

Due to the high incidence of comorbidities of physical and mental illnesses, it is important to conduct preventive examinations, personalized pharmacotherapy and psychotherapy, and educational programs for medical professionals. An integrative approach and timely recognition and treatment can reduce mortality, morbidity, and overall treatment costs (10).

The aims of our research were to examine the frequency of comorbidities and the most common psychiatric and somatic comorbidities and to determine the difference in the incidence of certain diseases by gender and age.

Patients and methods

Patients and study design

The research was organized as a cross-sectional study with historical data. It was approved by

the Ethics Committee of the Faculty of Medicine Osijek, Josip Juraj Strossmayer University

in Osijek. The study was conducted on 137 subjects who were hospitalized at the Clinic for Psychiatry of the Clinical Hospital Center Osijek. Data were collected from the hospital information system of the Clinical Hospital Center Osijek over a period of one year. Inclusion criterion was diagnosis of any somatic illness in psychiatric patients.

Methods

Data were categorized in several groups: demographic characteristics of respondents, psychiatric and somatic diagnoses classified

according to gender, age, and the legally determined ability to work (up to 65 years), and correlations of somatic and psychiatric diagnoses. To examine the correlation between somatic and psychiatric diagnoses, only diagnoses for which frequency was higher than 3% (N ≥ 7 for psychiatric, N ≥ 5 for somatic diagnoses) in total population and somatic diagnoses that are applicable in both genders came into consideration.

Statistical analysis

R software was used to perform statistical analysis of the collected data. Descriptive data are expressed in frequency and share for nominal variables and arithmetic and standard deviation for numerical variables that have a normal distribution. The normality of distribution was examined using the Kolmogorov-Smirnov test. Differences of category variables were tested by binomial, $\chi 2$, and Fisher's exact test, and the degree of correlation was examined by the ϕ test. Differences of numerical variables with normal distribution were tested by Student's t-test. The level of statistical significance was set at $p < 0.05$.

Results

The study included 137 respondents, of whom 95 (70%) were men and 42 (30%) were women. The mean age of men was 55.9 ± 12.1 (22 to 87) and women 56.9 ± 13.5 (16 to 80). Of the 137 respondents, 2% were aged between 18 and 30, 76% were between 30 and 65, and 23% were over 65. A statistically significant difference was found in the number of respondents by sex, in the group aged 35 to 65 years ($p < 0.0001$). Respondents were divided according to employment into employed, unemployed, and retired ones: A statistically significant difference was found between retired men and women ($p < 0.0001$) (Table 1).

Table 1. Demographic characteristics of respondents

	Male	Female	Total	p
Age	55.9±12.2	56.9±13.5		0.68
Age category				
16-30	2(20%)	1(2%)	3(2%)	0.56
30-65	73(77%)	30(71%)	103(76%)	**< 0.0001**
65 +	20(20%)	11(26%)	31(23%)	0.15
Employment status				
Employed	15(16%)	3(7%)	18(13%)	< 0.05
Unemployed	22(23%)	16(39%)	38(28%)	0.41
Retired	57(60%)	22(54%)	79(59%)	**< 0.0001**

The most common psychiatric diagnoses in men were post-traumatic stress disorder (PTSD) (25%), alcoholism (23%), recurrent depressive disorder (13%), while in women the most common ones were recurrent depressive disorder (19%), psychosis (10%), alcoholism, PTSD, and anxiety-depressive disorder (7%). A statistically significant difference was found in the incidence of alcoholism and PTSD, which were more common in men than in women (Table 2).

Table 2. Psychiatric diagnoses of respondents

	Male	Female	Total	p
Alcoholism	33(23%)	4(7%)	37(18%)	**< 0.0001**
Recurrent depressive disorder	18(13%	11(19%)	29(14%)	0.26
PTSD*	35(25%)	4(7%)	39(19%)	**< 0.0001**
Psychoorganic syndrome	7(5%)	2(3%)	9(4%)	0.18
Anxiety-depressive disorder	3(2%)	4(7%)	7(3%)	1
Psychosis	8(6%)	6(10%)	14(7%)	0.79
Another inorganic psychotic disorder	1(1%)	0(0%)	1(0%)	
Pervasive developmental disorder	0(0%)	1(2%)	1(0%)	
Mild mental retardation	4(3%)	1(2%)	5(2%)	0,27
Delirium tremens	3(2%)	0(0%)	3(1%)	
Organic insane disorder	1(1%)	3(5%)	4(2%)	0,62
Schizophrenia	6(4%)	3(5%)	9(4%)	0.5
Borderline depressive decompensation	4(3%)	3(5%)	7(3%)	1
Depressive disorder	10(7%)	3(5%)	13(6%)	0.09
Bipolar affective disorder	2(1%)	4(7%)	6(3%)	0.68
Crisis	1(1%)	4(7%)	5(2%)	0.37
OCD*	3(2%)	0(0%)	3(1%)	
Schizoaffective disorder	2(1%)	3(5%)	5(2%)	1
Organic emotionally labile disorder	0(0%)	3(5%)	3(1%)	
Anorexia nervosa	1(1%)	0(0%)	1(0%)	

*PTSD – Post-traumatic stress disorder, OCD – Obsessive-compulsive disorder

Of the somatic diagnoses, the most common diagnoses in both sexes were arterial hypertension (M = 33%, F = 46%), diabetes mellitus (M = 18%, F = 32%) and epilepsy (M = 15%, F = 8%). Statistically significant differences were found in the frequency of arterial hypertension (p = 0.03) and epilepsy (p = 0.002), which were more common in men (Table 3).

Table 3. Somatic diagnoses of respondents

	Male	Female	Total	p
Arterial hypertension	41(33%)	23(46%)	64(36%)	**0.03**
Diabetes mellitus	23(18%)	16(32%)	39(22%)	0.34
Epilepsy	19(15%)	4(8%)	23(13%)	**0.002**
COPD*	5(4%)	2(4%)	7(4%)	0.45
Liver cirrhosis	1(1%)	0(0%)	1(1%)	
Gastric ulcer	2(2%)	0(0%)	2(1%)	
Pneumonia	2(2%)	0(0%)	2(1%)	
Hashimoto's thyroiditis	0(0%)	1(2%)	1(1%)	
Multiple sclerosis	1(1%)	0(0%)	1(1%)	
Lumbosacral pain	2(2%)	0(0%)	2(1%)	
Esophagitis	0(0%)	0(0%)	0(0%)	
Chronic gastritis	5(4%)	0(0%)	5(3%)	
Venous ulcer	1(1%)	0(0%)	1(1%)	
Pulmonary embolism	0(0%)	1(2%)	1(1%)	
NHL*	1(1%)	0(0%)	1(1%)	
Angina pectoris	3(2%)	0(0%)	3(2%)	
Esophageal cancer	1(1%)	0(0%)	1(1%)	
Psoriasis	4(3%)	0(0%)	4(2%)	1
Prostate hyperplasia	5(4%)	0(0%)	5(3%)	
Parkinson's disease	3(2%)	0(0%)	3(2%)	
Acute renal failure	1(1%)	0(0%)	1(1%)	
Cystitis	1(1%)	0(0%)	1(1%)	
Hepatitis	1(1%)	0(0%)	1(1%)	
Cervicobrachial syndrome	0(0%)	1(2%)	1(1%)	
GERD*	1(1%)	0(0%)	1(1%)	
SLE*	0(0%)	2(4%)	2(1%)	
Urine retention	1(1%)	0(0%)	1(1%)	
Hodgkin's disease	1(1%)	0(0%)	1(1%)	

*COPD – Chronic obstructive pulmonary disease, NHL – Non-Hodgkin's lymphoma, GERD – Gastroesophageal reflux disease, SLE – Systemic lupus erythematosus

Since we were interested in the frequency of psychiatric diagnoses among respondents, we divided them into groups based on their employment status and age. The most common illness-related psychiatric diagnoses among retired respondents were recurrent depressive disorder (31%), PTSD (26%), and alcoholism (12%). Unemployed respondents were most often diagnosed with alcoholism (25%), recurrent depressive disorder (16%), and PTSD (14%). Similar diagnoses were most common among employed respondents: alcoholism (33%) and

PTSD (11%). $\chi 2$ showed a significant statistical difference in the number of patients with PTSD and recurrent depressive disorder among retired, unemployed, and employed respondents under the age of 65 (Table 4).

Table 4. Psychiatric diagnoses according to the employment status

	Retired		Unemployed	Employed	
	> 65	< 65	> 65	< 65	p
Alcoholism	5(12%)	10(12%)	13(25%)	9(33%)	0.8
Psychosis	5(12%)	0(0%)	4(8%)	2(7%)	
PTSD*	2(5%)	21(26%)	7(14%)	3(11%)	**0.0004**
Schizophrenia	2(5%)	5(16%)	2(4%)	0(0%)	
Borderline depressive decompensation	0(0%)	3(4%)	2(4%)	2(7%)	0.98
Depressive disorder	5(12%)	2(2%)	5(10%)	2(7%)	0.63
Bipolar affective disorder	0(0%)	4(5%)	1(2%)	1(4%)	0.5
Mixed anxiety-depressive disorder	0(0%)	3(4%)	3(6%)	1(4%)	0.85
Recurrent depressive disorder	5(12%)	25(31%)	8(16%)	2(7%)	**< 0.0001**
Organic emotionally labile disorder	3(7%)	0(0%)	0(0%)	0(0%)	
Mild mental retardation	0(0%)	2(2%)	0(0%)	1(4%)	
Crisis	1(2%)	1(1%)	1(2%)	287%)	0.96
Psychoorganic syndrome	10(24%)	5(6%)	0(0%)	0(0%)	
Organic delusional disorder	2(5%)	0(0%)	1(1%)	1(4%)	
Anorexia nervosa	0(0%)	0(0%)	1(2%)	0(0%)	
Schizoaffective disorder	0(0%)	0(0%)	4(8%)	0(0%)	
Pervasive developmental disorder	0(0%)	0(0%)	0(0%)	0(0%)	
Delirium tremens	1(2%)	0(0%)	0(0%)	1(4%)	
OCD*	0(0%)	0(0%)	0(0%)	0(0%)	

*PTSD – Post-traumatic stress disorder, OCD – Obsessive-compulsive disorder

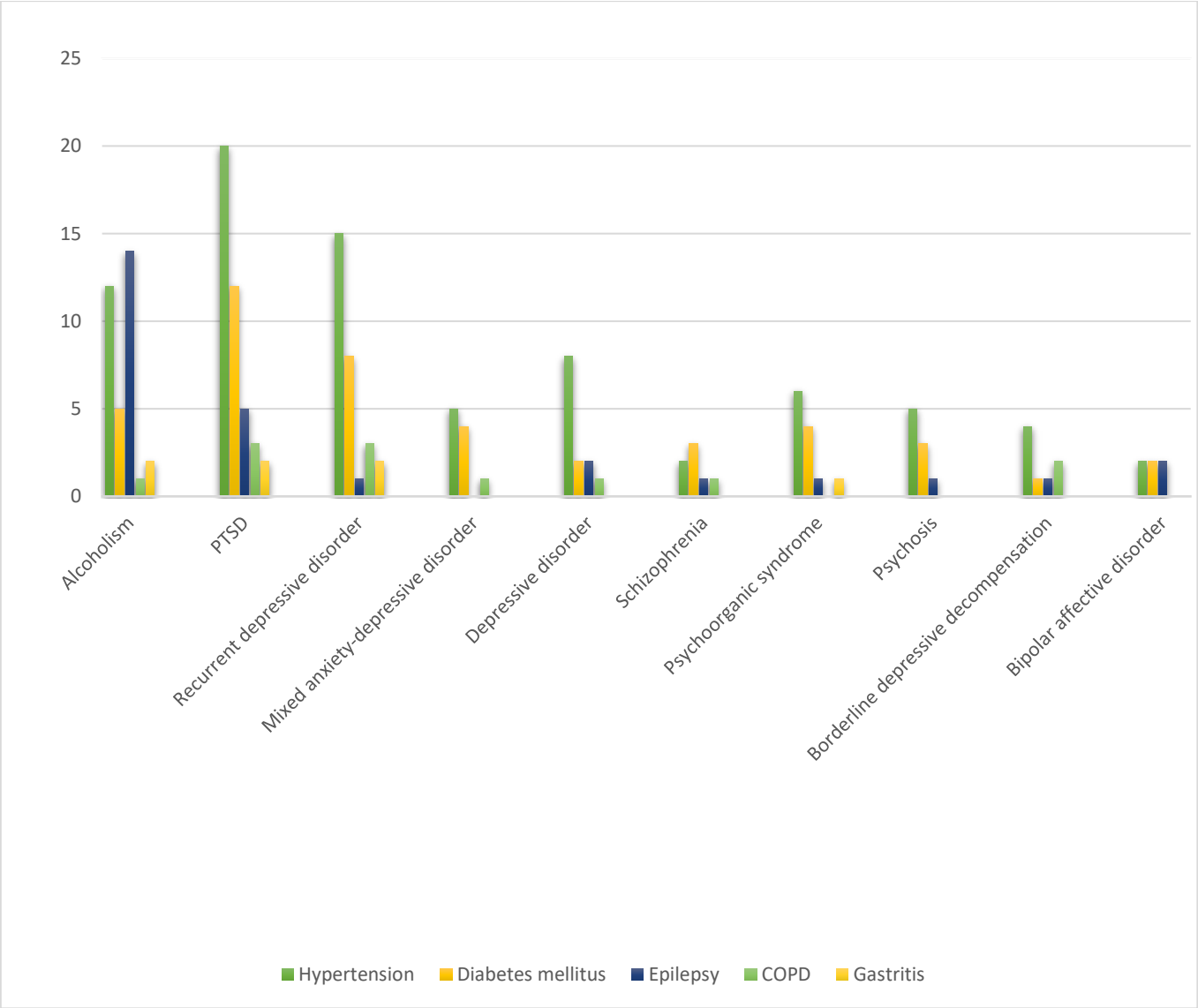

Figure 1. Correlation of somatic and psychiatric diagnoses

*** PTSD – Post-traumatic stress disorder, COPD – Chronic obstructive pulmonary disease**

With the aim of roughly determining the correlation of somatic and psychiatric diagnoses, a graph was made to reflect that correlation (Figure 1).

We took the most significant diagnoses from the graph and made a matrix in which we tested the statistical significance and correlation of the most common diagnoses:

1. Psychiatric diagnoses: alcoholism, recurrent depressive disorder, PTSD, mixed anxiety-depressive disorder, schizophrenia, depressive disorder

2. Somatic diagnoses: hypertension, diabetes mellitus, epilepsy, COPD, gastritis.

The ratios alcoholism-hypertension ($p = 0.03$), alcoholism-diabetes mellitus ($p < 0.0001$), alcoholism-COPD ($p < 0.001$) were statistically significant, which means that respondents treated for alcoholism had a lower risk for hypertension, diabetes, and COPD, although the correlation was almost equal to zero ($\Phi 1 = 0.03$, $\Phi 2 = 0$, $\Phi 3 = 0.004$) (Table 5).

Table 5. Correlation of somatic and psychiatric disorders

		HYPERTENSION				DIABETES MELLITUS				EPILEPSY				COPD				GASTRITIS		
		Yes	No	p	ϕ	Yes	No	p	ϕ	Yes	No	p	ϕ	Yes	No	p	Φ	Yes	No	p
Alcoholism	Yes	12	25	0.03	0.03	5	32	**<0.0001**	0.18	14	23	0.18		1	36	<0.001	0.004	2	35	0.62
	No	52	45			59	38			50	47			6	92			1	94	
Recurrent depressive disorder	Yes	15	14	0.678		8	21	1		1	28	**0.03**	0.03	3	26	0.17		2	27	0.3
	No	49	56			31	74			22	83			4	101			3	102	
PTSD	Yes	20	19	0.7		12	27	0.84		5	34	0.46		3	36	0.41		2	37	0.63
	No	44	51			27	68			18	77			4	91			3	92	
Psychoorganic syndrome	Yes	6	3	0.31		4	5	0.45		1	8	1		0	9			1	8	0.29
	No	58	67			35	90			22	103			7	118			4	121	
Mixed anxiety-depressive disorder	Yes	5	2	0.26		4	3	0.19		0	7			1	6	0.32		0	7	
	No	59	68			35	92			23	104			6	121			5	122	
Psychosis	Yes	5	4	0.74		3	6	0.72		1	8	1		0	9			0	9	
	No	59	66			36	89			22	103			7	118			5	120	
Schizophrenia	Yes	2	6	0.28		3	5	0.69		1	7	1		1	7	0.36		0	8	
	No	62	64			36	90			22	104			6	120			5	121	
Borderline depressive decompensation	Yes	4	3	0.7		1	6	0.67		1	6	1		2	6	0.056		0	7	
	No	60	67			38	89			22	105			5	121			5	122	
Depressive disorder	Yes	8	4	0.23		2	10	0.5		2	10	1		1	11	0.49		0	12	
	No	56	66			37	85			21	101			6	116			5	117	
Bipolar affective disorder	Yes	2	4	0.69		2	4	1		2	4	0.27		0	6			0	6	
	No	62	66			37	91			21	107			7	121			5	123	

* PTSD – Post-traumatic stress disorder, COPD – Chronic obstructive pulmonary disease

Discussion

Comorbidities of physical and mental disorders occur with high frequency, and they are most often present in people over 65 years of age. In this study, a statistically significant difference was found in the incidence of PTSD and alcoholism in men and women; they were significantly more common in men, while recurrent depressive disorder was more common in women.

In our research, PTSD is almost four times more common in men. It is estimated that 3 to 6% of the population suffers from PTSD. Seeing as some studies show that about 49.8% of people who were in the war develop PTSD, these findings can be related to the Croatian War of Independence in the early 1990s. PTSD was most often diagnosed in retired respondents under the age of 65 (26% of respondents), which

we can also attribute to the recent Croatian war history. Although several studies show increased incidence of somatic diseases in patients who suffer from PTSD, our study did not show a statistically significant correlation between PTSD and certain somatic diseases (11, 12, 13). One of the possible reasons could be a small number of participants in our study. PTSD is often associated with physical comorbidities ranging from nonspecific dizziness, tinnitus, and blurred vision to chronic pain, diabetes, cardiovascular, respiratory, and gastrointestinal diseases. There is also increased risk of cancer, arthritis, autoimmune and inflammatory diseases. In our study, the most common somatic disease in patients with PTSD was hypertension. A high ratio of patients with PTSD have unhealthy lifestyles and habits such as heavy smoking, low physical activity, and obesity, which lead to development of vascular, degenerative, and other types of somatic disorders (14). As many as 80% of people have at least one mental disorder with PTSD, the most common being depressive disorder, generalized anxiety disorder, and addictive disorder. Due to non-cooperation, the frequency of hospitalizations and relapses is high (15). Therefore, it is important to identify individuals suffering from this disease, encourage them to cope with the problem, and take care of their mental and physical health to avoid further consequences and comorbidities (16).

In our study, the most common mental disorder in women was recurrent depressive disorder (19%). The most common comorbidity with a recurrent depressive disorder was hypertension (4). Studies have shown that individuals with depression are more likely to develop hypertension, strokes, and ischemic heart disease. There is a pathophysiological connection between depression and hypertension because both disorders are characterized by increased sympathetic tone and increased secretion of adrenocorticotropic hormone and cortisol. Moreover, depressed patients may have difficulty adhering to their therapy regimen, resulting in poor blood pressure control (17). The prevalence of depression is 10 to 15%, with over 350 million people currently affected. Risk factors for developing depression disorder include stressful events, genetic predisposition, disability, illness, previous treatment for depression disorder and sleep problems. Somatic chronic diseases increase the risk of developing depression due to reduced quality of life, difficulty coping with diagnosis, pain, and rejection of the environment (4). Also, the prevalence of depression in people who suffer from at least one chronic illness is 9.3 to 23% and differs greatly from people who do not suffer from any chronic disorder (3.2 %). Increased prevalence of depressive disorders has been noticed in people suffering from cardiovascular diseases (17-27%), diabetes (11-31%), and arthritis (10-24%) (4, 17).

In this research, 25% of men and 7% of women were treated for alcoholism. It is estimated that 43% of the world's population consumes alcohol (18). In Croatia, about 6% of the population suffers from alcohol dependence, which amounts to about 250,000 people (19). Spirits (44.8 %) and beer (34.3 %) are most often consumed. Alcoholism is twice as common in men than in women, with the highest frequency between the ages of 20 and 24 (18). Alcoholics have twice the risk of developing other mental illnesses; these are most often anxiety disorders, affective disorders, personality disorders. Psychiatric disorders are thought to precede the development of alcoholism, except for obsessive-compulsive disorder and depression, which occur after alcohol use disorder (20). In addition, there is also a great link with various physical comorbidities.

In our study, the most common somatic diseases in patients treated for alcoholism were epilepsy and hypertension. Alcohol has a significant effect on the central nervous system, leading to symptoms of mania, depression, and epileptic seizures. Chronic alcohol consumption is related to multiple central and peripheral nervous system dysfunctions due to the direct action of alcohol or its derivatives and vitamin deficiencies associated with alcoholism (21). According to data from 2012, alcohol consumption was associated with 5.5% of cancers (7.2% in men and 3.5% in women) and

with 5.8% of deaths in oncological patients (22). The most common cancers associated with alcohol use are cancers of the oral cavity, pharynx, larynx, esophagus, liver, breast, and colon. The carcinogenic potential is linearly dependent on the amount of consumed alcohol (23). Alcohol consumption has a dual effect on the cardiovascular system; it has a cardioprotective effect in small doses (one standard drink), but it is harmful in large doses (24). The consumption of two standard drinks is considered to have a protective effect in diabetes mellitus but consuming four standard drinks a day results in negative effects. Since most of the alcohol is metabolized in the liver, liver diseases are not uncommon; chronic liver diseases that lead to cirrhosis are the most often (25). Primary alcoholic dementia accounts for 10% of all dementias (26).

Arterial hypertension is the most common somatic disease in this study. It affected 33% of men and 46% of women, a total of 36% of the respondents. Hypertension and coronary heart disease cause significant morbidity in patients, reduce the quality of life, and increase treatment costs. Psychosocial factors that lead to anxiety disorders play a role in the development of hypertension. Increased autonomic excitation via the hypothalamic-pituitary axis leads to an increase in circulating catecholamines, which increases the risk of hypertension and proinflammatory conditions, which in turn leads to the development of coronary heart disease (27). Also, hypertension intensifies symptoms of anxiety and the frequency of panic attacks. In one study, a significantly higher incidence of panic attacks was noticed in patients with hypertension (17%) compared to normotensive patients (11%) (28). Other anxiety disorders are also common; monitoring cardiac activity or avoiding certain activities often results in reduced quality of life in patients with hypertension (29).

Diabetes mellitus is the second most common somatic diagnosis in our respondents (22%). We found a higher incidence in women (32%) than in men (18%). 30% of patients with diabetes suffer from a mental disorder. Patients with schizophrenia are two to four times more likely to develop diabetes compared to the general population (30). The prevalence rates of depression and anxiety are significantly higher in diabetics; some studies have reported that the risk is increased by as much as 50-100%. The correlation is two-way, depression disorder results from years of uncontrolled or poorly controlled diabetes. Depression disorder, on the other hand, activates neurohormonal and neurotransmitter changes that stimulate the hypothalamic-pituitary axis and the adrenal gland, which releases more cortisol and other hormones responsible for insulin resistance (30, 31). The prevalence of diabetes in depressed adult patients is significantly higher in women than in men. A study conducted in Saudi Arabia reported that 37% of patients with type 1 diabetes mellitus, 37.9% of patients with type 2 diabetes mellitus, and 13.6% of patients with gestational diabetes suffer from depression. Another study reported that 46.15% of patients have these comorbidities, of which 36.7% suffer from severe depression. What is more, levels of glycosylated hemoglobin (HbA1c) are significantly higher in people with depression compared with those who do not suffer from it (30).

Epilepsy affected 15% of men and 8% of women, a total of 13% of respondents. It is estimated that the most common mental illness in comorbidity with epilepsy is depression, and its incidence is about 35%. In patients in whom epilepsy is poorly controlled, the incidence is about 50%, while in patients with well-controlled seizures it is about 10 to 20% (31). One study showed that 16.7% of patients with epilepsy have some sort of anxiety disorder; most people had frequent panic attacks (81.2%). Older age of patients and later onset of epileptic seizures are associated with a higher incidence of anxiety disorders (32).

Comorbidities of physical and mental illnesses are a major challenge in medicine. The mutual pathophysiological effect of one disease on another can significantly affect the course and prognosis of the disease. Due to the diverse symptoms experienced by people with multimorbidity, diagnoses are often missed, which can lead to major consequences. It is extremely important to improve cooperation in

treatment and the multidisciplinary approach to the patient in order to reduce the number of hospitalizations, emergency interventions, suicides and improve the patients' quality of life and life expectancy.

Acknowledgement. None.

References

1. Sartorius N. Comorbidity of mental and physical disorders: a key problem for medicine in the 21st century. Acta Psychiatrica Scandinavica 2018; 137(5):369-370.

2. Klesse C, Baumeister H, Bengel J, Härter M. Somatische und psychische Komorbidität. Psychotherapeut 2008; 53:49–62.

3. Šprah L, Dernovšek MZ, Wahlbeck K, Haaramo P. Psychiatric readmissions and their association with physical comorbidity: a systematic literature review. BMC Psychiatry 2017; 17(1):2.

4. Read JR, Sharpe L, Modini M, Dear BF. Multimorbidity and depression: A systematic review and meta-analysis. J Affect Disord 2017; 221:36-46.

5. Kašuba Lazić Đ, Cedilnik Gorup E. Bolesnik s istodobnim bolestima u obiteljskoj medicini. U: Katić M, Švab I i sur: Obiteljska medicina. Zagreb: Alfa Zagreb, 2013; 391-400.

6. Engidaw, N.A., Wubetu, A.D. & Basha, E.A. Prevalence of depression and its associated factors among patients with diabetes mellitus at Tirunesh-Beijing general hospital, Addis Ababa, Ethiopia. BMC Public Health. 2020:266.

7. Bădescu SV, Tătaru C, Kobylinska L, Georgescu EL, Zahiu DM, Zăgrean AM, Zăgrean L. The association between Diabetes mellitus and Depression. J Med Life. 2016; 9(2):120-5.

8. Zhang Y, Chen Y, Ma L. Depression and cardiovascular disease in elderly: Current understanding. J Clin Neurosci 2018; 47:1-5.

9. Härter M, Baumeister H, Bengel J, eds. Psychische Störungen bei körperlichen Erkrankungen. Berlin: Springer, 2007.

10. Filipčić I, Šimunović Filipčić I. Psihički poremećaji i tjelesne bolesti. Medicus 2017; 26 (2 Psihijatrija danas):205-208.

11. von Känel R, Begré S, Abbas CC, Gander ML, Schmid JP. Inflammatory Biomarkers in Patients with Posttraumatic Stress Disorder Caused by Myocardial Infarction and the Role of Depressive Symptoms. Neuroimmunomodulation, 2010; 17: 39-46.

12. van Kamp I, van der Velden PG, Stellato RK et. al. Physical and mental health shortly after a disaster: first results from the Enschede firework disaster study. Eur J Public Health, 2006; 16(3): 253-9.

13. Fischer CJ, Struwe J, Lemke MR. Longterm effect of traumatic experiences on somatic and psychic complaints of German World War Two refugees. Nervenartz, 2006; 77(1): 58-63.

14. Kadoic D, Obradovic M, Čandrilic M, Filakovic P. Neurobiological and clinicla consequences of posttraumatic stress disorder. Acta Clin Croat, 2000; 39: 89-94.

Disclosure

Funding. No specific funding was received for this study.
Competing interests. None to declare.

15. Mimica N, Uzun S, Kozumplik O, Žakić Milas D, Glavina T. Psihometrijski i klinički instrumenti za procjenu posttraumatskog stresnog poremećaja i ocjenu terapijskog učinka. Medicina Fluminensis 2018; 54(2):155-165.

16. Naguy A, Alamiri B. PTSD - Inevitable or preventable? Australas Psychiatry 2018; 26(6):670.

17. Rubio-Guerra AF, Rodriguez-Lopez L, Vargas-Ayala G, Huerta-Ramirez S, Serna DC, Lozano-Nuevo JJ. Depression increases the risk for uncontrolled hypertension. Exp Clin Cardiol. 2013 Winter; 18(1):10-2.

18. World Health Organization. Global status report on alcohol and health 2018. https://apps.who.int/iris/handle/10665/274603 (07 December 2021).

19. Rapić M, Vrcić Keglević M. ALKOHOLIZAM – ZABORAVLJENA DIJAGNOZA U OBITELJSKOJ MEDICINI. Medicina familiaris Croatica 2014; 22(2):25-32.

20. Powell BJ, Penick EC, Othmer E, Bingham SF, Rice AS. Prevalence of additional psychiatric syndromes among male alcoholics. J Clin Psychiatry 1982; 43(10):404-407.

21. Fouarge E, Maquet P. Conséquences neurologiques centrales et périphériques de l'alcoolisme [Neurological consequences of alcoholism]. Rev Med Liege. 2019; 74(5-6):310-313.

22. Praud D, Rota M, Rehm J, Shield K, Zatoński W, Hashibe M, La Vecchia C, Boffetta P. Cancer incidence and mortality attributable to alcohol consumption. Int J Cancer 2016; 15;138(6):1380-7.

23. Scoccianti C, Cecchini M, Anderson AS, Berrino F, Boutron-Ruault MC, Espina C, Key TJ, Leitzmann M, Norat T, Powers H, Wiseman M, Romieu I. European Code against Cancer 4th Edition: Alcohol drinking and cancer. Cancer Epidemiol 2016; 45:181-188.

24. O'Keefe JH, Bybee KA, Lavie CJ. Alcohol and cardiovascular health: the razor-sharp double-edged sword. J Am Coll Cardiol 2007; 50(11):1009-14.

25. Bruha R, Dvorak K, Petrtyl J. Alcoholic liver disease. World J Hepatol 2012; 4(3):81–90.

26. Gupta S, Warner J. Alcohol-related dementia: A 21st-century silent epidemic? Br J Psychiatry 2008; 193(5):351–3.

27. Player MS, Peterson LE. Anxiety disorders, hypertension, and cardiovascular risk: a review. Int J Psychiatry Med 2011; 41(4):365-77.

28. Davies SJ, Ghahramani P, Jackson PR, Noble TW, Hardy PG, Hippisley-Cox J, Yeo WW, Ramsay LE. Association of panic disorder and panic attacks with hypertension. Am J Med 1999; 107(4):310-6.

29. Tsartsalis D, Dragioti E, Kontoangelos K, Pitsavos C, Sakkas P, Papadimitriou GN, Stefanadis C, Kallikazaros I. The impact of depression and cardiophobia on quality of life in patients with essential hypertension. Psychiatriki 2016; 27(3):192-203.

30. Al-Atram AA. A review of the bidirectional relationship between psychiatric disorders and diabetes mellitus. Neurosciences Journal 2018; 23(2):91-96.

31. Kruse J, Petrak F, Herpertz S, Albus C, Lange K, Kulzer B. Diabetes and depression--a life-endangering

interaction. Z Psychosom Med Psychother 2006; 52(3):289-309.

32. Wiglusz MS, Landowski J, Cubała WJ. Prevalence of anxiety disorders in epilepsy. Epilepsy Behav 2018; 79:1-3.

Author contribution. Acquisition of data: RM, AL, DD, TB
Administrative, technical or logistic support: RM, AL, DD, TB
Analysis and interpretation of data: RM, AL, DD, TB
Conception and design: RM, AL, DD, TB
Critical revision of the article for important intellectual content: RM, AL, DD, TB
Drafting of the article: RM, AL, DD, TB
Final approval of the article: RM, AL, DD, TB
Guarantor of the study: RM, AL, DD, TB
Obtaining funding: RM, AL, DD, TB
Provision of study materials or patients: RM, AL, DD, TB
Statistical expertise: RM, AL, DD, TB
Other: RM, AL, DD, TB

Original article

Vitamin D Deficiency Among Medical Students in Osijek, Croatia

Stipe Vidović [1*], Željko Debeljak [2], Tatjana Bačun [3,4], Sven Viland [1], Milorad Zjalić [1], Marija Heffer [1]

1 Department of Medical Biology and Genetics, Faculty of Medicine, J. J. Strossmayer University of Osijek, Osijek, Croatia
2 Clinical Medical Center Osijek, Institute of Clinical Laboratory Diagnostics, Croatia
3 Clinical Medical Center Osijek, Department of Endocrinology, Osijek, Croatia
4 J. J. Strossmayer University of Osijek, Faculty of Medicine Osijek, Department of Internal Medicine and History of Medicine, Osijek, Croatia

*Corresponding author: Stipe Vidović, stipevidovic1@gmail.com

Abstract

Aim: This study aimed to evaluate serum levels of 25-OH D3 (calcidiol) among students of the Faculty of Medicine Osijek, Croatia, thereby determining to what extent vitamin D deficiency is present.

Methods: The present cross-sectional analysis was based on data collected from 60 participants. Blood sampling was done in March 2021. Concentrations of 25-OH D3 were measured using LC/MS-MS procedure on Shimadzu LCMS 8050 and RECIPE kit for serum levels of 25-OH-D3.

Results: The study was conducted on a sample of 60 respondents aged 19 to 28, of whom 16 were men and 44 were women. All subjects had a 25-OH D3 deficiency (<20 ng/ml), while 11 had an extreme deficiency. Mean 25-OH D3 concentration was 11.36 ng/ml, ranging from 7.70 ng/ml to 16.70 ng/ml. There was no statistical significance of 25-OH D3 concentration levels between the sexes (Student's t-test, P>0.05).

Conclusion: Vitamin D deficiency was detected in all subjects. In addition to the results of several other studies conducted worldwide that evaluated vitamin D status among medical students, this study further highlights the problem affecting this student subgroup.

(Vidović S*, Debeljak Ž, Bačun T, Viland S, Zjalić M, Heffer M. Vitamin D Deficiency Among Medical Students in Osijek, Croatia. SEEMEDJ 2022; 6(2); 67-74)

Received: Oct 18, 2022; revised version accepted: Nov 6, 2022; published: Nov 28, 2022

KEYWORDS: vitamin D deficiency; 25-hydroxyvitamin D concentration; medical students; hypovitaminosis D

Introduction

Over the past decade, there has been a growing number of studies focusing on vitamin D and its roles in human health and disease. Initially, it was thought to be only essential for rickettsial disease prophylaxis; however, contemporary research suggests the importance of vitamin D in maintaining individuals' well-being and overall health (1,2).

The active form of vitamin D, 1,25-dihydroxycholecalciferol (1,25-OH D3), has a pivotal role in maintaining mineral homeostasis and enhancing absorption of calcium and phosphate into the extracellular fluid by acting on the intestines, kidneys, and bones. Therefore, it regulates bone growth and reorganization by interfering with the activity of osteoclasts and osteoblasts (3).

Vitamin D receptors are expressed in almost all cell types, which may explain the multiple actions of vitamin D on different tissues (4). Although the proportion of the role of vitamin D and its effects on non-skeletal health is still debatable, it is associated with regulation of the innate and adaptive immune systems, reduction of inflammation, cell proliferation and differentiation, insulin and glucose secretion regulation, preventive effects on cardiovascular and neurodegenerative diseases, and even antiaging effects (5–9).

For most people, the primary source of vitamin D is skin exposure to ultraviolet radiation, specifically UVB rays, where 7-dehydrocholesterol is converted to pre-vitamin D3 in the skin during exposure to UVB rays (10). However, it can also be obtained through diet and dietary supplements (11).

Vitamin D testing has increased significantly in recent years, establishing the presence of vitamin D deficiency on a pandemic scale worldwide (12). It is estimated that more than a billion people worldwide have low vitamin D levels, with extensive observational data indicating that 40% of the European population and 24% of the US population have 25-OH D3 below 20 ng/ml (13).

Vitamin D deficiency can be diagnosed by measuring serum levels of 25-hydroxyvitamin D3 (14,15). Although there is no consensus on optimal levels of 25 OH-D3, most guidelines suggest that concentrations below 20 ng/mL indicate vitamin D deficiency (16). (Table 1).

Table 1. Recommended serum levels of 25-OH D3 for verification of deficiency and adequate levels of vitamin D; according to Croatian Guidelines for the Prevention, Detection and Therapy of Vitamin D Deficiency in Adults (11).

25-OH D3 (ng/mL)	Interpretation
<10 ng/mL	Extreme deficiency of vitamin D
<20 ng/mL	Deficiency of vitamin D
<30 ng/mL	Insufficiency of vitamin D
≥30 ng/mL	Adequate level of vitamin D
>100 ng/mL	Excess
>150 ng/mL	Intoxication

In 2016, Guidelines for Preventing, Detecting and Treating Vitamin D Deficiency in Adults were issued in Croatia, according to which recommended levels of 25-OH D3 are between 30 and 100 ng/ml (17).

Numerous conditions are associated with vitamin D deficiency, such as chronic diseases, obesity, and malabsorption syndromes. It also occurs during pregnancy. In addition, skin pigmentation, clothing style, diet, sunscreen

use, the season of the year, and latitude can also affect vitamin D synthesis and its serum levels, potentially leading to its deficiency, which increases the risk of developing skeletal and non-skeletal diseases (11,18).

This study was aimed at evaluating serum levels of 25-hydroxyvitamin D3 among medical students of the Faculty of Medicine Osijek in March 2021, thereby also determining to what extent vitamin D deficiency might be present among future healthcare professionals. They are potentially at a greater risk of developing hypovitaminosis D due to their work-related lifestyle, which could be even aggravated by the currently present COVID-19 pandemic.

Material and methods

The present cross-sectional analysis was based on data from 60 participants aged 19 to 28. Blood sampling was done in March 2021 at the Faculty of Medicine in Osijek and then analyzed at the Clinical Hospital Center Osijek, Croatia. Informed consent was obtained from all study participants. The research was approved by the Ethics Committee of the Faculty of Medicine Osijek, University of Osijek (Class: 602-04/22-08/02. No: 2158-61-46-22-149).

Subjects' blood was drawn into round bottom, polystyrene test tubes, 14 mL, 17 x 100 mm (Becton Dickinson, Croatia) to separate serum from cells. The blood was centrifuged at 3000 rpm for 10 minutes. After centrifugation, the serum was separated into other tubes using disposable tubes, which were stored in a refrigerator at -20 ˚ C until analysis. According to the manufacturer's instructions (Shimadzu Corp.), the sample was analyzed on an LCMS-8050 analyzer. The LCMS-8050 analytical system (Shimadzu, Japan) itself consists of NEXERA X2 HPLC (high-performance liquid chromatography) system connected to a mass spectrometer (MS). The LC-MS / MS method is characterized by high sensitivity, specificity, and the possibility of simultaneous analysis of multiple analytes. It is considered the gold standard for determining vitamin D concentration in serum.

Statistical analysis

Numerical data was described by arithmetic mean and standard deviation. Normality of distribution of numerical variables was determined by using the D'Agostino-Pearson test. Differences in normally distributed numerical variables between two independent groups were assessed by using the Student's t-test. All P values were two-sided. The significance level was set to Alpha = 0.05. The MedCalc Statistical Software version 20.106 was used for statistical analysis (https://www.medcalc.org/).

Table 2. Sample age, gender and 25-OH D3 concentrations (ng/ml) (N=number, SD=standard deviation).

Total number of participants	60
Male	16
Female	44
Male: female (ratio)	1:2.75
Age (males), mean(SD)	21.9(1.2)
Age (females), mean(SD)	21.7(2.2)
Age (years), mean(SD)	21.9(1.2)
25-OH D3 levels (ng/ml)	
N	60
Mean ±SD	11.37(1.59)
Minimum	7.67
Maximum	16.68
25-OH D3 levels; males (ng/ml)	
N	16
Mean (SD)	11.13(1.69)
Minimum	7.67
Maximum	13.78
25-OH D3 levels; females (ng/ml)	
N	44
Mean (SD)	11.46(1.53)
Minimum	8.29
Maximum	16.68

Results

The study was conducted on a sample of 60 respondents aged 19 to 28, of whom 44 (73.33%) were women and 16 (26.67%) were men. All subjects had a 25-OH D3 deficiency (<20 ng/ml), with 11 (18.33%) of them exhibiting an extreme deficiency according to recommended serum levels of 25-OH D3 (17). The mean 25-OH D3 concentration was 11.36 ng/ml, ranging from 7.70 ng/ml to 16.70 ng/ml.

The mean 25-OH D3 concentration in women was 11.45 ng /ml, while in men it was 11.13 ng/ml (Table 2). We examined differences in 25-OH D3 concentration levels with respect to gender. The results showed no statistical significance of 25-OH D3 concentration levels between the sexes (Student's t-test, P>0.05). Pearson's correlation coefficient suggests that the relationship between age and 25 OH-D3 concentration is not significant (r=0.06; P>0.05)..

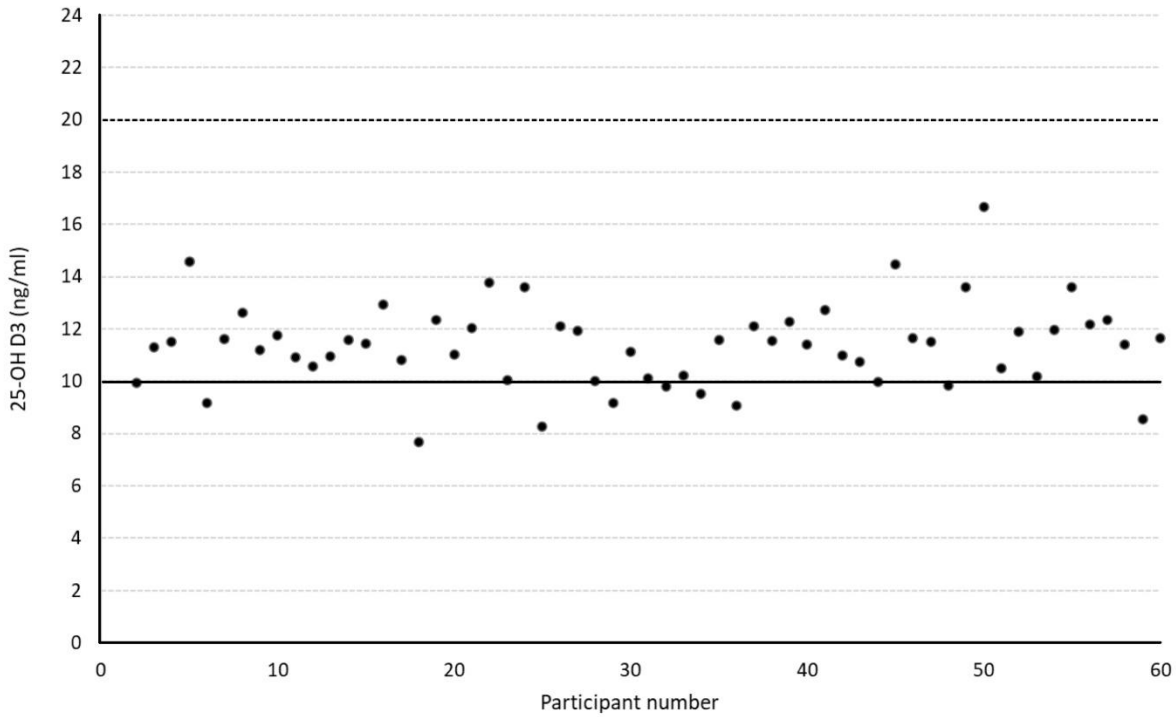

Figure 1. This scatter graph shows the 25-OH D3 status in the examined sample of 60 participants; expressed in ng/ml. The dashed black line indicates the threshold of vitamin D deficiency, while the solid black line indicates the threshold of extreme vitamin D deficiency. All subjects were vitamin D deficient (<20 ng/ml), where 11 (18.33%) of them had an extreme deficiency (<10 ng/ml).

Discussion

According to our knowledge, this is the second study in Croatia examining vitamin D levels among medical students. A study conducted in Rijeka, Croatia established a deficiency in half of the respondents, while we found hypovitaminosis among all of the participants (19). The results raise the question about the underlying cause and about the necessity of implementing prophylactic measures for this population in particular.

The incidence of hypovitaminosis D increased in certain subpopulations due to various risk factors, such as lack of sun exposure, use of sunscreen, long hours indoors, latitude, diet, age, and various chronic and acute diseases (11). A 2017 meta-analysis emphasized the presence of an occupational risk among healthcare professionals, specifically medical students and residents (20).

Several studies worldwide involved measuring vitamin D levels among medical students and found a significant prevalence of vitamin D deficiency. In a study conducted in Spain in 2011, 62% of students had lower than recommended levels of vitamin D (21).

Kardelen et al. determined vitamin D deficiency in 92% of medical students from Turkey, while Nadeem et al. found that only 13.6 % of healthy young medical students in Pakistan had vitamin D levels within the normal range (22, 23). A study conducted in Boston, USA in 1999 found deficiency among 34% of medical students (24).

Contrary to those findings, Leary et al. found a low presence of hypovitaminosis among medical students in the US; only 5% of the subjects were deficient in Florida and 13% in Pennsylvania (25).

In 2018, a study was also conducted in Osijek, Croatia, in the same period of the year as the current study. It also involved the measuring of vitamin D levels among young people aged 19 to 28. As in our study, a high incidence of hypovitaminosis was found, with 72.2% of the subjects having lower levels than 20 ng/mL. Judging by those findings, a high incidence of hypovitaminosis was present. However, a deficiency was significantly less present than in our study, where all of the subjects were medical students (26).

Circumstances that may have affected vitamin D levels

Sampling was carried out in March, when vitamin D levels are lower due to insufficient sun exposure and seasonal variation in the intensity of solar UV light (27). Research indicates that vitamin D concentrations for all age groups in Central Europe begin to decrease in early September and increase in late May (28). In this context, it has been found that medical students in Croatia do not get enough sunlight during the day (29).

A diet poor in vitamin D is another risk factor that may contribute to its low levels. A study from the UK found that students do not get enough vitamin D through their diet, where only 14% of respondents met recommended intake levels (30). A similar trend was noticed among students in China (31). In addition, a 2019 study found that medical students in Rijeka, Croatia, get only a fifth of the recommended vitamin D intake through diet (29).

The period of the COVID-19 pandemic is another circumstance that may affect vitamin D levels in this sample. The Croatian government, like many others, has implemented a series of measures to reduce the number of people affected by COVID-19, including social distancing and recommendations to stay at home, which could potentially limit sun exposure and in turn contribute to lowering vitamin D levels. Yamaguchi et al. found a significant increase in hypovitaminosis D among healthcare workers during the COVID-19 pandemic, where about 90% of the sample was deficient in vitamin D (32). This is essential, assuming that participants had a similar lifestyle in that period as our study sample, considering the duration of indoor activities in medical care and daily life routines.

Also, all study respondents live in the area around 45˚ latitude. Latitude is considered a statistically significant risk factor for vitamin D deficiency in the sense that it is inversely proportional to the level of circulating 25-OH D3 (10). Leary et al. found that medical students at higher latitudes had lower vitamin D levels. In that study, subjects (also medical students) were located at a similar latitude (42˚) as in our sample; but compared to our results, the prevalence of hypovitaminosis was significantly lower — 13 % of participants were vitamin D deficient (25).

Vitamin D supplementation

A 2018 study found that 30.5% of Croatian students practice some form of supplementation, among which medical students used almost twice as much as others (33). Jovanović et al., established that very few of their subjects (4.7%) used vitamin D supplementation (19). Cholecalciferol, ergocalciferol, calcidiol, and calcitriol are used; they are acceptable and straightforward replacements for lack of sun exposure and insufficient intake through diet. Considering

different pharmacokinetic characteristics, metabolism, and points of regulation, cholecalciferol, known as vitamin D3, is most often recommended and used to prevent and treat deficiency (34).

Although much has been said about the importance of preventive use and optimal vitamin D supplementation in health and disease, there is no uniform consensus on the recommended daily intake. The Institute of Medicine and the Endocrine Practice Guideline Committee defined specific guidelines for the general population, where recommended intake was 600 IU/day for people aged 1 to 70, with the upper tolerable intake limit of 4000 IU/day (16).

In 2016, Croatian Guidelines for the Prevention, Detection and Therapy of Vitamin D Deficiency in Adults defined "Vitamin D therapy for verified deficiency, depending on age and comorbidities"(17). According to the guidelines, vitamin D deficient people over 18 years of age without other comorbidities should take vitamin D supplementation of 6000 IU/day for eight weeks, then maintain with 1500-2000 IU/day. Considering that all subjects were deficient, following the previously mentioned recommendations could be one of the effective ways of optimizing vitamin D levels in the serum.

Conclusion

In addition to the results of several other studies conducted worldwide that evaluated vitamin D status among medical students, this study further highlights the problem affecting this student subgroup.

Also, it would be helpful to examine vitamin D levels among medical doctors who, through education, should have gained insight into the concept of a healthy lifestyle and proper prevention methods of various conditions, including hypovitaminosis.

Study limitations

The limitation of this study is that it was conducted on a small sample. Also, testing was done only once in the winter period. Moreover, there is a lack of assessment of participants' lifestyles correlated with vitamin D status, medical history of vitamin D-related diseases, and vitamin D supplementation.

Acknowledgement. None.

Disclosure

Funding. No specific funding was received for this study.

Competing interests. None to declare.

References

1. Chanchlani R, Nemer P, Sinha R, Nemer L, Krishnappa V, Sochett E, et al. An Overview of Rickets in Children. Kidney Int Rep. 2020; 5(7):980–90.

2. Khazai N, Judd SE, Tangpricha V. Calcium and vitamin D: skeletal and extraskeletal health. Curr Rheumatol Rep. 2008; 10(2):110–7.

3. Anderson PH, Turner AG, Morris HA. Vitamin D actions to regulate calcium and skeletal homeostasis. Clin Biochem. 2012; 45(12):880–6.

4. Wang Y, Zhu J, DeLuca HF. Where is the vitamin D receptor? Arch Biochem Biophys. 2012; 1;523(1):123–33.

5. Gil Á, Plaza-Diaz J, Mesa MD. Vitamin D: Classic and Novel Actions. Ann Nutr Metab. 2018; 72(2):87–95.

6. Nakashima A, Yokoyama K, Yokoo T, Urashima M. Role of vitamin D in diabetes mellitus and chronic kidney disease. World J Diabetes. 2016; 7(5):89.

7. Katicic D, Josipovic J, Pavlovic D. Vitamin D and cardiovascular diseases. Cardiol Croat. 2014; 9(5–6):263–72.

8. Sintzel MB, Rametta M, Reder AT. Vitamin D and Multiple Sclerosis: A Comprehensive Review. Neurol Ther. 2018; 7(1):59–85.

9. Wang H, Chen W, Li D, Yin X, Zhang X, Olsen N, et al. Vitamin D and Chronic Diseases. Aging Dis. 2017 ;8(3):346.

10. Wacker M, Holick MF. Sunlight and Vitamin D: A global perspective for health. Dermatoendocrinol. 2013; 5(1):51–108.

11. Holick MF. Vitamin D deficiency. N Engl J Med. 2007; 357(3):266–81.

12. Amrein K, Scherkl M, Hoffmann M, Neuwersch-Sommeregger S, Köstenberger M, Tmava Berisha A, et al. Vitamin D deficiency 2.0: an update on the current status worldwide. Eur J Clin Nutr. 2020; 74(11):1498–513.

13. Cashman KD, Dowling KG, Škrabáková Z, Gonzalez-Gross M, Valtueña J, De Henauw S, et al. Vitamin D deficiency in Europe: pandemic? Am J Clin Nutr. 2016; 103(4):1033–44.

14. El-Hajj Fuleihan G, Bouillon R, Clarke B, Chakhtoura M, Cooper C, McClung M, Singh RJ. Serum 25-Hydroxyvitamin D Levels: Variability, Knowledge Gaps, and the Concept of a Desirable Range: J Bone Miner Res. 2015 Jul;30(7):1119–33.

15. Herrmann M, Farrell CJL, Pusceddu I, Fabregat-Cabello N, Cavalier E. Assessment of vitamin D status – a changing landscape. Clin Chem Lab Med. 2017; 55(1):3–26.

16. Holick MF, Binkley NC, Bischoff-Ferrari HA, Gordon CM, Hanley DA, Heaney RP, Murad MH, Weaver CM, Endocrine Society. Evaluation, Treatment, and Prevention of Vitamin D Deficiency: an Endocrine Society Clinical Practice Guideline. J Clin Endocrinol Metab. 2011; 96(7):1911–30. doi: 10.1210/jc.2011-0385.

17. Vranešić Bender D, Giljević Z, Kušec V, Laktašic Žerjavić N, Bošnjak Pašic M, Vrdoljak E, Lkinas Kelećić D, Reiner Ž, Anić B, Krznarić Ž. Guidelines for the prevention, detection and therapy of vitamin D deficiency in adults. Lijec Vjesn. 2016 May;138(5–6):121–32.

18. Rosen CJ, Adams JS, Bikle DD, Black DM, Demay MB, Manson JE, Murad MH, Kovacs CS. The nonskeletal effects of vitamin D: an Endocrine Society scientific statement. Endocr Rev. 2012; 33(3):456–92.

19. Kehler T, Grubić Kezele T, Fužinac-Smojver A, Kauzlarić-Živković T. Association of vitamin D insufficiency and low physical activity with fatigue, headaches and psychological distress in college students, North-Mediterranean Croatia – a pilot study. Paediatr Croat. 2021; 65(2):59-65. https://doi.org/10.13112/PC.2021.10

20. Sowah D, Fan X, Dennett L, Hagtvedt R, Straube S. Vitamin D levels and deficiency with different occupations: a systematic review. BMC Public Health. 2017; 17(1):519.

21. González-Padilla E, Soria López A, González-Rodríguez E, García-Santana S, Mirallave-Pescador A, Groba Marco M del V, et al. Elevada prevalencia de hipovitaminosis D en los estudiantes de medicina de Gran Canaria, Islas Canarias (España). Endocrinol Nutr. 2011; 58(6):267–73.

22. Asli Derya K, Ismail Y, Beyhan O, Fatma O. Serum 25(OH) Vitamin D Levels of Adolescent and Young Medical Students. Int J Pediatr Res [Internet]. 2018 Jun 30 [cited 2022 Oct 1];4(1). Available from: https://www.clinmedjournals.org/articles/ijpr/international-journal-of-pediatric-research-ijpr-4-032.php?jid=ijpr DOI: 10.23937/2469-5769/1510032

23. Nadeem SB, Munim TF, Hussain HF, Hussain DF. Determinants of Vitamin D deficiency in asymptomatic healthy young medical students. Pak J Med Sci [Internet]. 2018 Sep 7 [cited 2022 Oct 1];34(5). Available from:

http://pjms.com.pk/index.php/pjms/article/view/15668

24. Tangpricha V, Pearce EN, Chen TC, Holick MF. Vitamin D insufficiency among free-living healthy young adults. Am J Med. 2002; 112(8):659–62.

25. Leary PF, Zamfirova I, Au J, McCracken WH. Effect of Latitude on Vitamin D Levels. J Osteopath Med. 2017; 117(7):433–9.

26. Šarić J. Koncentacija vitamina D u muškaraca i žena u dobi od 18 do 28 godina u zimskom radoblju [Internet] [info:eu-repo/semantics/masterThesis]. Josip Juraj Strossmayer University of Osijek. Faculty of Medicine Osijek; 2019 [cited 2022 May 17]. Available from: https://urn.nsk.hr/urn:nbn:hr:152:855195

27. Heidari B, Haji Mirghassemi MB. Seasonal variations in serum vitamin D according to age and sex. Casp J Intern Med. 2012; 3(4):535–40.

28. Pludowski P, Grant WB, Bhattoa HP, Bayer M, Povoroznyuk V, Rudenka E, Heorhi Ramanau H, Varbiro S, Rudenka A, Karczmarewicz E, Lorenc R, Czech-Kowalska J, Konstantynowicz J. Vitamin d status in central europe. Int J Endocrinol. 2014; 2014:589587.

29. Kenđel Jovanović G, Krešić G, Pavičić Žeželj S. Dietary vitamin D intake among university students and their habits concerning daily sunlight exposure – a cross-sectional study. Med Flum. 2021 ;57(4):396–406.

30. Dong H, Asmolovaite V, Marseal N, Mearbon M. Vitamin D status and dietary intake in young university students in the UK. Nutr Food Sci. 2022; 52(4):616–26.

31. Zhou M, Zhuang W, Yuan Y, Li Z, Cai Y. Investigation on vitamin D knowledge, attitude and practice of university students in Nanjing, China. Public Health Nutr. 2016; 19(1):78–82.

32. Funaki T, Sanpei M, Morisaki N, Mizoue T, Yamaguchi K. Serious vitamin D deficiency in healthcare workers during the COVID-19 pandemic. BMJ Nutr Prev Health. 2022; 5(1):134–6.

33. Žeželj S, Tomljanović A, Jovanović G, Krešić G, Peloza O, Dragaš-Zubalj N, Pavlinić Prokurica I. Prevalence, Knowledge and Attitudes Concerning Dietary Supplements among a Student Population in Croatia. Int J Environ Res Public Health. 2018; 15(6):1058.

34. Vieth R. Vitamin D supplementation: cholecalciferol, calcifediol, and calcitriol. Eur J Clin Nutr. 2020; 74(11):1493–7..

Author contribution. Acquisition of data: SV, ŽD, TB,MH
Administrative, technical or logistic support: SV, ŽD, TB, S Viland, MZ, MH
Analysis and interpretation of data: SV, ŽD, TB, MZ, MH
Conception and design: SV, TB, MZ, MH
Critical revision of the article for important intellectual content: SV, ŽD, TB, MH
Drafting of the article: SV, ŽD, MH
Final approval of the article: SV, ŽD, TB, MH
Guarantor of the study: TB, MH
Obtaining funding: TB, MH
Provision of study materials or patients: ŽD, TB, MH
Statistical expertise: SV, MH

Review article

Iron Chelation Therapy in COVID-19 Infection: A Review Article

Irena Krajina Kmoničeka [1], Anja Tomić [2], Josip Kocur [3]

[1] Department of Anesthesiology, Reanimatology and Intensive Medicine, Osijek University Hospital Centre, Osijek, Croatia
[2] Community Health Centre Vinkovci, Vinkovci, Croatia
[3] Department of Orthopedics and Traumatology, Osijek University Hospital Centre, Osijek, Croatia

*Corresponding author: Irena Krajina Kmoničeka, ikrajina20@gmail.com

Abstract

The recent outbreak of corona virus and coronavirus disease (COVID-19) caused by the SARS-CoV-2 virus is a global concern. Despite efforts to clarify the physiology and potential therapy, specific guidelines for the treatment of COVID-19 disease have yet to be established, and many therapeutic options are under investigation. Accumulating evidence suggests that dysregulation of iron homeostasis contributes significantly to the pathogenesis of COVID-19 through its toxic effects by the formation of reactive oxygen species (ROS). This review focuses on summarizing the available literature and relevant studies conducted to date on the possible therapeutic effects of iron chelation therapy in the treatment of COVID-19 disease. Scientific databases (PubMed, Scopus, Google Scholar) were searched for relevant articles using the following keywords: COVID-19, SARS-CoV-2, coronavirus, clinical management, iron chelators/chelation. Research articles, reviews, research letters, case reports, and commentaries were considered. Although there is ample evidence of the potential beneficial effects of using iron chelators as adjuvant treatment in COVID-19, further research on this topic is needed.

(Krajina Kmoničeka I, Tomić A, Kocur J. Iron Chelation Therapy in COVID-19 Infection: A Review Article. SEEMEDJ 2022; 6(2); 75-84)

Received: Mar 19, 2022; revised version accepted: Oct 28, 2022; published: Nov 28, 2022

KEYWORDS: COVID-19, SARS-CoV-2, iron chelating agents, COVID-19 therapy

The novel disease

In December 2019, a new virus from the coronavirus group (initially 2019-nCov) emerged and caused the appearance of unusual viral pneumonia in China. The disease is called coronavirus disease (COVID-19) and in March 2020, the World Health Organization declared COVID-19 a pandemic. The 2019nCov was later named SARS-CoV-2 due to its structural similarity to the SARS-CoV virus that caused the 2003 SARS outbreak (1). Vaccination campaigns against the SARS-CoV-2 virus are currently underway worldwide, but the COVID-19 pandemic is still out of control and continues to cause high mortality. Unfortunately, there is still no specific therapy for COVID -19 and patients rely on general and supportive therapies. Although drugs (antiviral drugs, monoclonal antibodies, corticosteroids, immunosuppressants) included in the recommended guidelines for the treatment of the infection show promising results, given the rising number of COVID-19 cases, additional therapeutic choices should be identified and thoroughly evaluated (2-4). The goal of therapy is to prevent the occurrence of a cytokine storm and to avoid significant damage to body tissues resulting in multiorgan failure and death. Most cases have a milder clinical course, but up to 14% of cases can be severe, and present with moderate to severe pneumonia requiring hospitalization. Severe cases are characterized by dyspnea, tachypnea (RR ≥ 30/min), hypoxemia (SpO2 ≤ 93%), PaO2/FiO2 ratio < 300, and/or pulmonary infiltrates involving more than 50% of the lung parenchyma. All of this can lead to severe disease requiring intensive care unit (ICU) treatment and can be life-threatening in 5% of cases characterized by respiratory failure that can provoke the development of acute distress syndrome (ARDS), septic shock, multiple organ dysfunction and death (5). Risk factors for fatal outcome include age, underlying comorbidities (hypertension, diabetes mellitus, obesity, heart failure, coronary artery disease), and disease severity, which increases by up to 49% in critically ill patients (6,7). In addition, coronavirus also affects numerous other organ systems, such as the cardiovascular system (e.g., myocardial damage, cardiomyopathy, and cardiac arrhythmia (8-11), the neurological system, and can also cause acute kidney injury and liver damage (12,13). Inflammation-induced coagulopathy, which causes an elevated coagulation state, is a consequence of damage to the endothelium and the action of pro-inflammatory cytokines (especially IL-6) (14-16). Endothelial cells are potential targets for SARS-CoV-2 due to the highly expressed ACE 2 receptors, which are thought to be the major (but not the only) port of entry into a cell for the virus (17). The virus also recognizes porphyrin in hemoglobin, with higher binding affinity than that to hACE2, resulting in oxygen deprivation (17). In addition to endothelial cells and porphyrin, transferrin receptors (TfR) are also considered as a possible target of viral action(18, 19). TfR is found on numerous tissues and cells, including cells of the respiratory system. Transferrin, a circulating glycoprotein that transports iron, delivers iron to cells when it binds to TfR. Studies in animal models have shown that viral infection did not occur when connection between virus and TfR was affected (18).

Iron and ferritin in inflammation

Iron metabolism is very important for the functioning of the whole body and ferritin plays a crucial role in this process. Ferritin is a protein that binds iron and is found in the bloodstream, cytosol and mitochondria. It is involved in crucial cellular activities, including immune regulation by making iron available and protecting cells from the toxic performance of free iron (20). By measuring serum ferritin levels, one can get an insight into iron status. During inflammation, there is often an increase in serum ferritin concentration with hypoferremia. Oral iron supplementation drugs have been shown to increase mortality in humans when taken during infection (20). Serum ferritin synthesis, apart from iron availability, is also regulated by inflammatory cytokines such as IL-1β and IL-6 (pro-inflammatory cytokine in COVID-19 infection) and increased hepcidin production, which in turn is stimulated by pro-inflammatory cytokines, especially IL-6 (21). To survive and

replicate in host cells, microbes require iron and to limit viral replication, the innate immune system takes control of iron metabolism by reducing iron bioavailability (2). To protect the host during active infection, ferritin reduces iron bioavailability to the pathogen. As a result, serum iron concentration decreases and serum ferritin concentration increases, limiting the availability of iron for erythropoiesis and leading to further exacerbation of anemia, which is called anemia of inflammation (AI) (22). Ferritin also plays a role in inflecting the immune response by inducing anti-inflammatory cytokines and limiting free radical-induced damage (23). Inflammation and infection produce large amounts of oxygen radicals (ROS) that leak into the fluids and tissues in the area of inflammation, causing cellular damage that can lead to endothelial dysregulation of the immune response, resulting in hyperinflammation and cytokine storms and multiple organ failure (24). When the concentration of non-transferrin bound iron in plasma is too high, it converts to its redox-active form called labile plasma iron. This further contributes to the production of ROS, leading to tissue lesion and, over time, fibrosis (5). These toxic free radicals are formed by the Fenton reaction, in which, in the presence of a harmful byproduct of aerobic metabolism hydrogen peroxide, ferrous iron (Fe^{2+}) is oxidized to ferric iron (Fe^{3+}), producing a hydroxyl radical and hydroxide ion.

In addition to ferritin, transferrin and its effect on iron must also be mentioned, as it has been shown that the concentration of transferrin changes during COVID-19 disease. Transferrin is a glycoprotein synthesized by the liver. It is found in the bloodstream, where it transports iron to TfR receptors on cells. When there is iron deficiency in the body and hypoxia, transferrin concentration increases, while it decreases during inflammation (18). Transferrin saturation with iron (TSAT) indicates how much iron is bound to transferrin and is an important marker for iron availability and the amount of systemic iron (18).

The role of iron in COVID-19 infection

Dysregulation of iron homeostasis, including iron overload, has also recently been recognized as an important element in the pathogenesis of COVID-19, along with high levels of proinflammatory CD4 and CD8 T cells, extensive cytokine release, and an increased coagulation state. As mentioned earlier, elevated ferritin levels not only indicate an acute phase response, but also play an important role in inflammation by contributing to the progression of cytokine storm (20). During cytokine storm there is an enormous and uncontrolled release of pro-inflammatory cytokines (IL-6, IL-10, TNF-α, IL-1β, IFN-γ, IL-2, IL-7 and IL-10, G-CSF, MIP-1 alpha, and others), which is especially prominent in more severe clinical forms of COVID-19 disease. As a result of the cytokine storm and the damaging cytopathic effect of the virus, there is destruction of the lungs and other organs and, at the same time, a further increase in cytokine levels. Besides the cytokine storm, high levels of intracellular iron generate ROS interaction with oxygen molecules and increases the risk of coagulopathy, oxidative stress and endothelial inflammation, all of which together can lead to disseminated coagulopathy and multiorgan failure (25). According to current clinical and experimental data, it is possible that significant oxidative stress may cause the progression of ARDS characterized by damage to the lung parenchyma, decreased lung capacity, endothelial and capillary membrane damage resulting in protein leakage (24). During this tissue damage and lysis, there is an additional increase in the level of ferritin, the synthesis of which is already elevated due to ongoing inflammation (26). Moreover, analysis of lavage fluid from patients with ARDS shows increased levels of iron and increased cellular levels of transferrin, ferritin, and lactoferrin, implying interruption of pulmonary iron homeostasis in ARDS (4).

As mentioned earlier, during COVID-19 infection, there is an iron overload and little attention is paid to this finding. Several studies suggest that patients with high ferritin levels have a much more severe form of COVID-19 disease, clinical deterioration of the patient's condition, a higher

mortality rate, and worse outcome in patients treated in the ICU (23,24). Hyperferritinemia is linked with considerably elevated mortality in septic patients, which has also been shown in patients with severe COVID-19 infection in ICU% (5). Patients with COVID-19 disease and ferritin levels above 300 μ g/l had a 9-fold higher risk of death4. Although little is well-known about the management of iron balance in SARS-CoV-2 patients, some conclusions can be drawn from other viral infections such as hepatitis B, hepatitis C, and HIV, in which iron overload leads to a worse prognosis (5,27). In HIV infection, for example, HIV 1 replication is dependent on host cell enzymes that require iron, and iron supplementation has been shown to lead to increased mortality in HIV-infected patients, indicating the importance of iron excess in HIV infection (2).

The level of transferrin and TSAT, mentioned earlier in the text, proved useful in assessing the severity of COVID-19 disease and survival. In patients hospitalized for COVID-19 disease, the serum concentration of transferrin decreases, although at the same time a low serum iron level is present (19, 28-31). It is possible that COVID-19 inflammation regulates the action of transferrin and prevents its increase when low iron levels are present (19). A very low concentration of transferrin was observed in patients who required oxygen therapy, and a continuous decrease in concentration was observed in patients who died (19, 28-31). In patients who survive, serum transferrin levels recover after some time. The TSAT decreases in COVID-19 patients, especially in patients who have a severe form of the disease and are in the ICU (19, 30). The drop in TSAT level is explained by the fact that at the beginning of the infection, the availability of iron for the pathogen is limited. After a few days, the TSAT level recovers and returns to normal range. It is interesting to note that TSAT levels were higher in intubated patients than in non-intubated patients, which may be explained by changes in the regulation of metabolism at different stages of the disease or by the effect of the tube on iron metabolism (19).

Overexpression of IL-6, IL-1 β , and IFN- γ during inflammation also leads to an increase in hepcidin levels (5). Hepcidin is an iron-regulating peptide hormone produced in the liver and released into the bloodstream in response to inflammation and increased iron levels in the body. The production of hepcidin in the liver is stimulated by IL-6 (32). It is a negative regulator of iron by sequestering iron in enterocytes and macrophages, increasing intracellular ferritin levels, and preventing iron efflux from storage cells by inhibiting ferroportin (33). It is possible that SARS-CoV-2 virus has a hepcidin-like effect because of the identical amino acid sequence between hepcidin and the coronavirus spike glycoprotein. By mimicking the action of hepcidin, SARSCoV-2 could remarkably increase circulating and tissue ferritin (especially in liver, spleen, bone marrow, and muscle) independent of inflammation, while causing serum iron deficiency and hemoglobin deficiency (4, 32). It is also possible that coronaviruses enter cells through complex mechanism by a mimic effect using their spike proteins and cleave their spike polypeptides using host furins and proteases, which promotes cell entry (32).

COVID-19 infection resembles hyperferritinemic syndromes due to high blood ferritin levels and inflammation triggered by the cytokine storm, as well as lymphopenia, decreased NK count and activity, abnormal liver function tests, coagulopathy, pleurisy, pericarditis, lung consolidation, pulmonary edema, and myocarditis (34,35). Because iron chelation is the basis for treating iron overload, as it is in other hyperferritinemic syndromes, and because impaired iron metabolism has been observed in COVID-19 infection, iron chelator therapy may be beneficial.

There are several theories about how increases in ferritin and free iron may occur during COVID-19 infection. An in-silico model suggests and considers direct interaction between several viral proteins and hemoglobin, but side effects on inflammation or tissue damage are not considered (36, 37). The viral proteins (ORF1ab, ORF10, ORF3a) originate from infected plasma cells and together remove heme from the b-

chain of hemoglobin, remove iron from heme, and consequently sequester iron-free protoporphyrin IX (PPIX). As a result, a toxic amount of iron is released, functional hemoglobin levels are impaired and hemoglobin metabolism is disturbed. Another theory, as addressed previously in the text, is that AI may be the cause of the decreased hemoglobin level (2, 22).

Iron chelator therapy

Iron chelators have several beneficial properties such as chelating iron, inhibiting the redox properties of free iron, and preventing the involvement of iron in Fenton reactions. They inhibit the production of hydroxyl radicals and the production of other ROS which lead to oxidative damage and ferroptosis (38). Another useful mechanism of iron chelators is the downregulation of hepcidin and the removal of iron from iron-binding proteins, showing their anti-ferritin effect (2,39). FDA-approved iron chelators such as deferoxamine (DFO), deferiprone, and deferasirox have so far been used as iron overload therapy in a number of pathogens in vivo and in vitro, particularly (DFO) (17). Each of the iron chelators has different efficacy in iron overload therapy. DFO could be effective against SARS-CoV-2 because it forms a stable complex with iron, scavenging iron-mediated hydroxyl radical formation and acting as an antiviral (4). What is more, iron chelators can reduce the availability of cellular iron involved in the replication of RNA viruses such as West Nile virus, HIV, and hepatitis C virus, a property that could be used in the treatment of COVID -19 infections (17). The chelator deferasirox has a different effect, binding cytosolic iron discharged from ferritin (5).

Lactoferrin, a glycoprotein that is part of the body's natural immunity, is one of the potential naturally occurring iron chelators. It is produced by exocrine glands and neutrophils and found in human milk and all secretions. It has a variety of therapeutic effects. Apart from iron binding and effect on the immune system, it also diminishes inflammation by affecting the formation of cytokines and ROS, thus reducing iron overload. It also inhibits the joining of heparan sulfate proteoglycans, which prevents viruses from cell entry (40).

Iron chelation therapy in COVID-19

As more research indicates that endothelial inflammation is an important pathophysiological mechanism responsible for the multiorgan involvement and organ failure in SARS-CoV-2 infection, many researchers believe that iron chelators may prove useful in improving the systemic manifestations of COVID-19 (41). Experimental studies in animals with bleomycin-induced pulmonary fibrosis, in which fibrosis and worsening lung function are associated with increased iron aggregation in the lungs, have shown that iron chelator therapy is beneficial (42).

Due to the lack of adequate therapy, an increasing number of investigators are suggesting that targeted iron therapy may help treat the more severe forms of COVID-19, as iron is likely required for viral replication and functions of SARS-CoV-2 (5). Previous research and findings have shown that iron chelation may have an effect on proinflammatory cytokines and free radicals, which are closely related with severe COVID-19 disease and may lead to tissue destruction, with acute lung injury and ARDS being the most severe outcomes. Because of all these factors, iron chelators represent a potential COVID-19 treatment (5). Iron chelators could alleviate ARDS and contribute to the control of SARS-CoV-2 through several mechanisms: reduction of iron attainability, inhibition of viral multiplication, increase in the titer of neutralizing antiviral antibodies and B cells, prevention of endothelial inflammation, and inhibition of pulmonary fibrosis and lung decay by reducing pulmonary iron accumulation (41). As mentioned before, iron chelator DFO could be useful as a potential therapy for COVID-19 infection because it reduces the replication of some RNA viruses, as shown by in vitro studies, and also reduces the availability of iron in serum and body tissues, which could prevent pulmonary fibrosis after COVID-19 infection (39). In vitro, it also lowers levels of IL-6

and endothelial inflammation, which could reduce the severity of COVID-19 infection and multi-organ damage and failure (39). In a mouse model, preconditioning with DFO was shown to protect the lungs from mechanical ventilation damage by reducing ROS formation in mitochondria and macrophages (43).

There is only one study of 25 patients that evaluated the effect of tocilizumab and an adjuvant iron chelator in severe COVID-19 pneumonia and whether the prescribed therapy would reduce mortality (44). Eleven patients received therapy with tocilizumab and the adjuvant iron chelator deferasirox and over 80% had a favorable outcome. The therapy proved to be a good option for patients with significant hyperferritinemia and severe COVID-19 disease. Two trials are currently underway to check the efficacy and safety of DFO compared to the standard of care or tocilizumab in patients with COVID-19 (NCT04333550, NCT04361032), the results of which are eagerly awaited (5).

Vlahakos et al have proposed possible therapeutic guidelines for iron chelator therapy (45) Several parameters indicative of patient deterioration would be monitored (e.g., oxygen demand ≥60%, ferritin levels ≥ 1000 ng/ml and CRP level > 10-fold above baseline, platelets < 100 000 × 109/L and lymphocyte counts < 1000 × 109/l) and their deterioration would indicate progressive severity of COVID-19 infection and predict the need for more aggressive critical treatment. It has been suggested that oral iron chelator therapy could be administered 10-14 days after the onset of severe COVID-19 infection. Iron chelators have been successfully used for half a century to treat diseases with excessive iron accumulation (45). It is possible that intravenous iron chelator therapy may provide sufficient and rapid lowering of plasma iron levels to relieve cytokine storm in patients with severe COVID-19 infection in ICU. In moderate cases, oral chelators can prevent the development of a severe inflammatory response. Scientists all over the world agree that treatment of patients with COVID-19 infection should begin as soon as possible and at the appropriate dose. However, it is essential to conduct adequately powered randomized trials before using iron chelators in patients with severe COVID-19 infection (45).

In addition to iron chelators, hepcidin antagonists could be used as a potential therapy to lower iron levels instead of iron chelators in the supportive care of COVID-19 in the future, since all infections trigger inflammation that increases hepcidin levels as the main regulator of iron, causing anemia. It is also known that ferritin formed during inflammation contains less iron than normal ferritin (39,46,47). In addition, cytokines are overexpressed during COVID-19, leading to an increase in hepcidin levels (17). DFO decreases the level of IL-6, an important inflammatory mediator that triggers a cytokine storm. In addition, there is evidence that the other pharmacological benefit of DFO is the downregulation of hepcidin (39). It has been observed that replication of coronaviruses in iron-deficient cells is suboptimal compared to iron-rich cells (2).

Some encouraging in vitro studies on the effects of the naturally occurring iron chelator lactoferrin on SARS-CoV and on SARS-CoV-2 viruses have shown that lactoferrin inhibits the initial phase of viral infection (40,42,48).

Iron chelator therapy and its beneficial effects on pneumonia and secondary fibrogenesis suggest that iron chelators should be taken into account to improve the long-term outcome and survival of patients with COVID-19, especially those with severe COVID-19 infection (5). Some of the known iron chelators, such as DFO, deferasirox, and deferiprone, as well as the natural iron chelator lactoferrin, may be efficient in the therapy of COVID-19 (4).

Conclusion

According to the literature, iron chelator therapy could have a number of beneficial effects in patients with COVID -19 infection, especially in severe forms of the disease, without causing harm in severe COVID-19 patients. Unfortunately, there are currently not enough adequate randomized prospective trials to confirm the benefits of iron chelator treatment, and the current evidence base is poor. Several

clinical trials need to be conducted first to prove the efficacy and safety of iron chelator use, and further research is needed in order to establish new therapeutic guidelines that may include iron chelators as supportive treatment for COVID -19 disease.

Acknowledgement. This paper was supported by the Croatian Science Foundation grant IP-06-2016-2717 and the European Structural Fund 2014–2020 as financial support for the PhD student I. Bazina.

References

1. Zhou P, Yang X-L, Wang X-G. et al. A pneumonia outbreak associated with a new coronavirus of probable bat origin. Nature 2020; 579: 270–273. DOI: 10.1038/s41586-020-2012-7

2. Liu W, Zhang S, Nekhai S, Liu S. Depriving Iron Supply to the Virus Represents a Promising Adjuvant Therapeutic Against Viral Survival Curr Clin Microbiol Rep. 2020; 1-7. DOI:10.1007/s40588-020-00140-w

3. Coronavirus Disease 2019 (COVID-19). Treatment guidelines. Available from: https://www.covid19treatmentguidelines.nih.gov/. Site Updated: August 4, 2021. Accessed 10 Aug 2021

4. Habib HM, Ibrahim S, Zaim A, Ibrahim WH. The role of iron in the pathogenesis of COVID-19 and possible treatment with lactoferrin and other iron chelators. Biomed Pharmacother. 2021; 136:111228. DOI:10.1016/j.biopha.2021.111228

5. Perricone C, Bartoloni E, Bursi R. Cafaro G, Guidelli GM, Shoenfeld Y, Gerli R. COVID-19 as part of the hyperferritinemic syndromes: the role of iron depletion therapy. Immunol Res. 2020; 68(4): 213–224. DOI: 10.1007/s12026-020-09145-5

6. Wu Z, McGoogan JM. Characteristics of and important lessons from the Coronavirus Disease 2019 (COVID-19) outbreak in China. JAMA 2020; 323(13): 1239. DOI: 10.1001/jama.2020.2648

7. Kordzadeh-Kermani E, Khalili H, Karimzadeh I. Pathogenesis, clinical manifestations and complications of coronavirus disease 2019 (COVID-19). Future -Microbiol. 2020; 15: 1287-1305. DOI: 10.2217/fmb-2020-0110

8. Xu Z, Shi L, Wang Y, Huang L, Zhang C, Liu S, Zhao P, Liu H, Zhu L, Tai Y, Bai C, Gao T, Song J, Xia P, Dong J, Zhao J, Wang F-S. Pathological findings of COVID-19 associated with acute respiratory distress syndrome. Lancet Respir Med. 2020; 8(4):420-422. DOI: 10.1016/S2213-2600(20)30076-X

9. Xiong TY, Redwood S, Prendergast B, Chen M. Coronaviruses and the cardiovascular system: acute and long-term implications. Eur Heart J. 2020; 41(19):1798-1800. DOI: 10.1093/eurheartj/ehaa231

10. Chen L, Li X, Chen M, Feng Y, Xiong C. The ACE2 expression in human heart indicates new potential mechanism of heart injury among patients infected with SARS-CoV-2. Cardiovasc Res. 2020; 116(6):1097-1100. DOI: 10.1093/cvr/cvaa078

11. Nunes Kochi A, Tagliari A P, Battista Forleo G, Fassini GM, Tondo C. Cardiac and arrhythmic complications in patients with COVID-19. J Cardiovasc Electrophysiol. 2020; 31(5):1003-1008. DOI: 10.1111/jce.14479

12. Cheng Y, Luo R, Wang K, Zhang M, Wang Z, Dong L, Li J, Yao Y, Ge S, Xu G. Kidney disease is associated with in-hospital death of patients with COVID-19. Kidney Int. 2020; 97(5):829-838. DOI: 10.1016/j.kint.2020.03.005

13. Wong SH, Lui RN, Sung JJ. Covid-19 and the digestive system. J Gastroenterol Hepatol. 2020; 35(5):744-748. DOI:10.14309/ajg.0000000000000691

14. Connors JM, Levy JH. COVID-19 and its implications for thrombosis and

Disclosure

Funding. None.
Competing interests. None to declare.

anticoagulation.: Blood 2020; 135(23):2033-2040. DOI: 10.1182/blood.2020006000

15. T Poll. The immunopathology of sepsis and potential therapeutic targets. Nat Rev Immunol. 2017; 17(7):407-420. DOI:10.1038/nri.2017.36

16. Ranucci M, Ballotta A, Di Dedda U, Baryshnikova E, Dei Poli M, Resta M, Falco M, Albano G, Menicanti L. The procoagulant pattern of patients with COVID-19 acute respiratory distress syndrome. J Thromb Haemost. 2020; 18(7):1747-1751. DOI: 10.1111/jth.14854

17. Maiti BK. Heme/Hemeoxygenase-1 System Is a Potential Therapeutic Intervention for COVID-19 Patients with Severe Complications. ACS Pharmacol Transl Sci. 2020 Sep 28;3(5):1032-1034. DOI: 10.1021/acsptsci.0c00136.

18. Tang X, Yang M, Duan Z, Liao Z, Liu L, Cheng R, Fang M, Wang G, Liu H, Xu J, Kamau MP, Zhang Z, Yang L, Zhao X, Peng X, Lai R. Transferrin receptor is another receptor for SARS-CoV-2 entry. bioRxiv 2020. 10.23.350348; doi: https://doi.org/10.1101/2020.10.23.350348

19. Suriawinata, E., Mehta, K.J. Iron and iron-related proteins in COVID-19. Clin Exp Med (2022). https://doi.org/10.1007/s10238-022-00851-y

20. Kernan KF, Carcillo JA. Hyperferritinemia and inflammation. Int Immunol. 2017; 29(9)401-9. DOI: 10.1093/intimm/dxx031

21. Goud PT, Bai D, Abu-Soud HM. A Multiple-Hit Hypothesis Involving Reactive Oxygen Species and Myeloperoxidase Explains Clinical Deterioration and Fatality in COVID-19. Int J Biol Sci 2021; 17(1):62-72. DOI:10.7150/ijbs.51811.

22. Parrow NL, Fleming RE, Minnick MF. Sequestration and scavenging of iron in infection. Infect Immun. 2013; 81(10):3503–14. DOI:10.1128/IAI.00602-13

23. Cheng L, Li H, Li L, Liu C, Yan S, Chen H, Li Y. Ferritin in the coronavirus disease 2019 (COVID-19): A systematic review and meta-analysis. J Clin Lab Anal. 2020;34(10):e23618. DOI:10.1002/jcla.23618

24. Deng F, Zhang L, Lyu L, Lu Z, Gao D, Ma X, Guo Y, Wang R, Gong S, Jiang W. Increased levels of ferritin on admission predicts intensive care unit mortality in patients with COVID-19. Med Clin (Barc). 2021; 156(7):324-331. DOI:10.1016/j.medcli.2020.11.030

25. Wagener FADTG, Pickkers P, Peterson SJ, Immenschuh S, Abraham NG. Targeting the Heme-Heme Oxygenase System to Prevent Severe Complications Following COVID-19 Infections. Antioxidants (Basel). 2020; 9(6):540. DOI:10.3390/antiox9060540

26. Khiroya H., Turner A. The role of iron in pulmonary pathology. Multidiscip. Respir. Med. 2015; 10:34. DOI: 10.1186/s40248-015-0031-2

27. Gómez-Pastora J, Weigand M, Kim J, Wu, Strayer J, Palmer AF, Zborowski M, Yazer M, Chalmers JJ. Hyperferritinemia in critically ill COVID-19 patients – Is ferritin the product of inflammation or a pathogenic mediator? Clin Chim Acta. 2020; 509: 249–251. DOI:10.1016/j.cca.2020.06.033

28. Knovich MA, Storey JA, Coffman LG, Torti SV, Torti FM. Ferritin for the clinician. Blood Rev. 2009 May;23(3):95-104. doi: 10.1016/j.blre.2008.08.001.

29. Claise C, Saleh J, Rezek M, Vaulont S, Peyssonnaux C, Edeas M. Low transferrin levels predict heightened inflammation in patients with COVID-19: New insights. International Journal of Infectious Diseases: 2022; 116:74-79. DOI: 10.1016/j.ijid.2021.12.340.

30. Bolondi, G., Russo, E., Gamberini, E. Circelli A, Cosimo M, Meca C, Brogi E, Viola L, Bissoni L, Poletti V, Agnoletti V. Iron metabolism and lymphocyte characterisation during Covid-19 infection in ICU patients: an observational cohort study. World J Emerg Surg 15, 41 (2020). https://doi.org/10.1186/s13017-020-00323-2

31. Lanser L, Burkert FR, Bellmann-Weiler R, Schroll A, Wildner S, Fritsche G, Weiss G. Dynamics in Anemia Development and Dysregulation of Iron Homeostasis in Hospitalized Patients with COVID-19. Metabolites. 2021; 11(10):653. https://doi.org/10.3390/metabo11100653

32. Ehsani S. COVID-19 and iron dysregulation: distant sequence similarity between hepcidin and the novel coronavirus spike glycoprotein. Biol Direct. 2020; 15(1):19. doi: 10.1186/s13062-020-00275-2.

33. Carota G, Ronsisvalle S, Panarello F, Tibullo D, Nicolosi A, Li Volti G. Role of Iron Chelation and Protease Inhibition of Natural Products on COVID-19 Infection. J Clin Med. 2021; 10(11):2306. DOI:10.3390/jcm10112306

34. Colafrancesco S, Alessandri C, Conti F, Priori R. COVID-19 gone bad: A new character in the spectrum of the hyperferritinemic syndrome? Autoimmun Rev. 2020; 19(7): 102573. DOI:10.1016/j.autrev.2020.102573

35. Hanley B., Lucas S.B., Youd E., Swift B, Osborn M. Autopsy in suspected COVID-19 cases. J Clin Pathol 2020; 73(5):239-242. DOI: 10.1136/jclinpath-2020-206522

36. Liu W, Li H. (2020) COVID-19: Attacks the 1-beta chain of hemoglobin and captures the porphyrin to inhibit human heme metabolism. Available from: https://chemrxivorg/articles/COVID-19_Disease_ORF8_and_Surface_Glycoprotein_Inhibit_Heme_Metabolism_by_Binding_to_Porphyrin/11938173 Accessed 2 Aug 2021. DOI:10.26434/chemrxiv.11938173.v8

37. Read R. Flawed methods in "COVID-19: attacks the 1-beta chain of hemoglobin and captures the porphyrin to inhibit human heme metabolism." ChemRxiv. 2020. May 5, v2. Available from: https://chemrxiv.org/engage/chemrxiv/article-details/60c74ae1567dfe162cec4e4a Accessed 8 Aug 2021 DOI:10.26434.chemrxiv.12120912

38. Alvarez S. NFS1 undergoes positive selection in lung tumours and protects cells from ferroptosis. Nature. 2017; 551 (7682): 639–643. DOI: 10.1038/nature24637

39. Abobaker A. Can iron chelation as an adjunct treatment of COVID-19 improve the clinical outcome? Eur J Clin Pharmacol. 2020; 76(11):1619-1620. DOI:10.1007/s00228-020-02942-9

40. Lang, J., Yang, N., Deng, J., Liu, K., Yang, P., Zhang, G., Jiang C. Inhibition of SARS Pseudovirus Cell Entry by Lactoferrin Binding to Heparan Sulfate Proteoglycans. PLoS ONE 2011; 6(8):e23710.. DOI:10.1371/journal.pone.0023710

41. Dalamaga M, Karampela I, Mantzoros CS. Commentary: Could iron chelators prove to be useful as an adjunct to COVID-19 Treatment Regimens? Metabolism. 2020; 108:154260. DOI:10.1016/j.metabol.2020.154260

42. Campione E, Lanna C, Cosio T, et al. Lactoferrin Against SARS-CoV-2: In Vitro and In Silico Evidences. Front Pharmacol. 2021;12:666600. DOI:10.3389/fphar.2021.666600

43. Zhu W, Huang Y, Ye Y, Wang Y. Deferoxamine preconditioning ameliorates mechanical ventilation-induced lung injury in rat model via ROS in alveolar macrophages: a randomized controlled study. BMC Anesthesiol 2018; 18(1):116DOI: 10.1186/s12871-018-0576-7

44. Birlutiu V, Birlutiu RM, Chicea L. Off-label tocilizumab and adjuvant iron chelator effectiveness in a group of severe COVID-19 pneumonia patients: A single center experience. Medicine (Baltimore). 2021; 100(18):e25832. DOI:10.1097/MD.0000000000025832

45. Vlahakos, VD, Marathias, KP, Arkadopoulos, N, Vlahakos, DV. Hyperferritinemia in patients with COVID-19: An opportunity for iron chelation? Artif Organs. 2021; 45:163–167. DOI: 10.1111/aor.13812

46. Herbert V, Jayatilleke E, Shaw S, Rosman A, Giardina P, Grady R, Bowman B, Gunter

EW. Serum ferritin iron, a new test, measures human body iron stores unconfounded by inflammation. Stem Cells. 1997; 15(4):291–296. DOI: 10.1002/stem.150291

47. Ganz T. Anemia of inflammation. N Engl J Med. 2019; 381(12):1148–1157. DOI:10.1056/NEJMra1804281.

48. Hu, Y., Meng, X., Zhang, F., Xiang, Y., and Wang, J. (2021). The In Vitro Antiviral Activity of Lactoferrin against Common Human Coronaviruses and SARS-CoV-2 Is Mediated by Targeting the Heparan Sulfate Co-receptor. Emerging Microbes & Infections 2021; 10(1):317-330 DOI:10.1080/22221751.2021.1888660

Author contribution.
Acquisition of data: IKK; AT, JK
Administrative, technical or logistic support: IKK; AT, JK
Analysis and interpretation of data: IKK; AT, JK
Conception and design: IKK; AT, JK
Critical revision of the article for important intellectual content: IKK; AT, JK
Drafting of the article: IKK; AT, JK
Final approval of the article: IKK; AT, JK
Guarantor of the study: IKK; AT, JK
Obtaining funding: IKK; AT, JK
Provision of study materials or patients: IKK; AT, JK
Statistical expertise: IKK; AT, JK